The Extragalactic Distance Scale Key Project VIII. The Discovery of Cepheids and a New Distance to NGC 3621 Using the Hubble Space Telescope'

Daya M. Rawson & Jeremy R. Mould

Mount Stromlo and Siding Spring Observatories, Institute of Advanced Studies, Australian National University, Weston Creek, ACT 2611, Australia

Lucas M. Macri & John P. Huchra

Harvard Smithsonian Center for Astrophysics, Cambridge, MA 02138, USA

Robert C. Kennicutt & Paul Harding

Steward Observatories, University of Arizona, Tucson AZ 85721, USA

Wendy L. Freedman, Robert J. hill & Randy L. Phelps

Carnegie Observatories, Pasadena CA 91101, USA

Barry F. Madore & Nancy A. Silbermann

IPAC, California Institute of Technology, Pasadena CA 91125, USA

John A. Graham

DTM, Carnegie Institution of Washington, Washington, DC 20015, USA

Laura Ferrarese & Holland C. Ford

John Hopkins University and Space Telescope Institute, Baltimore MD 21218, USA

Garth D. Illingworth

Lick observatory, University of California, Santa Cruz CA 95064, USA

John G. Hoessel & Mingsheng Han

University of Wisconsin, Madison, WI, 53706, USA

Shaun M. Hughes

1 Royal Greenwich Observatory, Cambridge CB3 OHA, UK

Abhijit Saha

Space Telescope Science Institute, Baltimore MD 21218, USA

Peter B. Stetson

Dominion Astrophysical Observatory, Victoria, BC V8X 4M6, Canada

[1]Based 011 observations with the NASA/ESA *Hubble Space Telescope*, obtained at the Space Telescope Science Institute, operated by AIJ{A, Inc. under NASA contract, No. NAS5-26555.

Received _____ ., accepted _____

ABSTRACT

We report on the discovery of Cepheids in the field spiral galaxy NGC 3621, based on observations made with the Wide Field and Planetary Camera 2 011 board the *Hubble Space Telescope* (11 S'1'). NGC3621 is one of 18 galaxies observed as a part of *The HST Key Project* on *the Extragalactic Distance Scale*, which aims to measure the Hubble Constant to 1 0% accuracy. 69 Cepheids with periods in the range 9 60 days have been observed over 12 epochs using the F555W filter, and 4 epochs using the F814W filter. The HST F555W and F814W data have been transformed to the Johnson V and Cousins I magnitude systems, respectively. Photometry was performed using two independent packages, DAOPHOT II/ALLFRAME and DoPHOT.

Period-luminosity relations in the V and I bands have been constructed using 23 high-quality Cepheids present in our set of 69 variables. Distance moduli relative to the LMC of 10.70 ± ().07 mag and 10.56 ± 0.09 mag are obtained using the ALLFRAME and DoPHOT data, respectively. True distance moduli of 29.20 ± 0.18 mag and 29.06 ± 0.18 mag, corresponding to distances of 6.9 ± 0.7 Mpc and 6.5 ± 0.7 Mpc, are obtained by assuming values of μ_0 = 18,50:1 0.10 mag and $E(V-I)$ = 0.08 mag for the distance modulus and reddening of the LMC, respectively.

Subject headings: galaxies: individual(NGC 3621) galaxies: distances stars: Cepheids

1_s Introduction

These observations of the spiral galaxy NGC 3621 form a part of a Key Project for the *Hubble Space Telescope* (11 S'1'), This project, known as *The HST Key Project on the Extragalactic Distance Scale* (1''rcd] nan et al. 1994a, 1994b, 1994c, Mould et al. 1995, and Kennicutt, Freedman and Mould 1995), aims to measure the Hubble Constant to IO% accuracy. This will be achieved by obtaining distances based on Cepheid variable stars to eighteen different galaxies, whit]) will provide a firm basis for the calibration of several secondary indicators: the Tully-Fisher relation, the Surface Brightness Fluctuation Method, the Expanding Photosphere Method, the Planetary Nebula Luminosity Function, the Globular Cluster Luminosity Function, and the Type 1a Supernova Standard Candle Method. The HST, with its enhanced resolution over ground-based telescopes and its position in space which removes many of the problems plaguing terrestrial observers, is the ideal instrument for the stringent demands of this type of project. Observations of Cepheids in M100 using HST (Ferrarese et al. 1996) have already yielded Cepheid distances to galaxies in the Virgo Cluster, thus displaying the capabilities of the WFPC2 instrument in detecting Cepheids in galaxies outside of the Local Group.

NGC 3621 is a relatively isolated spiral with a morphological classification of Sc II.8 (Sandage & Tammann 1981) or Sc III-IV (de Vaucouleurs et al. 1991) and a low galactocentric redshift of 526 km/s (de Vaucouleurs et al. 1991), indicative of a comparatively small distance relative to that of the Virgo cluster (Mould et al. 1995). Its complex pattern of partially resolved, irregular spiral arms makes it an excellent candidate for the detection of Cepheids, while its high inclination (i = *60°)* and well-ordered 11-1 rotation (Gardiner & Whiteoak 1 977) indicates that it is an ideal object for the calibration of the Tully-Fisher relation as applied to field spirals.

We describe the observations and preliminary reductions in §2. '1'11(! photometryand calibration of the instrumental magnitudes is discussed in §3. The search for Cepheids using two independent photometric algorithms and the resulting set of variables are described in §4. Period-luminosity relations and distance moduli are presented and discussed in §5, and our conclusions are given in §6.

2. Observations and Reductions

2.1, Observations

Observations of NGC 3621 using the Wide Field and Planetary Camera 2 (WFPC2) system on the 11 ST commenced on December 27, 1994 with the first of 24 F555W (approximately Johnson V) images. The observations were split over 12 epochs within a 60 day window; 11 of them were cosmic-ray split and one was a single exposure. In addition, 9 F814W (approximately Cousins I) images divided among four epochs, and 4 F439W images over two epochs were obtained. For both the F555W and F814W filters, a single short exposure of 180 seconds was obtained to provide a linearity check on the magnitudes derived by the photometric routines. The WFPC2 footprint for the observations, superimposed 011 a wide-field image of the galaxy (kindly made available by Sandage & Bedke 1985), is shown in Figure 1, while a mosaic of the WFPC2 images can be seen in Figure 2.

The WFPC2 includes four 800 x 800 CCD detectors. Three of these, the Wide Field Cameras, have a pixel size of 0.1 arcseconds as projected 011 the sky, for a total field of vim of 1.3 x 1.3 arcminutes each. The remaining CCD, the Planetary Camera, has a pixel size of 0.04 (i arcseconds as projected on the sky, for a total field of view of 36 X 36 arcseconds. A more detailed exposé on the WFPC2 instrument can be found in *The HST WFPC2 Instrument Handbook* (Burrows et al. 1994). All observations were made with the telescope guiding in fine lock with a stability of approximately 3 mas. The gain and readout noise were 7 e^-/DN and 7 e^-, respectively. The CCD was operated at a temperature of -88° C for all observations.

Exposure times and dates for each observation are given in Table 1. The sampling strategy, as discussed by Freedman et al. (1 994a), has been designed specifically for the Key Project with the purpose of maximising the probability of detecting a Cepheid with

a period in the chosen window of 1 0 60 days. It follows a power-law distribution in time which allows for an optimum sampling of the light curve for Cepheids in this period range and reduces the risk of aliased detections. No follow-up observation to anchor the lollg-period variables more accurately is planned for this galaxy. Figure 3 shows a plot of the variance in the chosen sampling from an ideal sampling as a function of period. The plot is normalised sue]] that low values indicate uniform sampling was achieved and high values indicate clumping and redundancies in the actual sampling.

2.2. Data Reductions

The HST data have been calibrat ed using the pipeline processing at the Space Telescope Institute (STScI). The full reduction procedure, given in Holtzman et a]. (1995a), consists of: a correction of A/l) errors, the subtraction of a bias level for each chip, the subtraction of a superbias frame, the subtraction of a dark frame, a correction for shutter shading, and a division by a flat field. The names of the STScI reference files used for this calibra tion arc listed in the notes to Table 1. Furthermore, each of the frames was corrected for vignetting and geometrical distortions in the WFPC2 optics (using files kindly provided by I). Stetson and J. Holtzman, respectively). A more complete description of the calibration steps can be found in hill et al. (1996) and Stetson et al, (1996).

1 Ioltzman et al. (1995b) have described the effect on photometry of charge transfer inefficiency (CTI) in the Loral WFPC2 chips. The principal effect at very low light level is a loss of sensitivity from bottom to top of each chip amounting to ().04 mag for a star at row 800 relative to an equivalent star at hypothetical row ().

Subsequent investigations (Holtzman, private communication) have made use of the pre-flash capability built into WFPC2 (but not a user commandable facility). Pre-flash

intensities from $30e^-$ to $1\ 000e^-$ were added to observations of standard stars in w Centauri, and aperture photometry was carried out systematically as a function of pre-flash level and y-coordinate. These observations demonstrated that observations with $0e^-$ background show a *0.04* mag ramp relative to $30e^-$ background observations and to observations at all other brighter background levels. For our purposes, this confines the CTI problem to the calibration observations of Holtzman et al. and implies that no ramp correction is required for any of our observations, where the background level is always greater than $70e^-$.

There is a small difference in the long- and short-exposure zero points for the WFPC2, derived from photometry of w Centauri, of the order of 0.05 magnitudes (Hill et al. 1 996). We use the long-exposure zero points in this paper.

Hot pixels not accounted for in the subtraction of the dark frames, or "superdarks," are found not to present substantial problems to the photometry programs. A filter which screens against sharp spikes, such as hot pixels, is implemented in the FIND routine of DAOPHOT (Stetson 1990). This filter will likewise guard against low-valued bad pixels in the image. Background galaxies or other extended objects are also filtered out. These types of objects undergo further filtering in subsequent steps of the photometry. DoPHOT (Schechter, Mateo and Saha 1 993) also contains routines for detection and removal of hot pixels and filtering of non-stellar objects.

3. Photometry and Calibration

3.1. Photometric Reductions

Photometry of NGC 3621 was obtained by two groups implementing independent soft ware packages; 1). M .R. and J .R. M. at Mount St romlo Observatory, Australia using D AOPHOT II/ALLFRAME (Stetson 1994) and L.M. M. and J.]).]]. at the Harvard-Smithsonian Center for Astrophysics, Cambridge, USA using a version of DoPHOT (Schechter, Mateo and Saha 1993) specially modified to deal with HST WFPC2 data (Saha et al. 1 996). Each package performs photometry using independent techniques, and a comparison of results yields a fundamental check on the validity of the photometry. This provides a very powerful tool for detecting the presence of systemat ic errors which might go undetected if only one package were used.

Both packages make use of a Point Spread Function (PS1'), but whereas D AOPHOT 11 uses a PSF created from independent images of u])-crowded fields, 1)01'110'1' constructs a PSF by fitting a function to the brightest stars in the frame being reduced. In each case, 1'S1"s appropriate to the filter and chip of each image are used. The I)sl"s used for the ALLFRAME reductions were made using images of un-crowded regions of NGC 2419, and I'al 4 (hill et al. 1996), with the implicit assumption that the PSF for a given filter/clli]) combination does not vary with time (or, if it does, that the variation can be absorbed into the aperture correction; see below).

The ALLFRAME reduction started with the creation of a preliminary star list using D AOPHOT 11 and ALLSTAR on each image. D AOMASTER was then u sed to deri ve coordinate transformations between each epoch. ALLFRAME was then run on this preliminary star list to obtain more accurate photometry and transformations. This information was used to obtain a deep image of NGC 3621 , averaging together all the

images, and discarding bright points which did not appear in a significant fraction of the frames. DAOPHOT 11 was once again used on this image to provide the master star list, which was then used by ALLFRAME in the final photometric reduction step.

The DOPHOT reduction started by combining the pair of exposures of each of the cosmic-ray split F555W and F814W epochs into single, cosmic-ray-free images. These images were co-added to create master images for each filter. DOPHOT was then run on these images to create the master star lists, which were later used in the photometric reduction of each frame.

3.2. Calibration

The calibration of photometry for NGC 3621 was achieved using the method outlined in Holtzman (1995b) and Hill (1996). Slightly different methods are employed for both the DOPHOT and ALLFRAME photometry. The general equations which convert the instrumental magnitudes into the standard system are:

$$V = F555W - 0.052(V - I) + 0.027(V - I)^2 \quad (1)$$

$$I = F814W - 0.063(V - I) + 0.025(V - I)^2 \quad (2)$$

In the preceeding equations, the instrumental magnitudes ($F555W$ and $F814W$) have been fully calibrated and corrected for exposure time and for changes in the gain state of the camera (the 11 ST calibration measurements were made with the camera in a gain state of 14, whereas the NGC 3621 observations were made in the gain state of 7). The gain ratios for each chip are listed in Table A 1.

The calibration of photometry from ALLFRAME is achieved in several steps. First, an aperture correction to the ALLFRAME magnitude is made. This involves converting

the instrumental magnitude calculated from the best fit of the PSFs to a 0.5-arcsecond aperture magnitude. This correction is obtained by comparing photometric magnitudes for the brightest isolated stars in the field Of each chip within a 0.5-arcsecond radius calculated using DAOGROW (Stetson 1990) and the corresponding ALLFRAME magnitudes for those stars. The aperture corrections used are given in Table A 1. An ALLFRAME zero point of 25 is subtracted from the result. The final equations for ALLFRAME photometry are presented in Table A2.

The calibration of photometry from DoPHOT followed the steps described in Saha et al. (1996), First, the instrumental fit magnitudes of each frame arc corrected for small variations due to position and transformed into instrumental aperture magnitudes. This is achieved using correction coefficients derived by A. Saha from observations of stars in the Leo I dwarf galaxy. Next, the instrumental aperture magnitudes are transformed to 0.5-arcsecond aperture magnitudes using coefficients determined by A. Saha from a large set of field stars found in the NGC 3621 master frames.

Typical values for the difference between the ALLFRAME and DoPHOT magnitudes of the brightest stars (m_{F555W} <23.5, m_{F814W} < 22.5) are of the order of -0.01 mag in F555W and +0.05 mag in F814W (see Figures 4a-b). Typical uncertainties in the photometry of stars in the range of our Cepheids (23 < m_{F555W} < 26, 22,5 < m_{F814W} < 24.5) amount to 0.04 mag in F555W and 0.06 mag in F814W for ALLFRAME and 0.11 mag in F555W and 0.09 mag in F814W for DoPHOT. ALLFRAME photometry of the fifty brightest uncrowded stars in each chip are presented in Tables A 3-A6 for future comparisons of our photometry with other observations of NGC 3621 Cepheids.

4. Cepheid Search

4.1. ALLFRAME Search

The scare}] for Cepheid variables obtained from the Al,1 .FRAME photometry was achieved in three main steps. The first step was a simple siglna-based classification of all objects as either variable or non-variable. Any star with a single point more than 1.5σ from the mean magnitude was selected as a possible variable star. This method dots not screen against cosmic ray hits, but dots provide a list of stars which are likely to be variable.

This list of stars was then presented to a program based on a phase dispersion minimisation (PDM) technique (Stellingwerf 1978). The algorithm seeks to minimise the dispersion of the light curve at a constant phase, relative to a mean curve. The minimum in dispersion will generally be lower for a true Cepheid variable than for other sources of variability such as stars with multiple cosmic ray hits. A cut-off of the dispersion, Θ, of ().9 was implemented. Uncertainties in the periods were calculated by manually checking the phasing of bracketing periods. The light curves produced by the 1'1)M program were fu rtl ı er weeded out by eye, to pick out all candi dates likely to be Cepheids.

4.2. DoPHOT Search

The search for Cepheid variables obtained from the 1)01'11 () 'J' photometry started with a basic χ^2 variability statistic (described in Saha & Hoessel 1 990), which flags all objects with $\chi^2_\nu \geq$] .75 as variable. Periods for all variable objects were calculated using the A-statistic developed by Lafler & Kinman (1 965), with uncertainties given by the variation of A with trial period. objects with A ≥ 3 were selected for visual examination of their folded lightcurves to identify the Cepheid candidates and to remove data points affected b y cosmic rays.

4.3. Mean Magnitudes

Two methods are used to obtain mean magnitudes for each of the Cepheids, as a cross-check on the validity of each magnitude. The first one is an intensity-averaged magnitude,

$$m = -2.5 \log_{10} \frac{1}{N} \sum_{i=1}^{N} 10^{-0.4 \times m_i}, \tag{3}$$

while the second one is a phase-weighted magnitude,

$$m_{PW} = -2.5 \log_{10} \sum_{i=1}^{N} 0.5 \times (\phi_{i+1} - \phi_{i-1}) \times 10^{-0.4 \times m_i}, \tag{4}$$

where N is the total number of epochs and m_i and ϕ_i are the magnitude and phase of the i-th epoch, in order of increasing phase. In the case of the cosmic-ray split pairs of observations, the two magnitudes were weighted by the inverse square of the uncertainty in their photometry. This greatly reduces contamination due to cosmic rays and spurious magnitude estimates. In practice, obvious cosmic ray hits were removed from the data, their presence being identifiable by a major increase in intensity for one of the cosmic-ray split frames and a large uncertainty in the resulting photometry.

Phased light curves that are evenly sampled yield intensity-averaged and phase-weighted magnitudes that coincide closely. However, when the sampling is not uniform the phase-weighted average provides a more accurate determination. Typical differences between the two methods are of the order a few hundredths of a magnitude. This dots not significantly impact the distance modulus, a result which is consistent with previous papers in this series (Kelson et al. 1996, Ferrarese et al. 1996 and Silbermann et al. 1996).

Only four epochs of data have been taken for the I-band photometry. This gives rise to under-sampling of the light curves and decreases the precision of both methods of averaging. One way to compensate for this is to make use of the correspondence between V and I

light curves for Cepheids, as discussed by Freedman (1988). This takes advantage of the fact that, as a first approximation, one light curve can be mapped onto the other by simple numerical scaling. The ratio of V to I amplitude is found to be 1:0.51. Using this result, we can make an estimate of the correction to the average I magnitude that is required by the under-sampling. This is achieved by calculating the difference between the V-band average for all epochs and for just those epochs with both V- and I-band observations. This result, is rescaled by the 1:0.51 amplitude ratio and summed to the mean I magnitude. The correction is calculated using both methods of averaging and it amounts to no more than $\pm$ 0.1 magnitudes, with an average of approximately 0.04 magnitudes. This Procedure has been used in previous papers in this series.

4.4. The Cepheids Found in NGC 3621

The ALLFRAME and DoPHOT variable searches produced a total of sixty-nine Cepheids (identified as C01-C69) and one Population II Cepheid (identified as W01). Table 2 lists, for each of these stars, the identification number, the chip in which it is found, the ALLFRAME period, the J2000.0 coordinates, the ALLFRAME phase-weighted magnitudes for the V and I bands, and comments on the variable. The comments describe the image quality, sampling of the light curve and amplitude of the variability, and indicate the Presence of other irregularities such as high sky gradients and cosmic rays nits. This classification]) system was applied uniformly across the entire sample of Cepheids to achieve a rigorous and consistent determination of the high-quality variables used in the final fit to the Period-Luminosity function. A total of 24 Cepheids were selected based on this classification.

While ALLFRAME photometry is available for all candidates, DoPHOT photometry does not exist for three of the stars: C07 (which was too close to the border of the chip,

in an area not searched by DoPHOT), C34 (located in a very crowded region), and C46 (also located in a very crowded region). A comparison of V- and I-band phase-weighted magnitudes determined by each reduction scheme (Figure 5) shows agreement at the 0.2 mag level for most variables. A comparison of period determinations by the Stellingwerf and Lafler-Kinman methods (Figure 6) shows agreement at the 1 5% level for all Cepheids.

The Cepheids are identified in the field of each of the WFPC2 chips in Figures 7a-d using circles which are numbered following the convention given in Table 2. Finding charts for each of the stars are displayed in Figures 8a-l. Each of the charts encompasses a 50 by 50 pixel segment of the chip. The ALLFRAME V- and I-band light curves are presented in Figures 9a-1, and the data used to generate these curves is presented in in Tables A7 and A8. Figure 10 shows the location of all Cepheids in a color-magnitude diagram of NGC 3621 stars. Based on this CMD, one of the high-quality variables (C08) was removed from the sample due to its unusually red ($V - I = 2.03 \pm 0.06$) color. This resulted in a change of -0.04 mag and +0.01 mag in the V- and I-band distance moduli, respectively, for both the ALLFRAME and DoPHOT data sets.

5. Period-Luminosity Relations and Distance Modu i

5.1 Theory

The method used to derive V- and I band apparent distance modu is the same one that was used in other papers in this series. The period-luminosity relations of LMC Cepheids (Madore & Freedman 1991), scaled to an assumed true distance modulus of 18.50±0.10 mag and corrected for an estimated average line-of-sight reddening of $E(V \quad I) = 0.08$ mag (see Bessel 1991 for a recent review of MC reddening) are:

$$M_V \qquad 2.76 \log P(d \qquad .0) \quad 4.16, \tag{5}$$

$$M_I \qquad 3.06 (\log P(d) \quad 1.0) \quad 4.87 \tag{6}$$

fitting the data from NGC 3621, we follow the procedure given in Freedman et al (1994a). We fix the slope o best fit to tha given in the equations above and scale the equations in the magnitude axis until the minimum rms dispersion between the data and ie fit is obtained By using the slopes given above, we avoid any bias that would arise from incompleteness at faint magn udes in the NGC 3621 data set The magnitude shifts resultant from this method yield V and I-band apparen distance moduli relative to the MC.

A reddening correction due to the presence of interstellar dust must be applied in order to obtai the true distance modulus (see Madore & Freedman 1991 for a complete description of this correction). The mean reddening relative to the MC reddening, $\Delta E(V \quad I)$, is given by ie difference V- and I-band distance oduli This can be converted into an absolute value by adding the assumed value of MC reddening quoted above. The true distance modulus is calculated as $\mu_0 = \mu \quad \mathcal{R}_I \times \Delta E(V \quad I)$, where $\mathcal{R}_I \approx 1.40$.

5.2. Results

The procedure described in the preceding subsection was carried out and V- and I-band apparent distance moduli relative to the LMC were determined, with values of 11.16 ± 0.10 mag and 10.97:1 0.06 mag for the ALLFRAME data, and 11.11 ± 0,10 mag and 10.884 0.07 mag for the DoPHOT data, The quoted uncertainties reflect *only* the rms dispersion of the NGC 3621 P-L relations.

Given these results and assuming $E(V - I)_{\rm LMC}$ = 0.08 mag, the mean reddening values are 0.27 ± 0,05 mag and 0.31 ± 0.05 mag for the ALLFRAME and DoPHOT data, respectively. These rather high values of color excess are consistent with the comparatively low surface brightness of the region of NGC 3621 observed by HST (see Figure 1). The unreddened distance moduli relative to the LMC are 10.70 ± 0.07 mag and 10.56 ± 0.09 mag for the ALLFRAME and DoPHOT data, respectively.

True distance moduli of 29.204 0.18 mag and 29.06 ± 0.18 mag for the ALLFRAME and 1)01' 110'1" data, respectively, are obtained by assuming $\mu_{0,\rm LMC}$ = 18.50 ± 0.10 mag . These are equivalent to distances of 6.9 ± 0.7 Mpc and 6.5 ± 0.7 Mpc. A full description of the different contributions to the uncertainties is presented in Table 3.

Figures 11 and 12 show the V- and I-b and period-luminosity relations of the NGC 3621 Cepheids. For comparison with Equations (5) and (6), the NGC 3621 period-luminosity relations based on ALLFRAME results are:

$$m_V = -2.76(\log P(d) - 1.0) + 25.73 \quad (7)$$

$$m_I = -3.06(\log P(d) - 1.0) + 24.70, \quad (8)$$

5.3. Discussion

Three potential causes for concern are the effect of magnitude selection effects for the fainter Cepheids, variations from chip to chip, and differences between the two sets of results for each method of photometry.

Due to the intrinsic width of the 1'-1, relation and the limiting magnitude of the sample, we detect only the brightest of the short-period variables, giving rise to a lower apparent distance modulus for shorter periods. The distance modulus increases as the lower limit in the period is raised, levelling off as it approaches 18 days. This variation in distance modulus is of the order of 0.04 magnitudes. By imposing a lower limit on the period of 18 days, we ensure that our sample is as representative as possible.

Variability in measurements across the four chips of the WFPC2 instrument may give rise to systematic differences in the distance moduli derived from each chip. This variability could arise from a number of possible sources, including variations in the sky value (particularly in regions with severe crowding). Another area for concern is the manner in which the zero points have been derived, which assumes flat-fielding has taken into account any inherent differences from chip to chip. These problems are tested for by obtaining distance moduli for each chip, which are in agreement within their errors. Thus, variability from chip to chip is not a problem.

The comparisons of ALLFRAME and DoPHOT magnitudes and periods presented in previous sections indicate that the two data sets are in good agreement. The apparent distance moduli for the V- and I-band P-L relations presented above are also consistent within their errors, indicating no significant differences between the two methods of photometry.

6. Conclusions

We have discovered a total of 69 Cepheid stars in the Sc field spiral galaxy NGC 3621. We have fitted standard V- and I-band period-luminosity relations to the Cepheids with high-quality light curves and periods longer than 18 days and obtained true distance moduli of 29.20 ± 0.18 and 29.06 ± 0.18 magnitudes from the ALLFRAME and DoPHOT data, respectively. These correspond to distances of 6.9 ± 0.7 and 6.5 ± 0.7 Mpc. Mean reddenings were deduced from the apparent V- and I-band moduli using a standard reddening curve, and they amount to $E(V-I) = 0.27 \pm 0.05$ and 0.31 ± 0.05 magnitudes. There is good agreement, within the uncertainties, between the ALLFRAME and DoPHOT results.

With an inclination angle of 60°, NGC 3621 is an excellent calibrator for the Tully-Fisher relation, but is not so edge-on that extinction and confusion pose problems for discovery and photometry of Cepheids. Figure 13 shows the location of NGC 3621 in the Tully-Fisher diagram for galaxies with accurate Cepheid distances. The data used to generate this figure is listed in Table 4. The least-squares fit to the data points in Figure 13 is (Mould et al. 1996):

$$H^{abs}_{-0.5} = -21.3 - 11(log\Delta V(0)_{20} - 2.5), \tag{9}$$

where $\Delta V(0)_{20}$ is the 21-cm profile width and $H^{abs}_{-0.5}$ is a measure of the infrared flux. The quantities are fully defined in the original references. The intercept in this regression is 0.07 mag and 0.28 mag brighter than those obtained respectively by Aaronson et al. (1980) and Freedman (1990). The regression is indistinguishable within the errors from the calibration obtained when 17 Virgo galaxies are placed at the distance of M100 and added to the calibration (Mould et al. 1995).

Environment dependence of the Tully-Fisher relation is an important issue for the extragalactic distance scale, as the most nearly unbiased measurement of distances in the free Hubble expansion at 10^4 kill/sccisf[)~galaxy clusters (Aaronson & Mould 1986). This 11 ST Key Project will be able to add many more galaxies to the Tully-Fisher diagram to test the identity of field and cluster Tully-Fisher relations.

7. Acknowledgments

We would like to thank Doug Van Orsow, the program coordinator for this Key Project, as w c]] as the rest of the STScI and NASA support staff that have made this project possible. The HST Key Project on the Extragalactic Distance Scale is supported by NASA through grant GO-2227-87A from STScI. This work has made use of the NASA/IPAC Extragalactic Database (NED), which is operated by the Jet Propulsion Laboratory, Caltech, under contract with the National Aeronautics and Space Administration.

REFERENCES

Aaronson, M., 1977, Ph.D. Thesis, Harvard University

Aaronson, M. et al. 1980, ApJ 239, 12

Aaronson, M. et al. 1982, ApJS 50, 241

Aaronson, M. & Mould, J.R. 1986, ApJ 303, 1

Bessell, M.S. 1991, A&A 242, L17

Burrows, C.J. et al., 1994, *The Wide Field and Planetary Camera 2 Instrument Handbook.* (Baltimore: STScI)

deVaucouleurs, G., deVaucouleurs, A., Corwin Jr., H., Buta, R., Paturel, G. and Fouqué, P., 1991, *Third Reference Catalogue of Bright Galaxies.* (Berlin: Springer-Verlag)

Ferrarese, L. et al. 1996, ApJ 464, 568

Fisher, J.R. & Tully, R.B. 1981, ApJS 47, 139

Freedman, W.L. 1988, ApJ 326, 691

Freedman, W.L. 1990, ApJ 355, L35

Freedman, W.L. et al. 1994a, ApJ 427, 628

Freedman, W.L. et al. 1994b, ApJ 435, L31

Freedman, W.L. et al. 1994c, *Nature* 371, 757

Gardiner, L.T. and Whiteoak, J.B. 1977, Aust. J. Phys. 30, 187

Hill, R.J. et al. 1996, submitted for publication in ApJ

Holtzman, J.A. et al. 1995a, PASP 107, 156

Holtzman, J.A. et al. 1995b, PASP 107, IO(L5

Kelson, D.D. et al. 1996, ApJ 463, 26

Kennicutt, R. C., Freedman, W.L., and Mould, J.R. 1995, AJ 110, 1476

Lafler, J. and Kinman, T.D. 1965, ApJS 11, 216

Madore, B.F., and Freedman, W.L. 1991, PASP 103, 933

Mould, J. R, et al. 1995, ApJ 449, 413

Mould, J .R. et al. 1996, in *The Extragalactic Distance Scale*, Livio, Donahue & Panagia, eds. (Cambridge: Cambridge University Press)

Saha, A. and Hoessel, J.G. IWO, AJ 99, 97

Saha, A. et al. 1996, ApJ 466, 55

Sandage, A. and Tammann, G. 1981, *Revised Shapley-Ames Catalog of Bright Galaxies.* (Washington: Carnegie)

Sandage, A. and Bedke, J. 1985, AJ 90, 1992

Schechter, P.L., Mateo, M., and Saha, A. 1993, PASP 105, 134'2

Silbermann, N.A. et al. 1996, accepted for publication in ApJ

Staveley-Smith, L. & Davies, R.D. 1987, MNRAS 224, 953

Stellingwerf, R.F. 1978, ApJ 224, 953

Stetson, P.B. 1990, PASP 102, 93'2

Stetson, P.B. 1994, PASP 106, 250

Stetson, P.B. et al. 1996, in preparation

Tanvir, N.R. et al. 1995, Nature 377, 27

Wevers, B.M.H.R. 1984, Ph.D. Thesis, University of Gröningen

This manuscript was prepared with the AAS LaTeX macros v4.0.

Figure Captions

Figure 1: - A wide-field image of NGC 3621 (courtesy Sandage & Bedke 1985), with the footprint of the WFPC2 field of view (see Figure 2)

Figure 2.- A mosaic of the WFPC2 images of NGC 3621. Single-chip images, marking the location of the variables, can be found in Figures 7a-d.

Figure 3.- The sampling efficiency of the V-band observations. Large dips indicate the inability of our sampling scheme to detect Cepheids with those periods.

Figures 4a-b.- A comparison of the ALLFRAME and DoPHOT $F555W$ and $F814W$ magnitudes for each of the four WFPC2 chips.

Figure 5.- A comparison of the ALLFRAME and DoPHOT V- and I-band mean magnitudes for all Cepheids.

Figure 6.- A comparison of the ALLFRAME and DoPHOT periods for all Cepheids.

Figures 7a-d.- V-band images of the four WFPC2 chips. The circles indicate the position of each of the Cepheids, labeled as in Table 2.

Figures 8a-l.- Finding charts for all the Cepheids.

Figures 9a-[illegible].- V- and I-band phased light curves for all the Cepheids.

Figure 10.- Color-magnitude diagram of the Cepheids and the field stars in NGC 3621.

Figure 11.- V-band period-luminosity relations of high-quality Cepheids (see Table 2) obtained with ALLFRAME (top) and DoPHOT (bottom) photometry.

Figure 12.- I-band period-luminosity relations of high-quality Cepheids (see Table 2) obtained with ALLFRAME (top) and DoPHOT (bottom) photometry.

Figure 13.- Calibrators of the Infrared Tully-Fisher Relation (see Table 4).

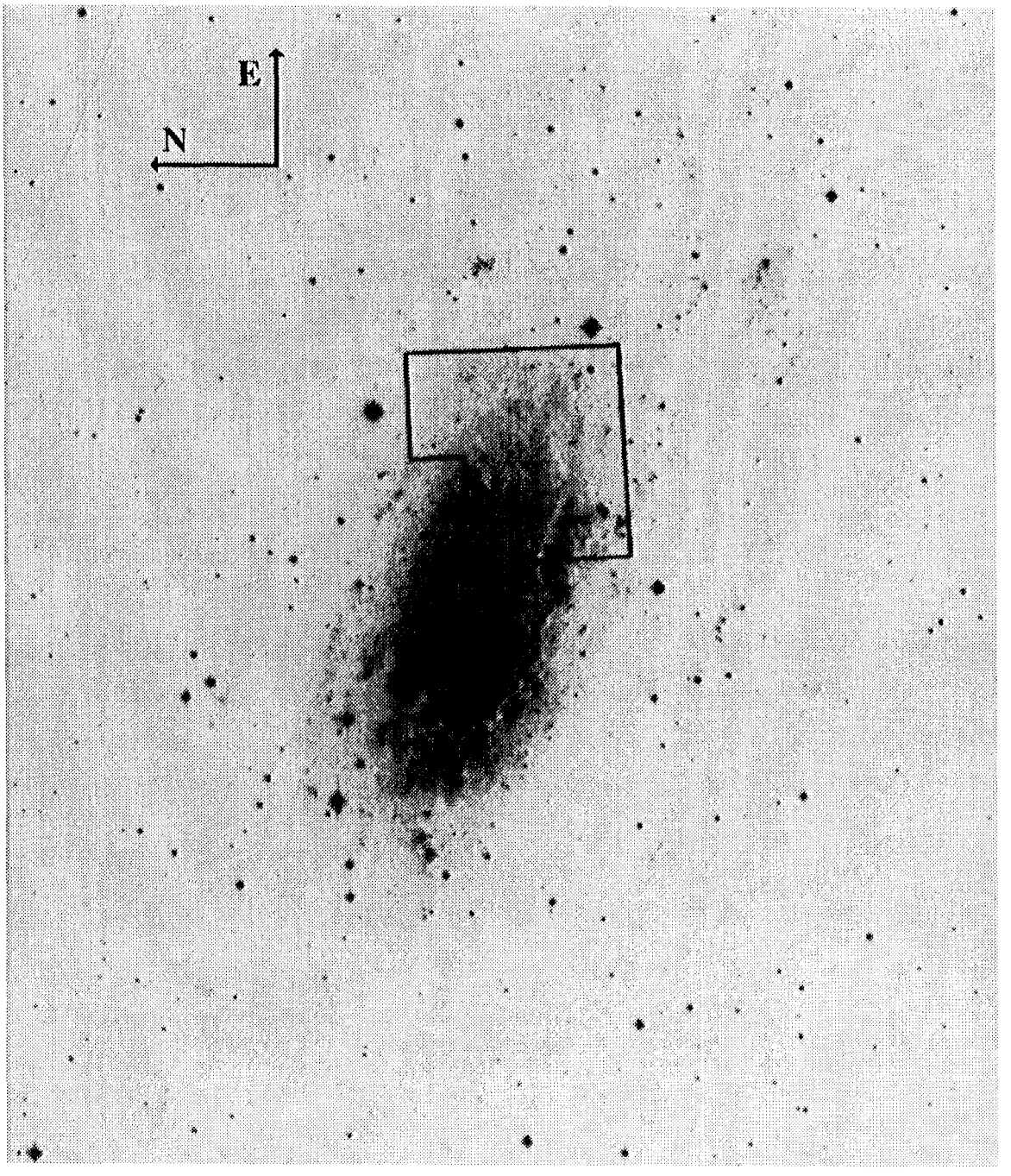

Figure 1.- A Wicl(:-field image of NGC 3621 (courtesy Sandage & Bedke 1985), with the footprint of the WFPC 2 field of view (see Figure 2)

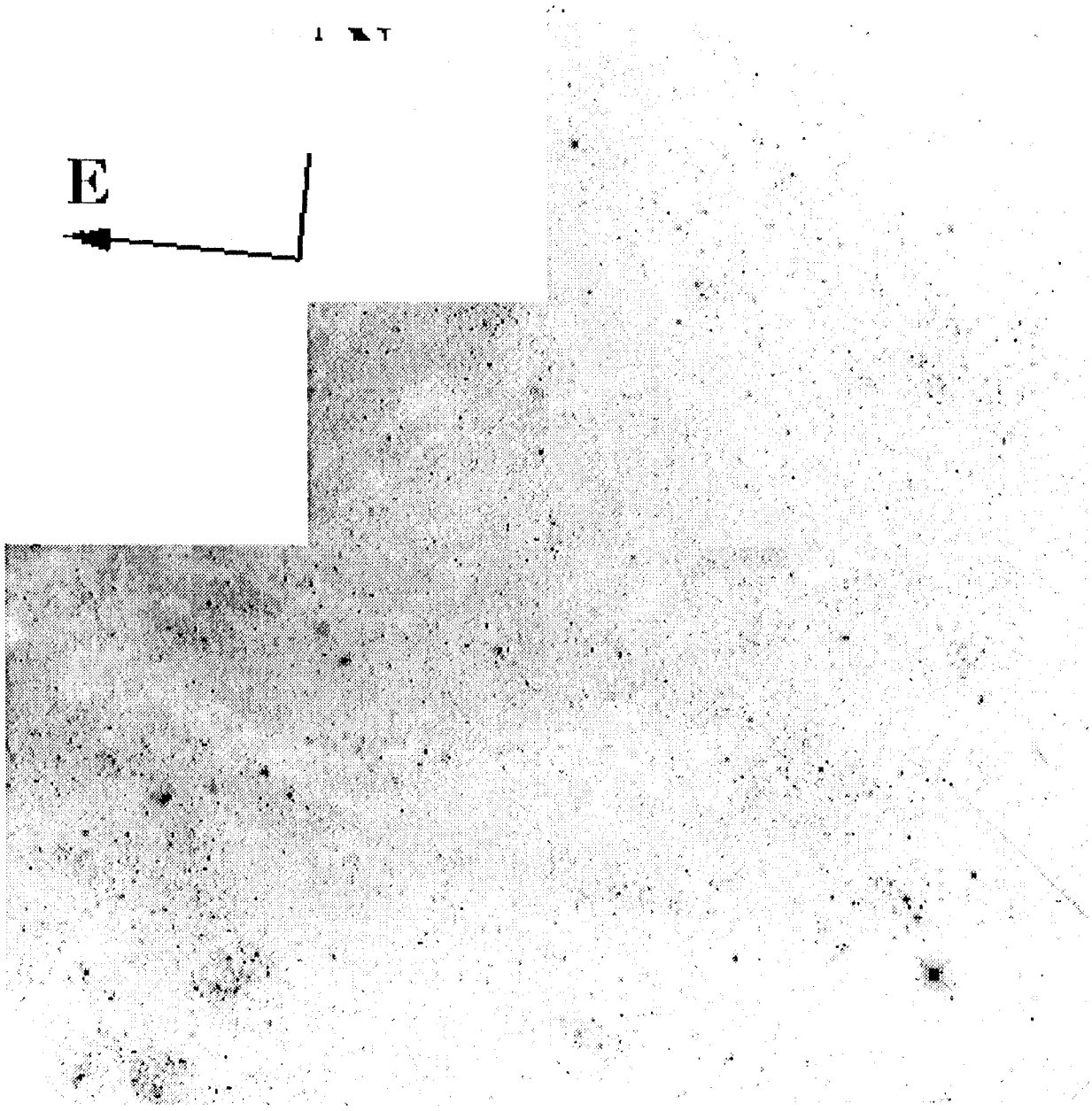

Figure 2.- A mosaic of the WFPC2 images of NGC3621, Single-chip images, marking the location of the variables, can be found in Figures 7a-d.

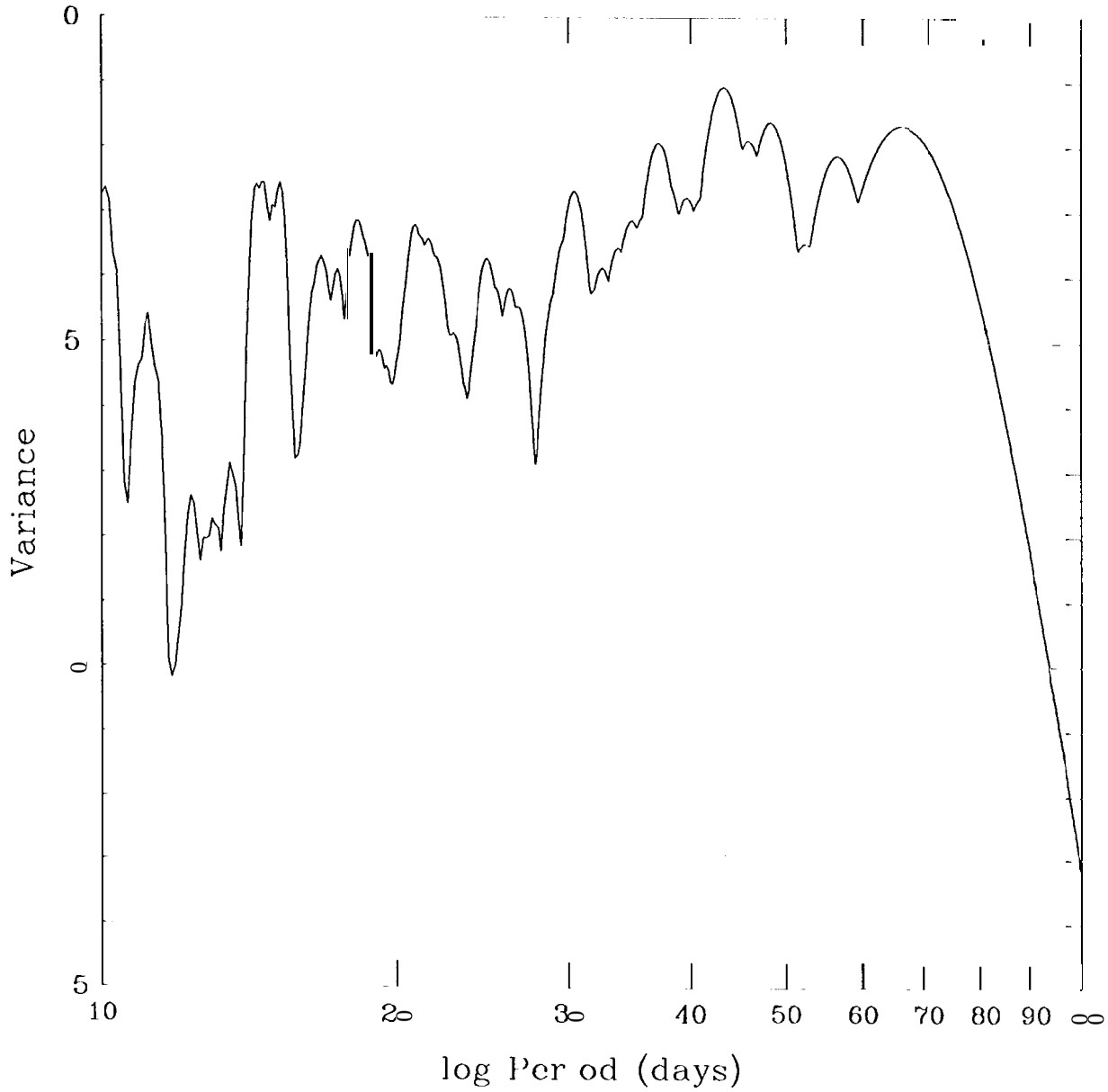

Figure 3. The sampling efficiency of the V-band observations. Large dips indicate the inability of our sampling scheme to detect Cepheids with those periods.

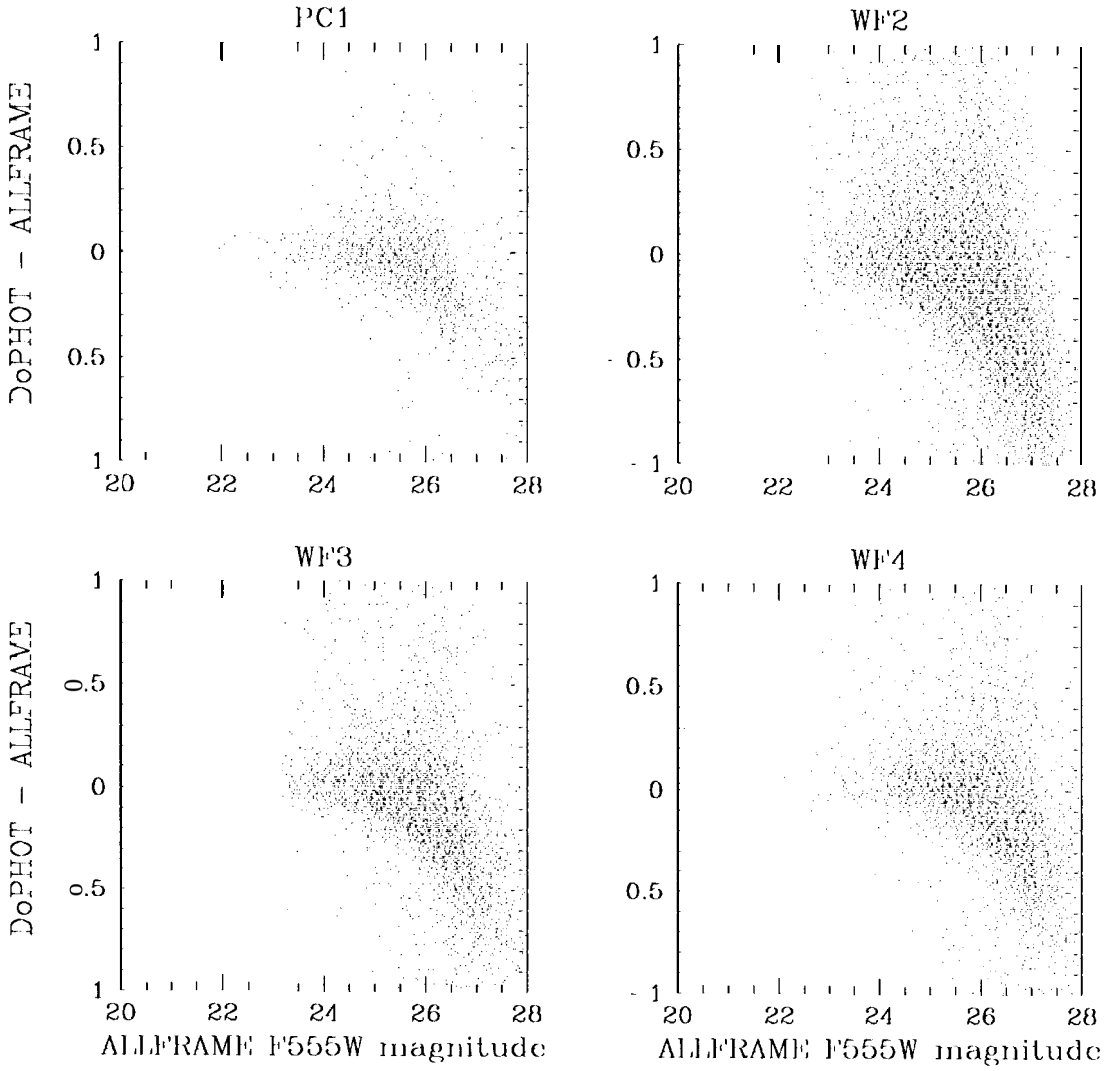

Figure 4a.- A comparison of the ALLFRAME and DoPHOT $F555W$ magnitudes for each of the four WFPC2 chips. The lines of best fit for bright ($m_{F555W} < 23.5$) stars are 0.01, -0.03, 0.00 and 0.03 for the PC1, WF2, WF3 and WF4 chips, respectively.

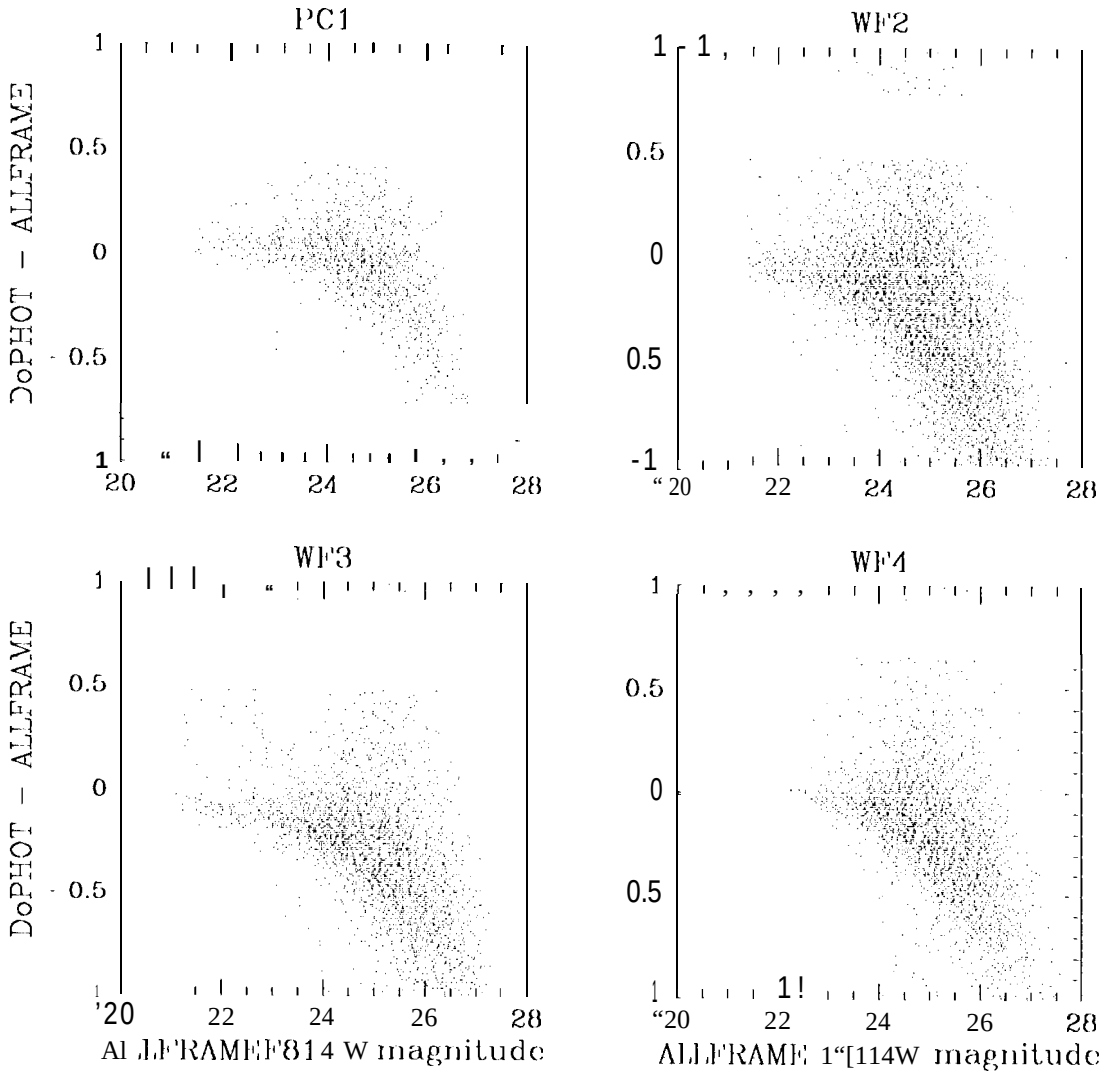

Figure 4b.- A comparison of the ALLFRAME and DoPHOT $F814W$ magnitudes for each of the four WFPC2 chips. The lines of best fit for bright ($m_{F814W} < 22.5$) stars are 0.04, - 0.06, - 0.10 and - 0.01 for the PC1, WF2, WF3 and WF4 chips, respectively.

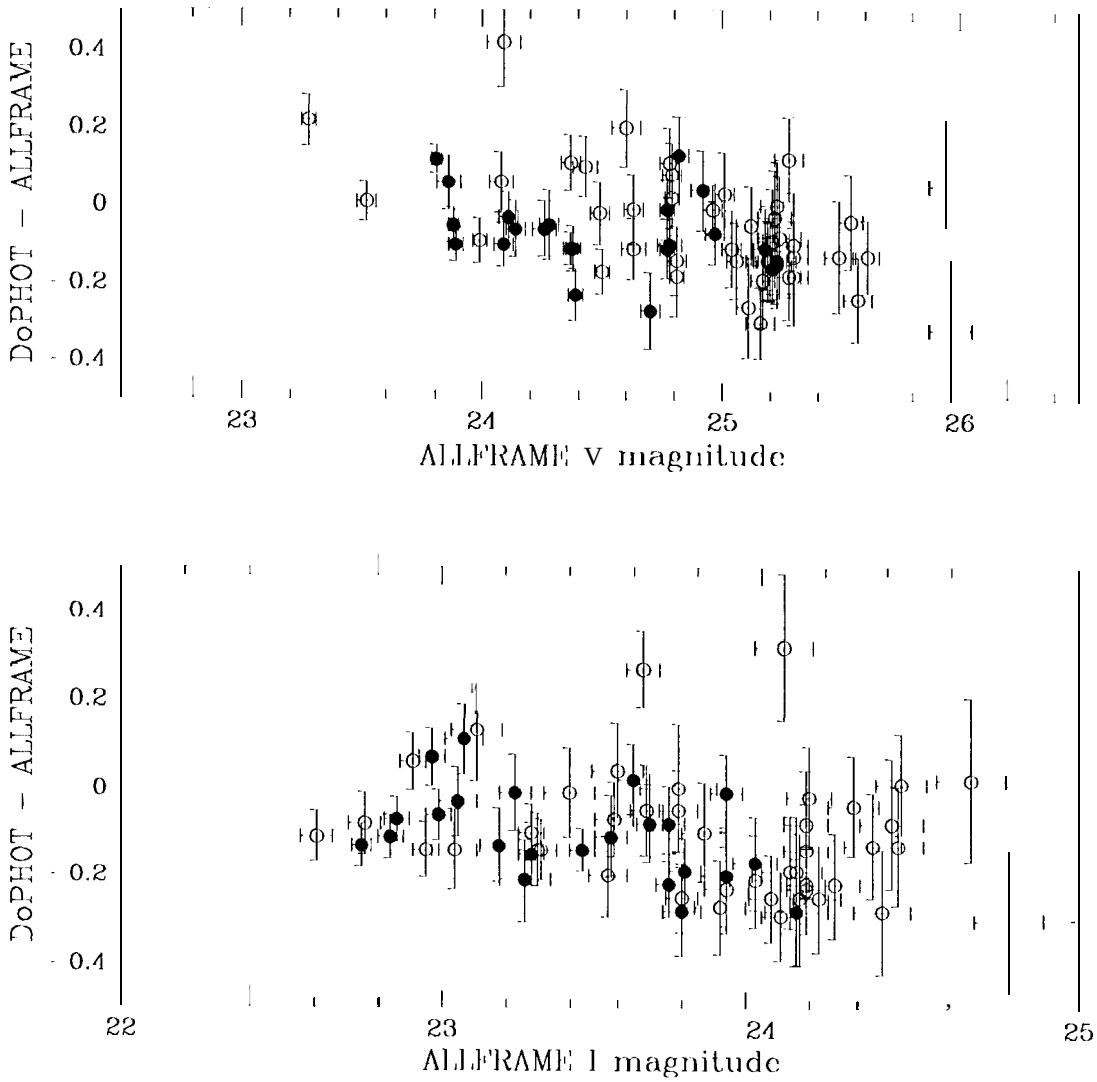

Figure 5.- A comparison of the ALLFRAME and DoPHOT V- and I-band mean magnitudes for all Cepheids in the sample. Filled circles identify the Cepheids that were used to construct the period-luminosity relations.

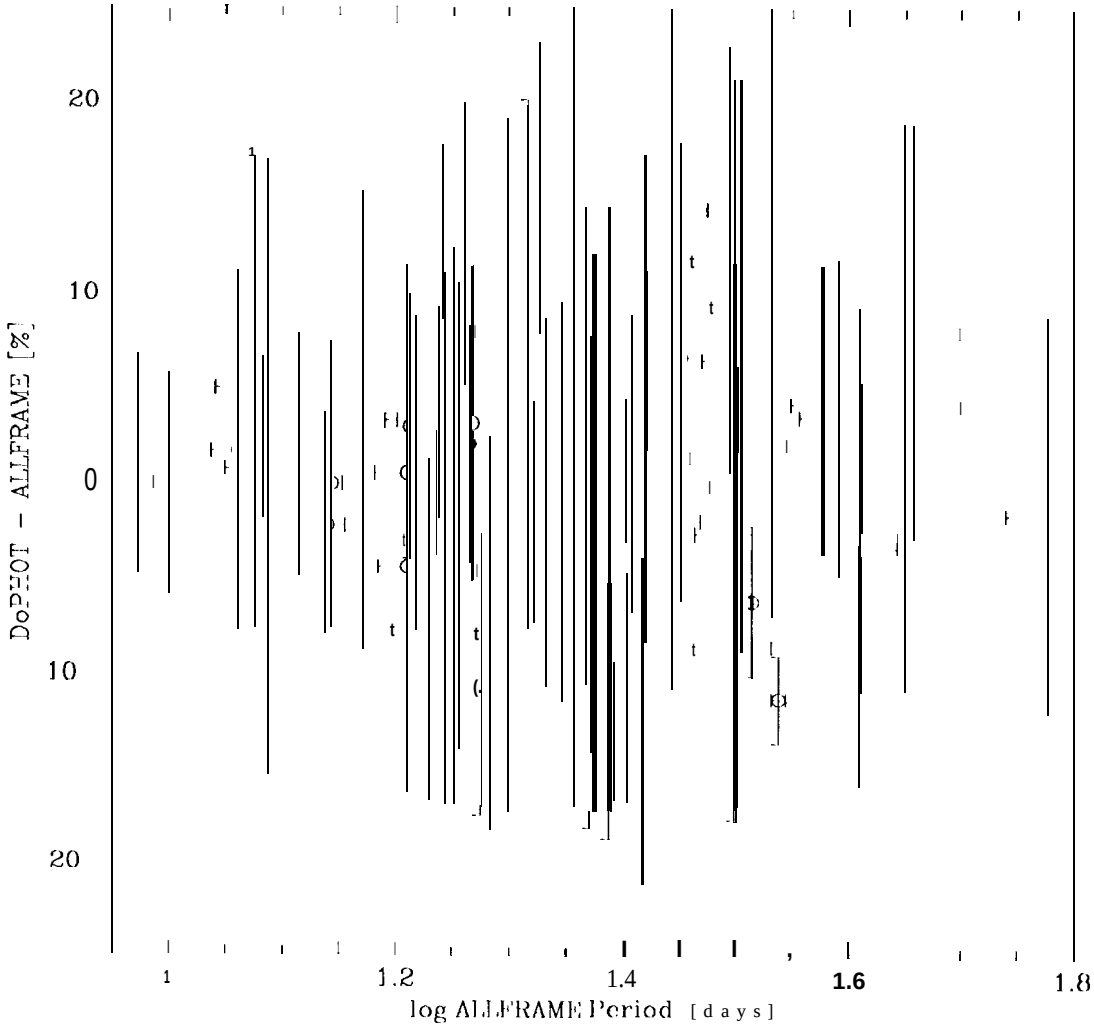

Figure 6.- A comparison of the ALLFRAME and DoPHOT periods for all Cepheids in the sample. Filled circles identify the Cepheids that were used to construct the period-luminosity relations.

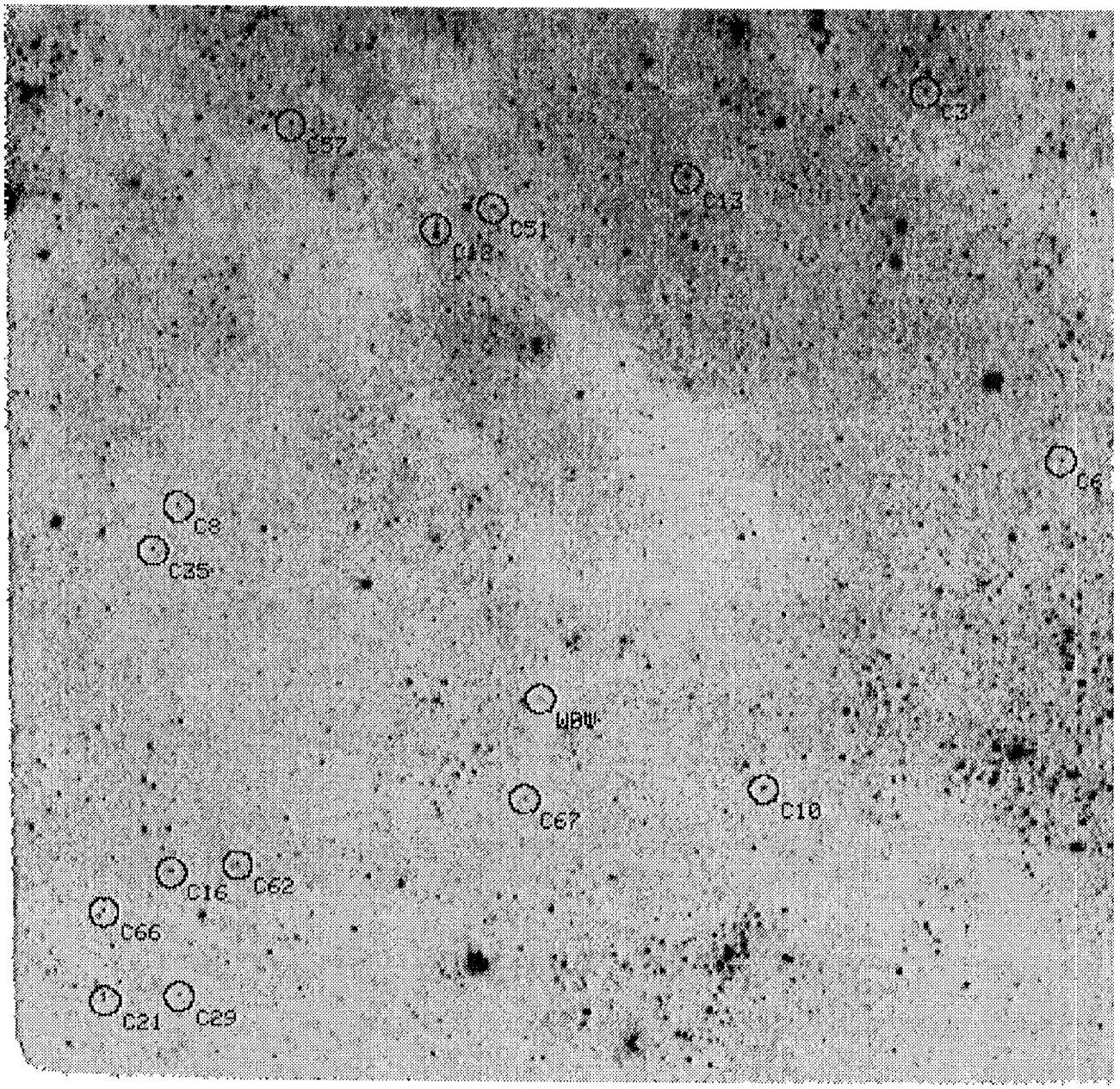

Figure 7a.- V-band image of the PC1 chip. The circles indicate the position of each of the newly identified Cepheids, labeled as in Table 2.

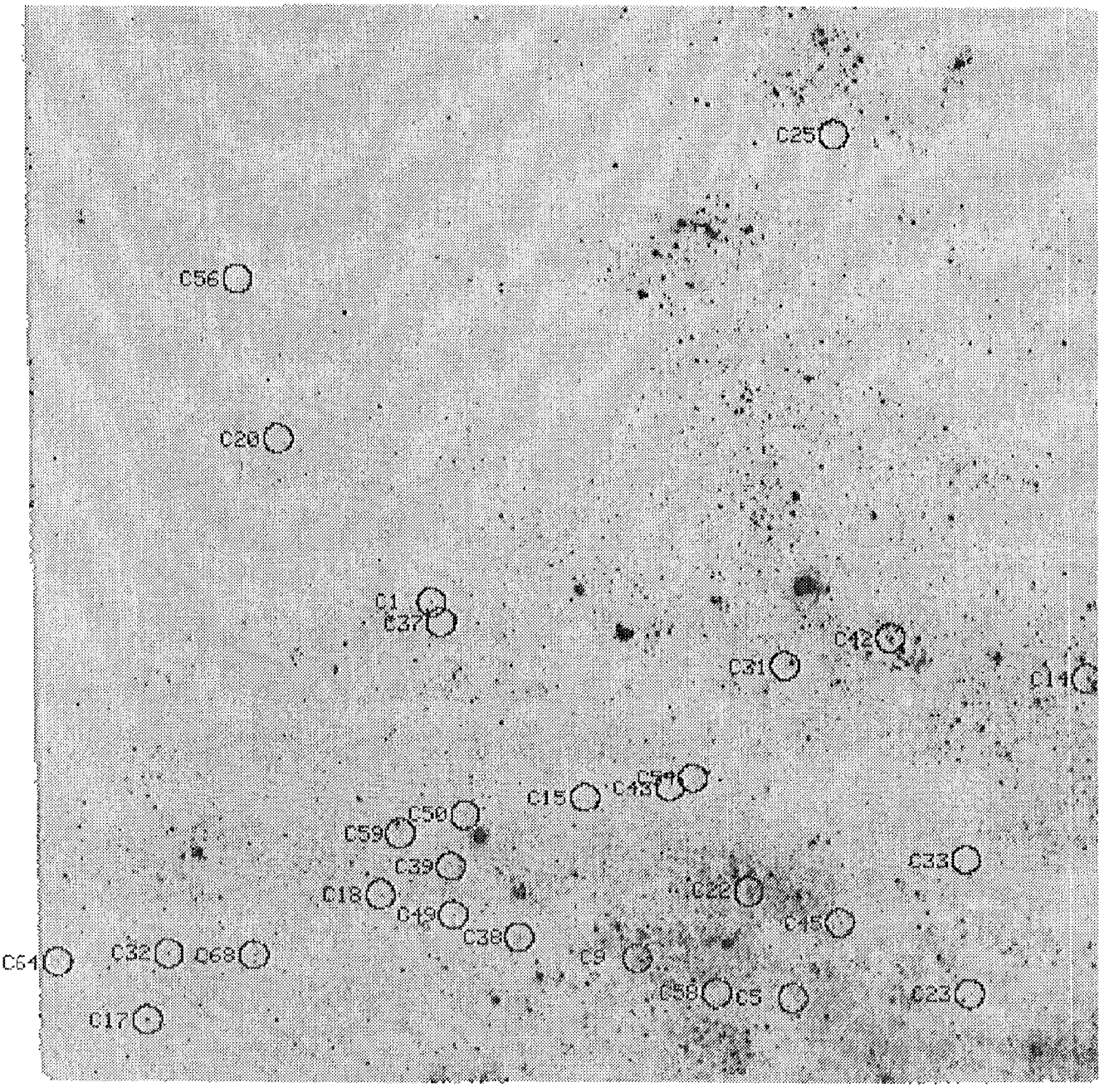

Figure 7b.- V-band image of the WF2 chip. The circles indicate the position of each of the newly identified Cepheids, labeled as in Table 2.

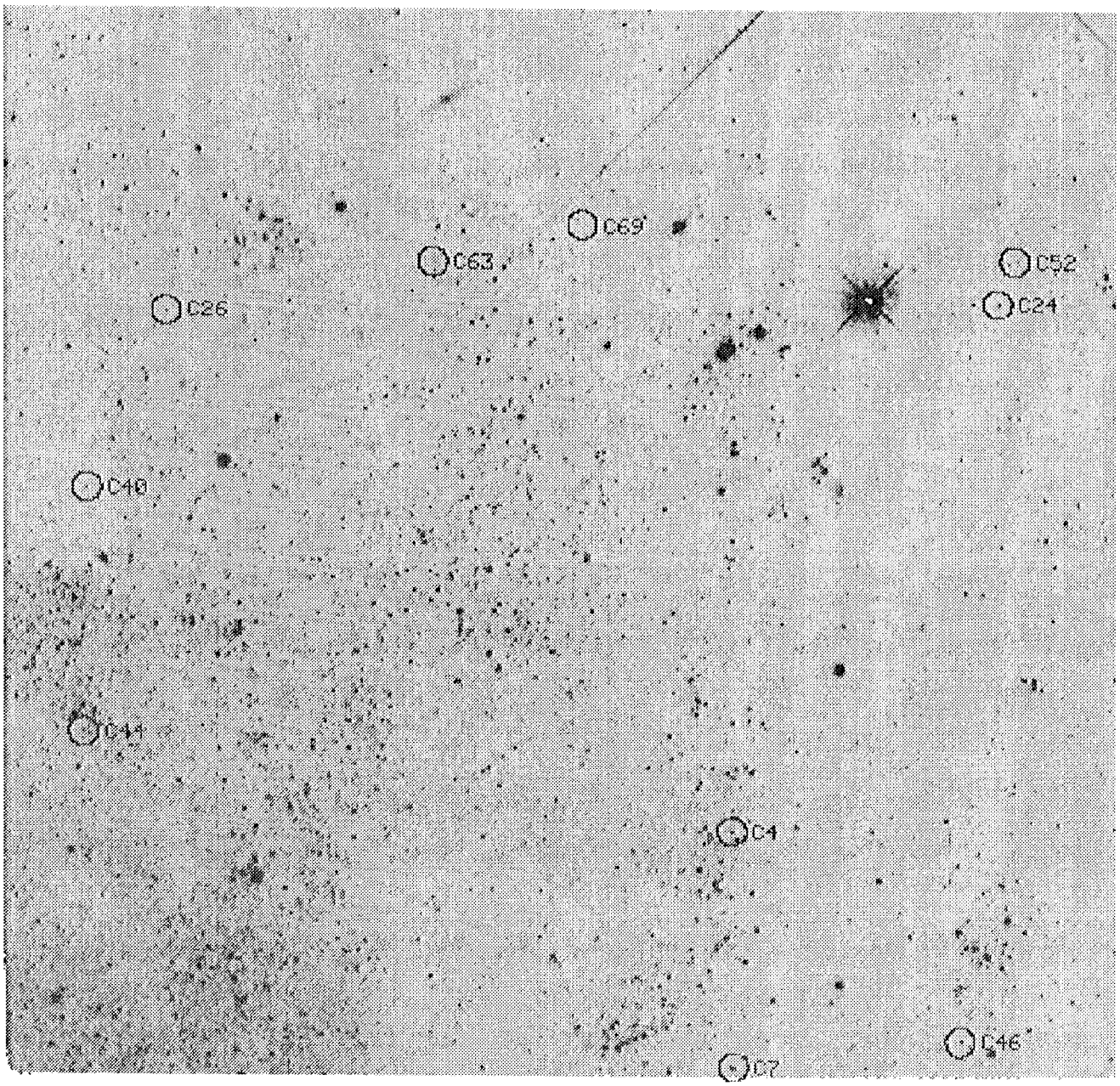

Figure 7c.- V-band image of the WF3 chip. The circles indicate the position of each of the newly identified Cepheids, labeled as in Table 2.

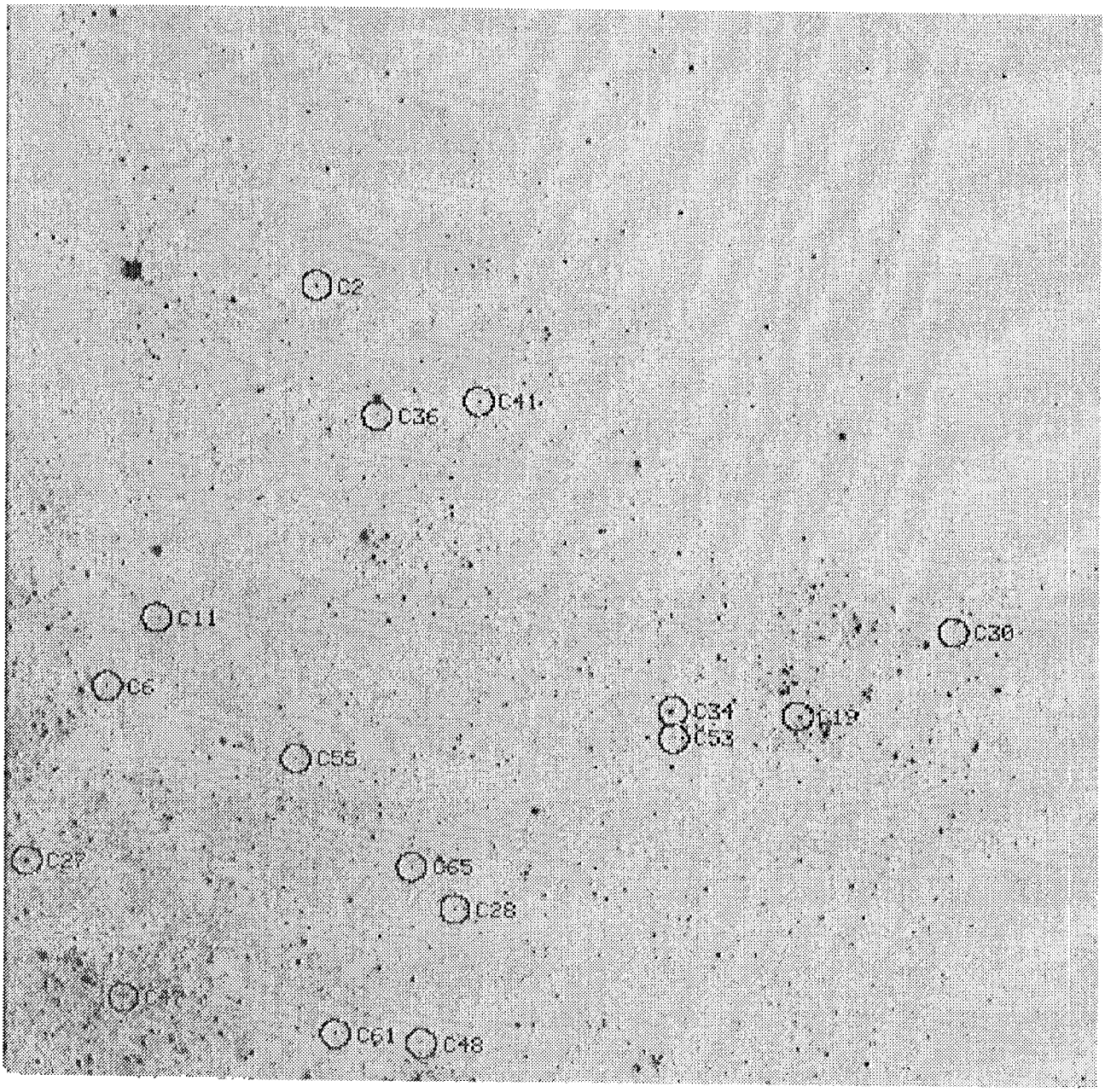

Figure 7d. V-band image of the WF4 chip. The circles indicate the position of each of the newly identified Cepheids, labeled as in Table 2

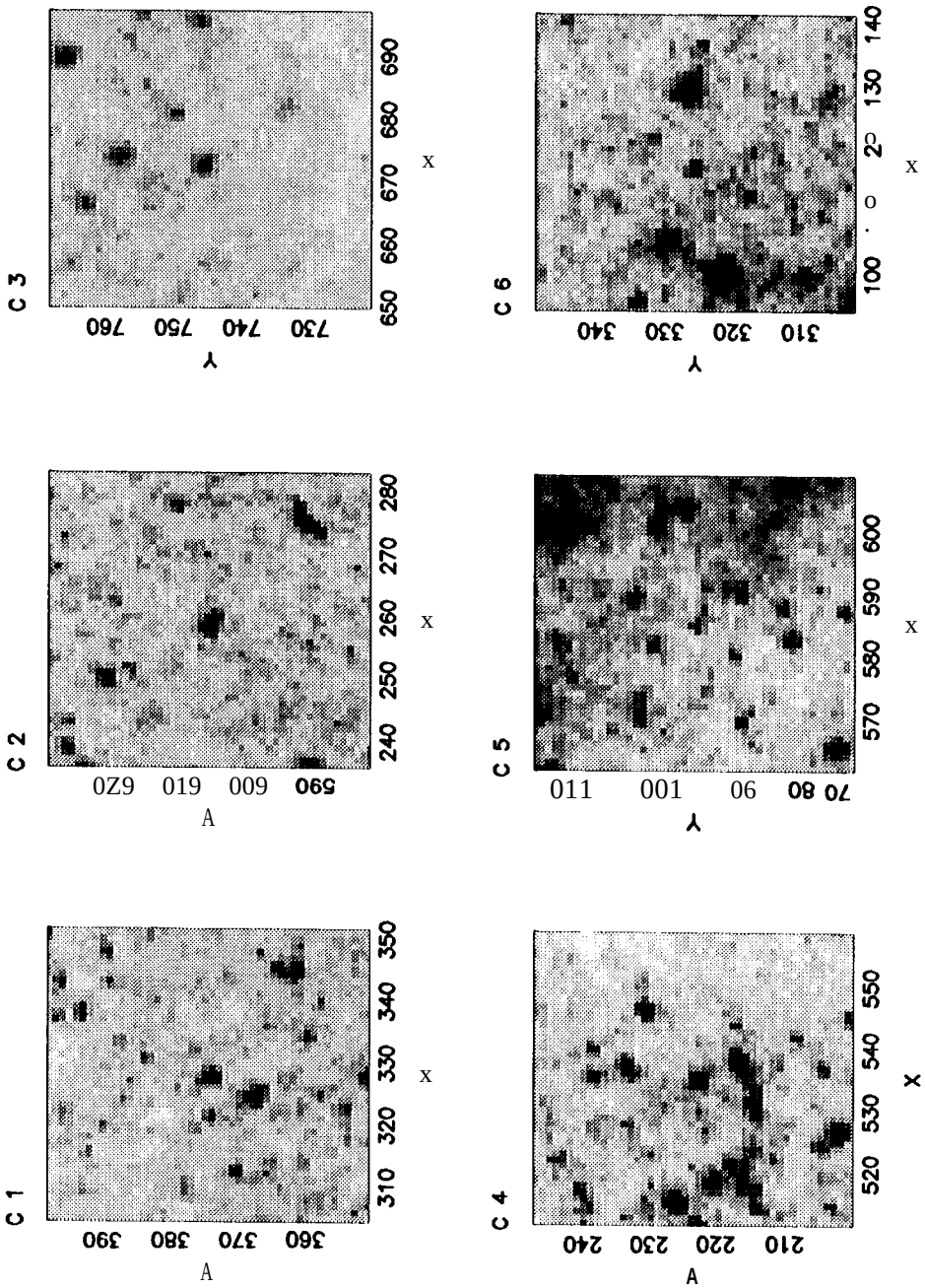

Figure 8a.- Finding charts for Cepheids C01 - C06

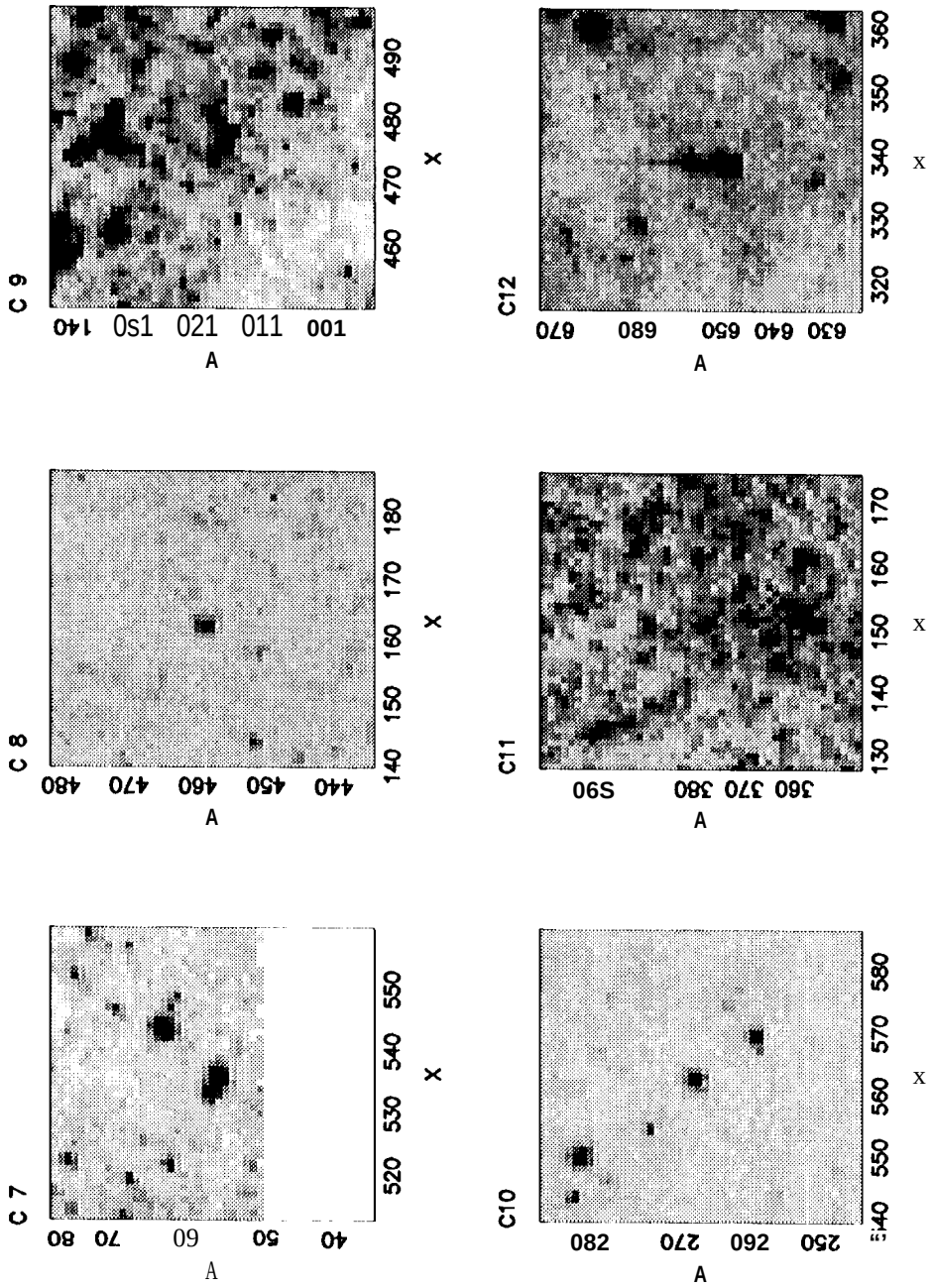

Figure 8b.- Finding charts for Cepheids C07 - C12

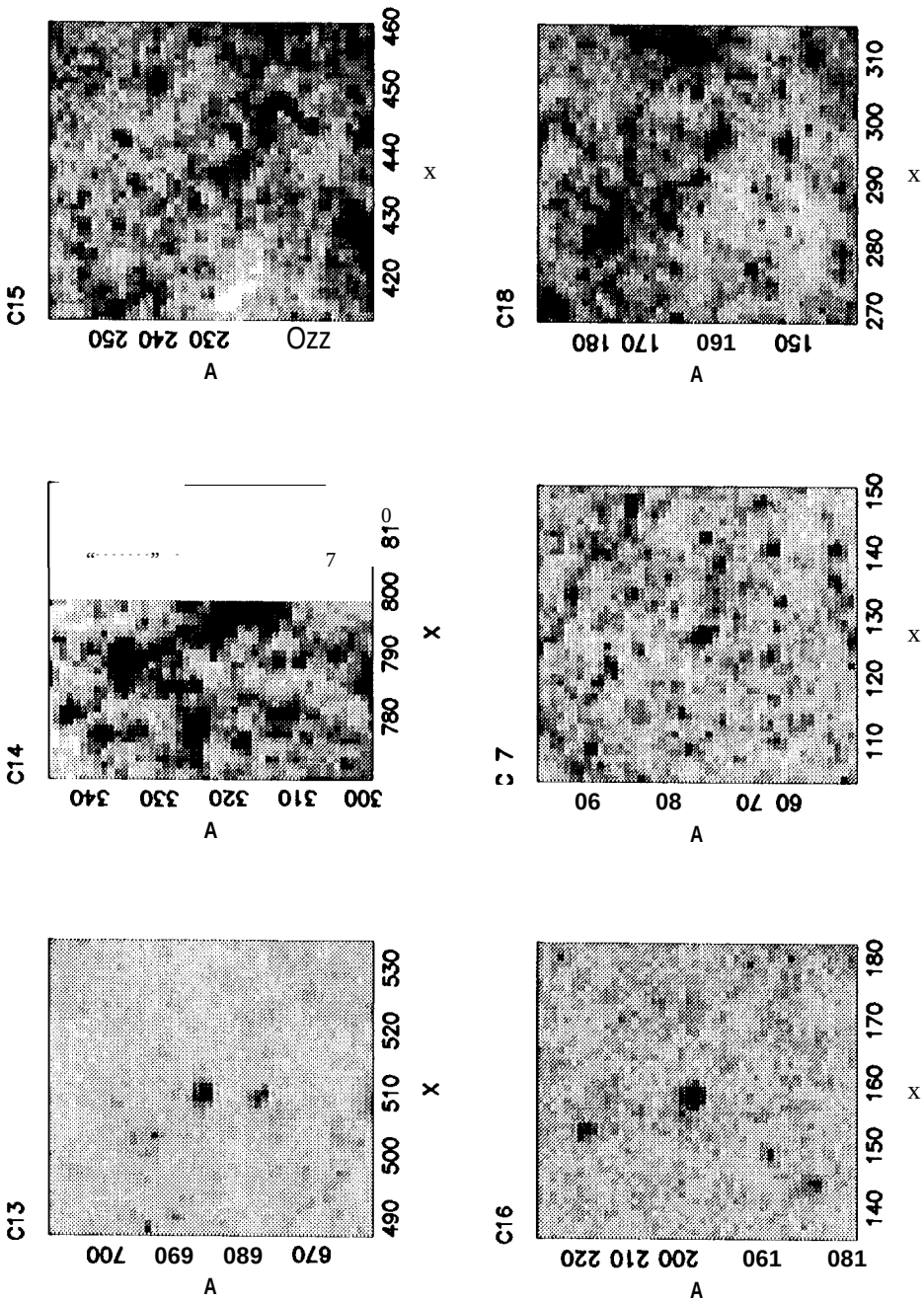

Figure 8c.- Finding charts for Cepheids C13 - C18

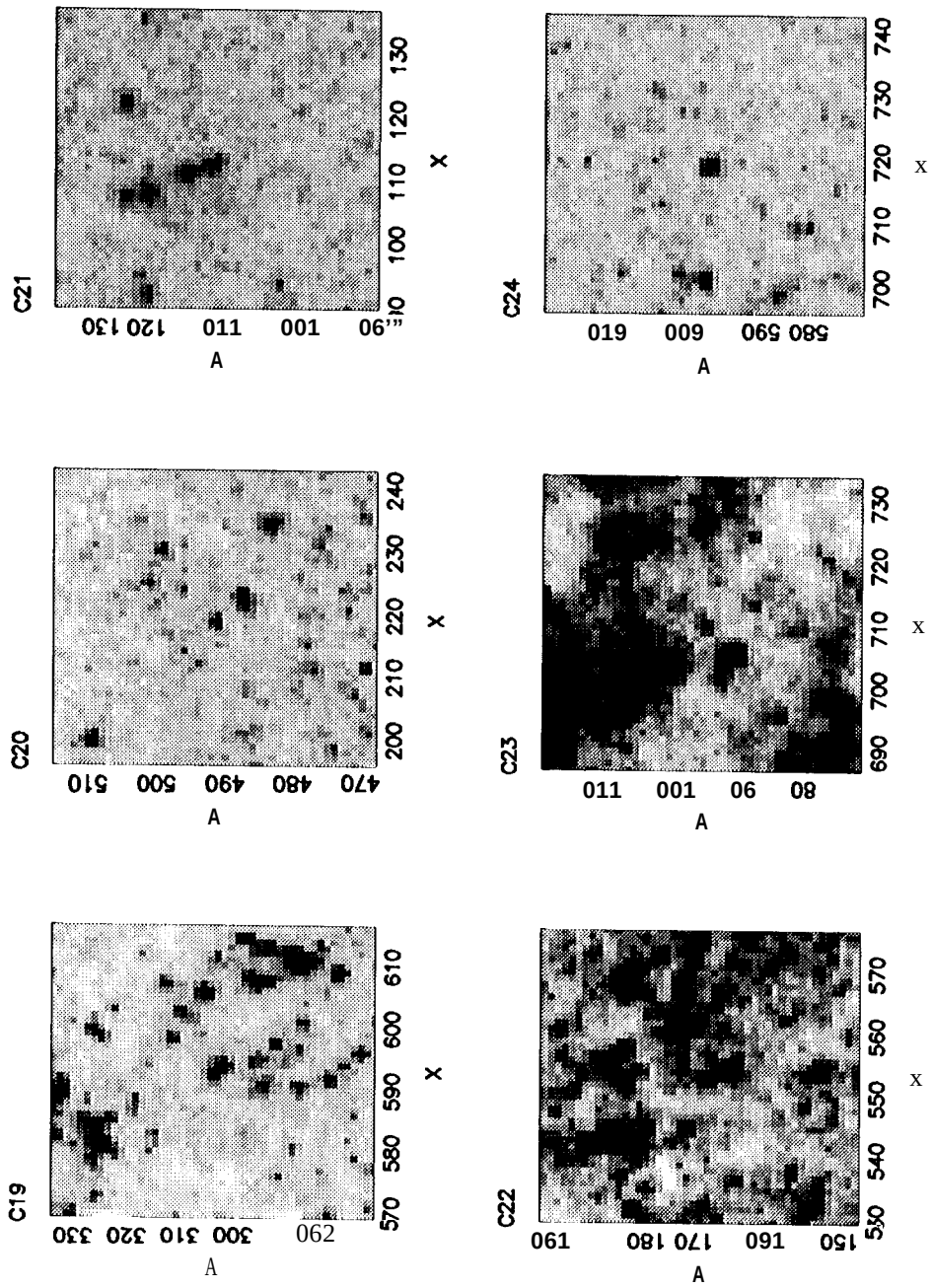

Figure 8d.- Finding charts for Cepheids C19 - C24

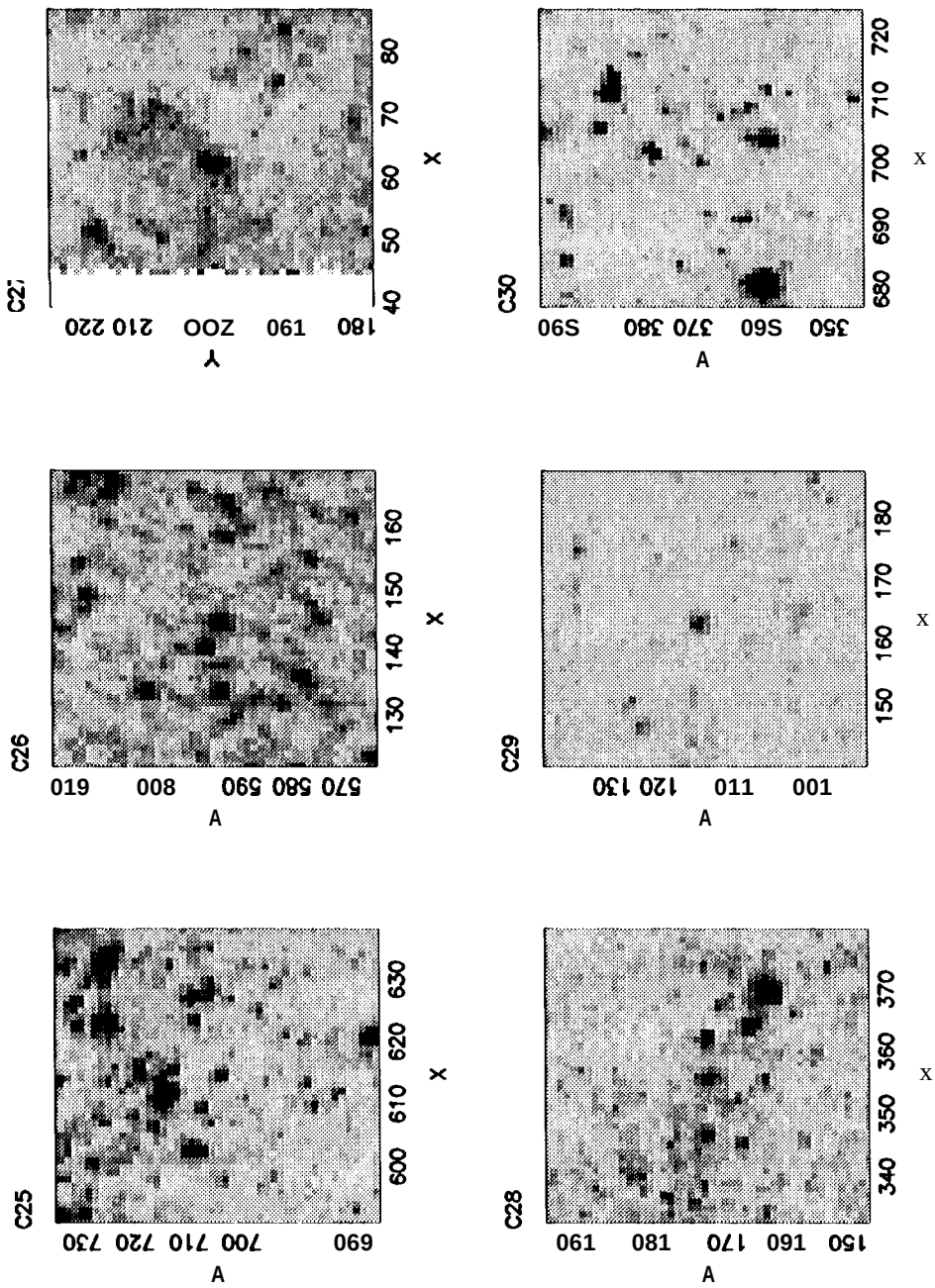

Figure 8c.- Finding charts for Cepheids C25 - C30

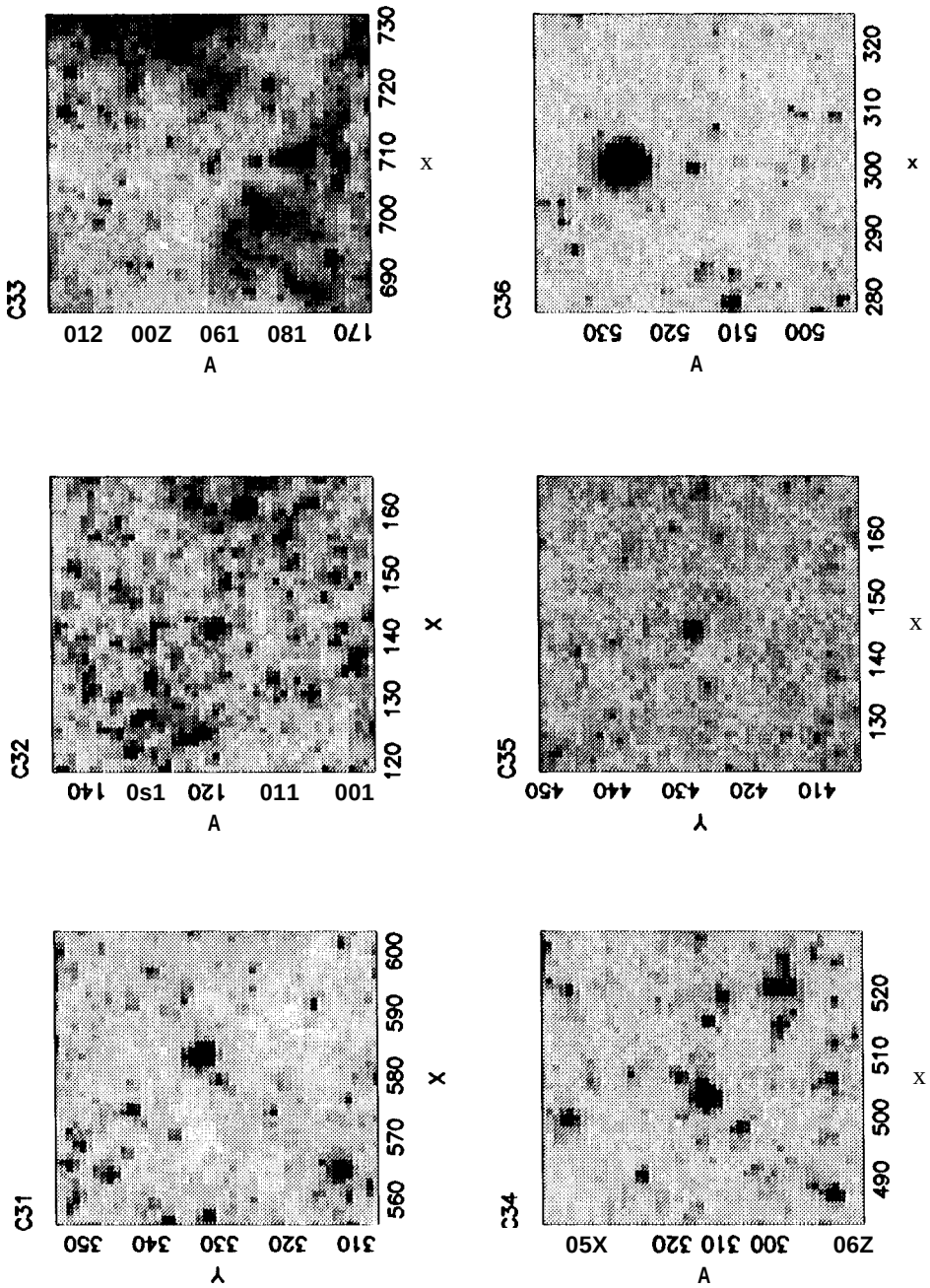

Figure 8f.- Finding charts for Cepheids C31 - C36

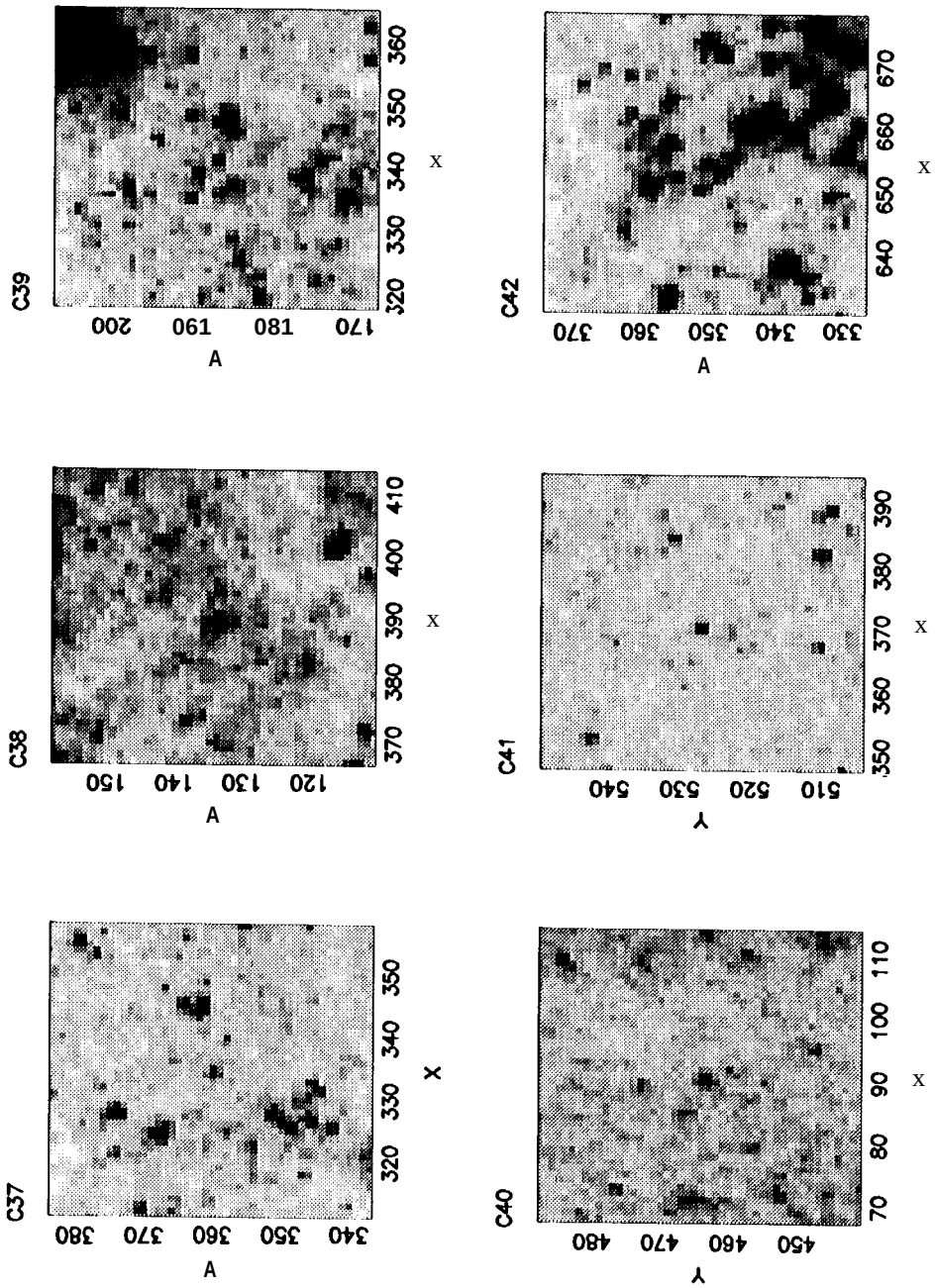

Figure 8g.- Finding charts for Cepheids C37 - C42

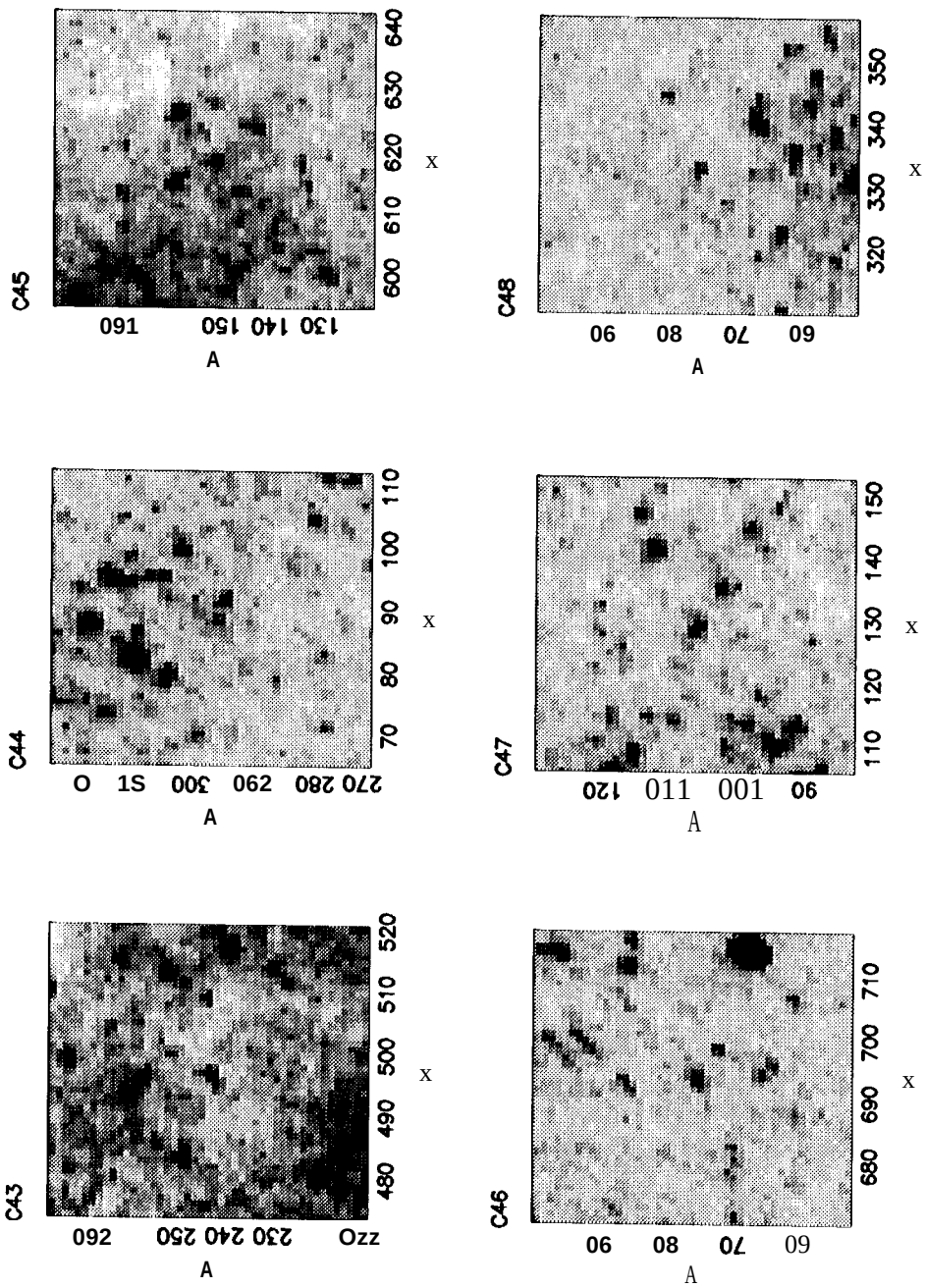

Figure 8h.- Finding charts for Cepheids C43 - C48

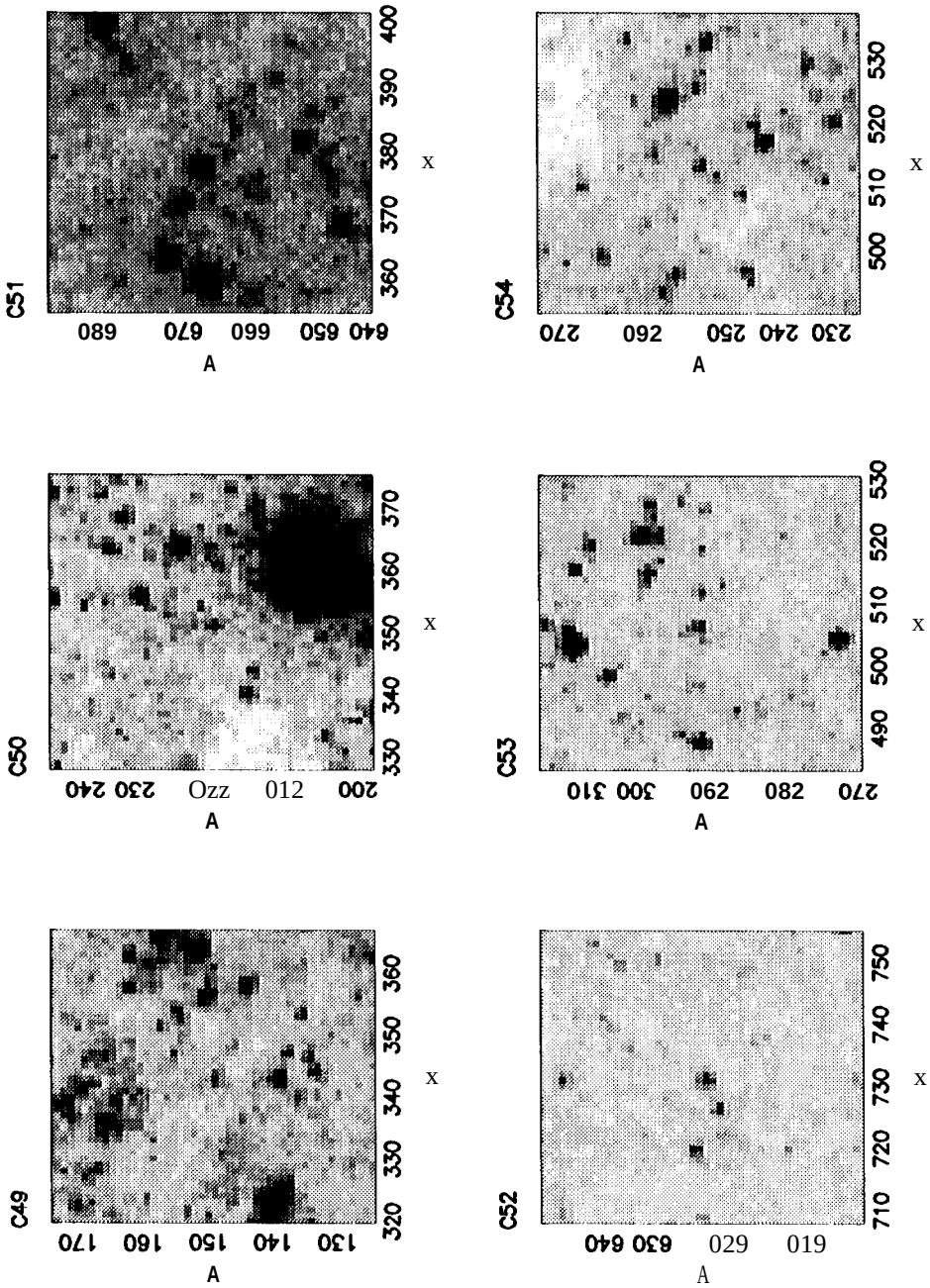

Figure 8i.- Finding charts for Cepheids C49 - C56

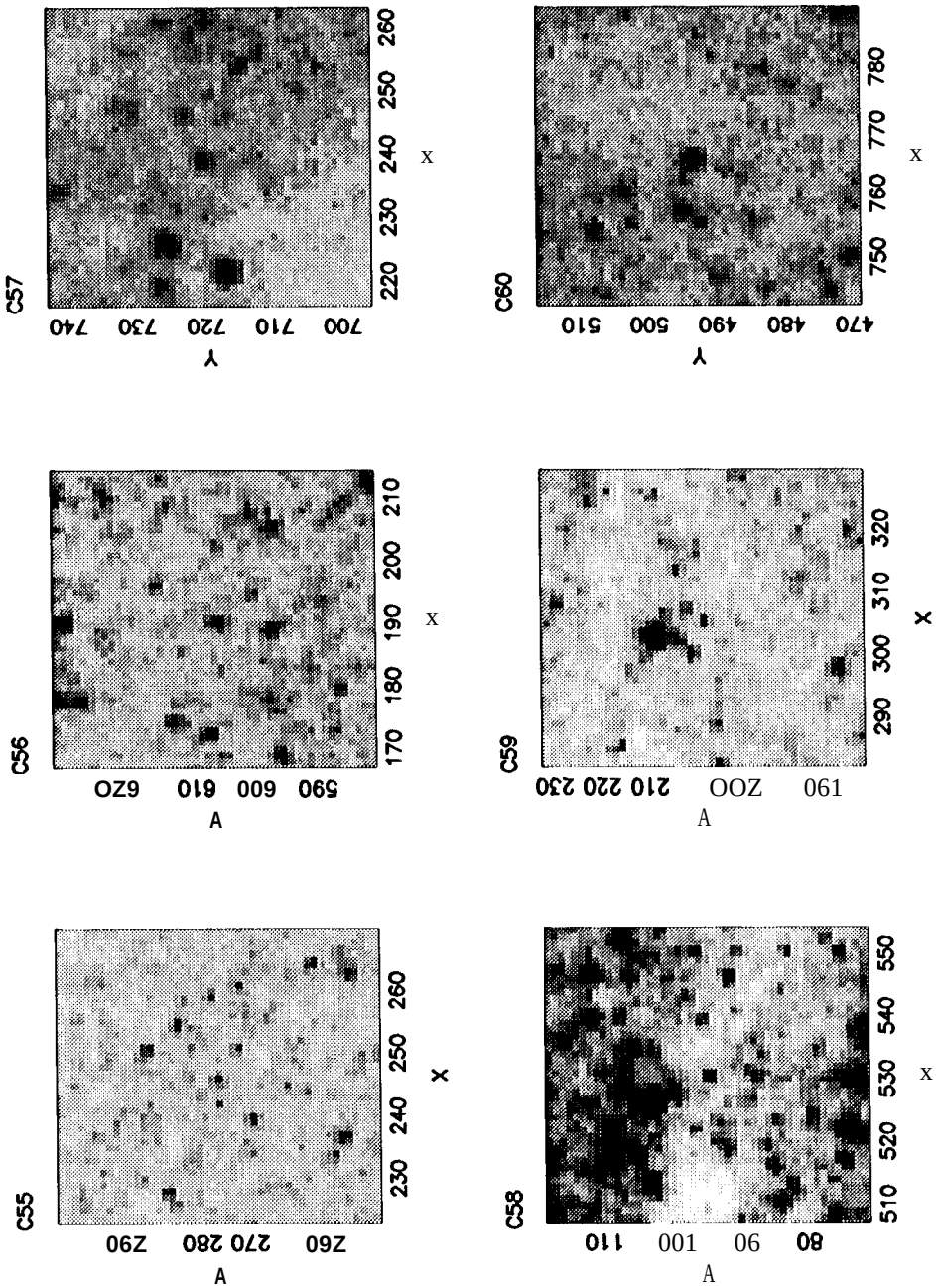

Figure 8j.- Finding charts for Cepheids C57 - C60

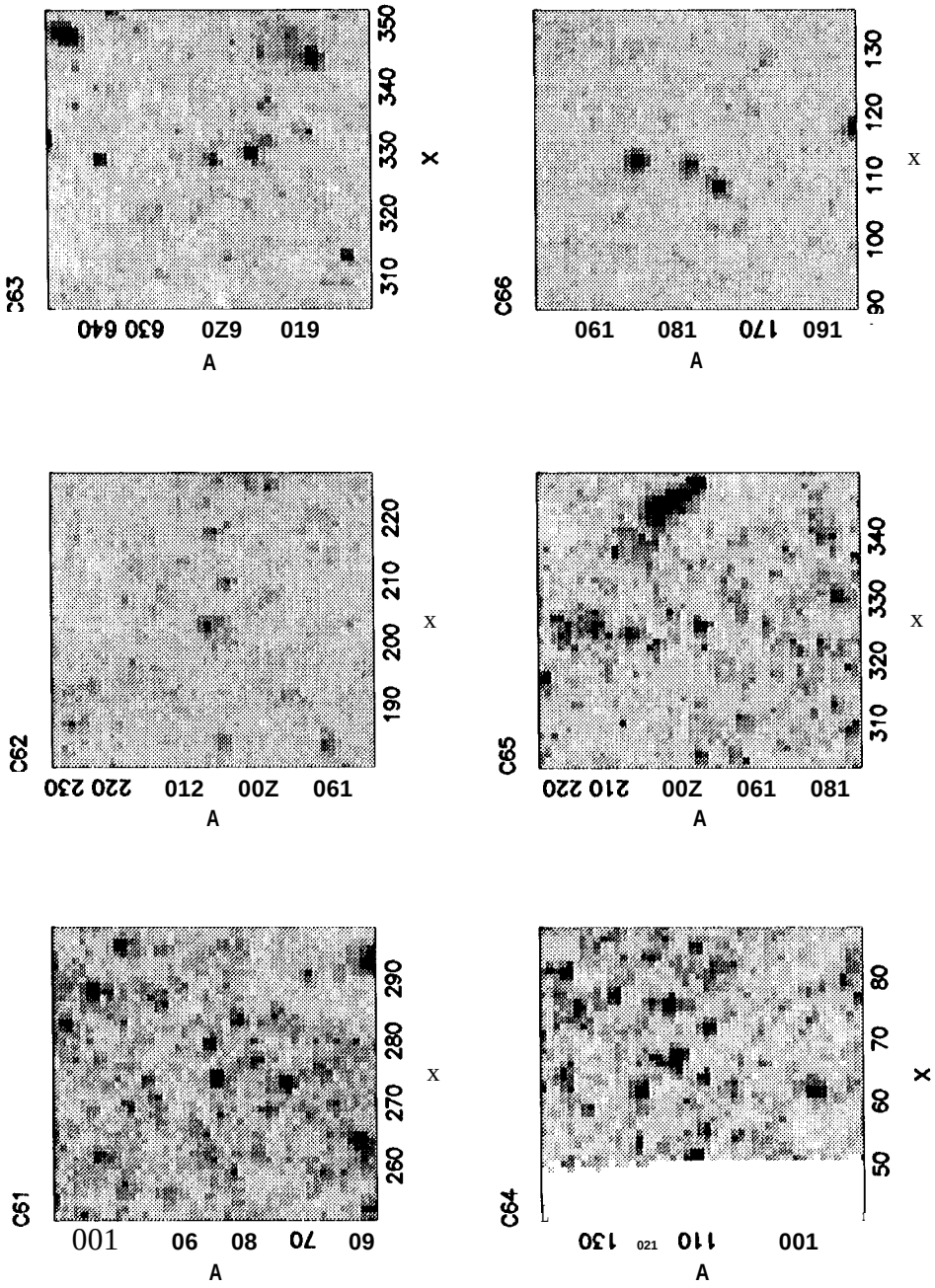

Figure 8k.- Finding charts for Cepheids C61 - C66

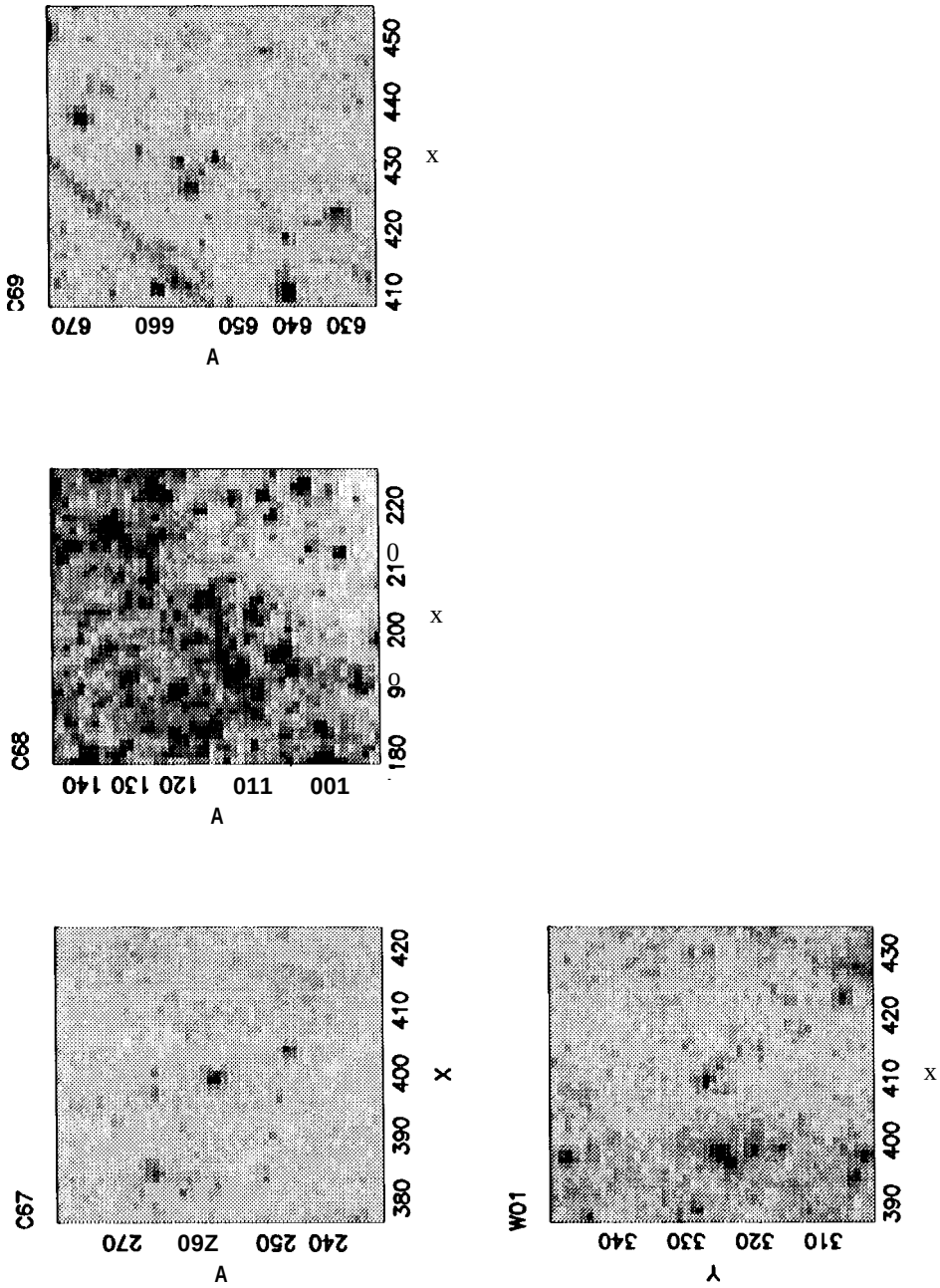

Figure 8l.- Finding charts for Cepheids C67 - C69 and W01

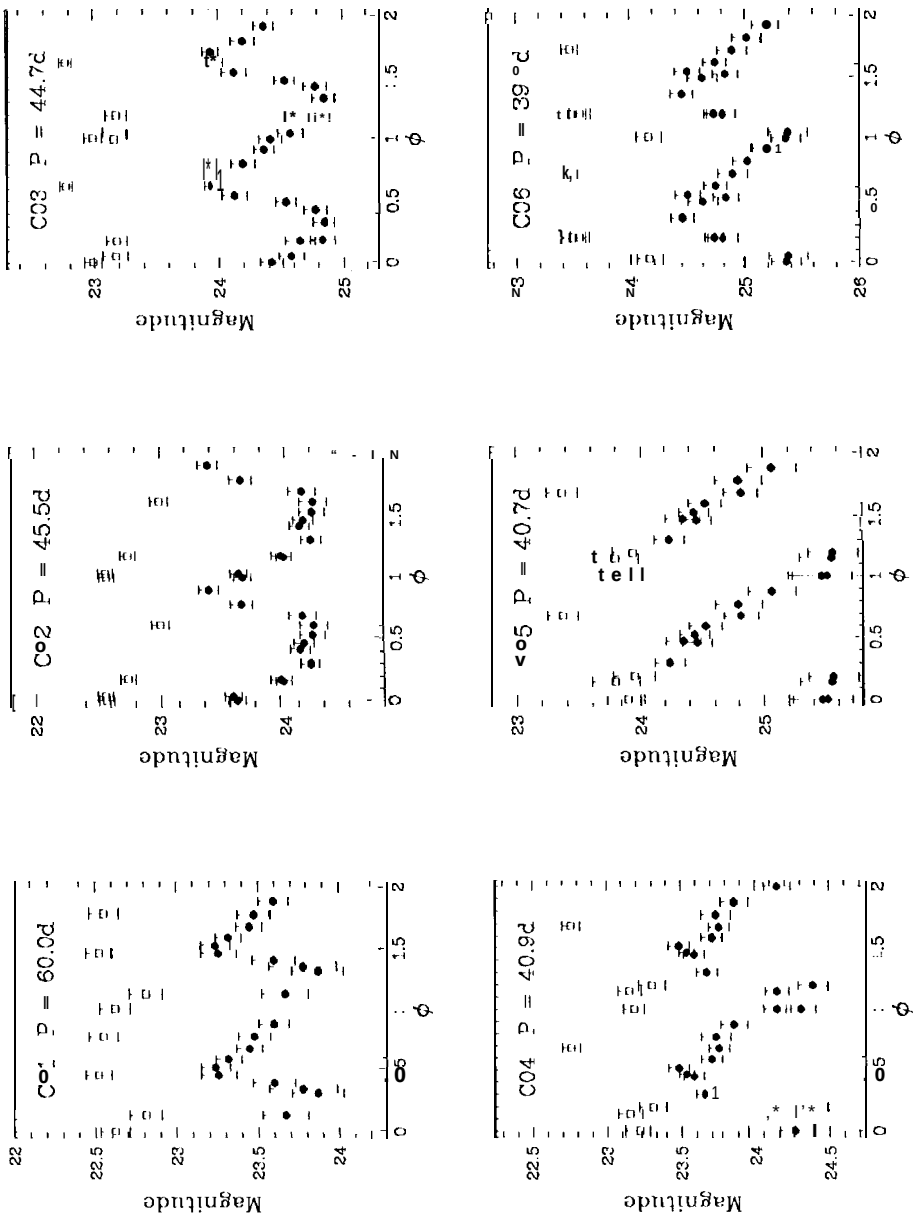

Figure 9a.- Light curves for Cepheids C01 - C06. Filled and open symbols indicate V- and I-band photometry, respectively

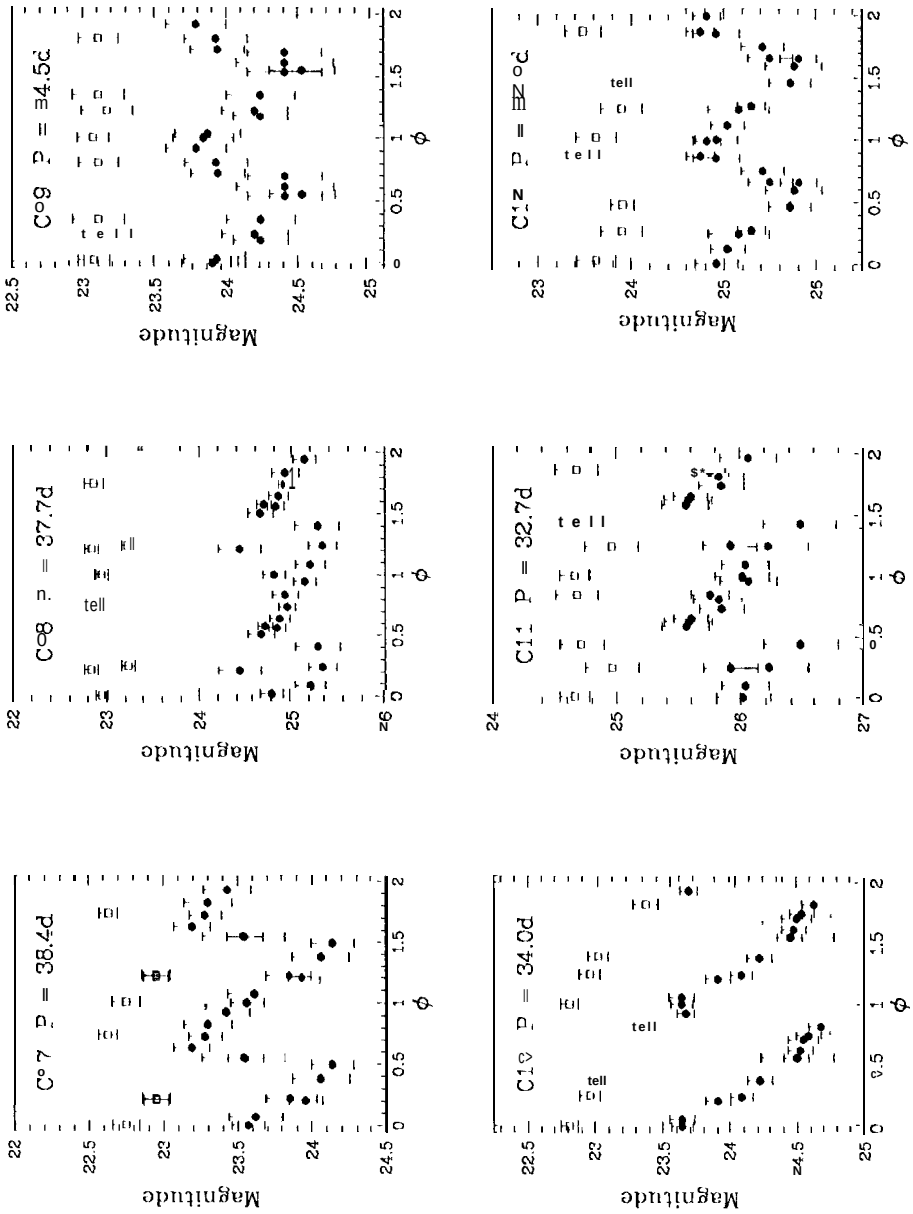

Figure 9b.- Light curves for Cepheids C07 - C12. Filled and open symbols indicate V- and I-band photometry, respectively.

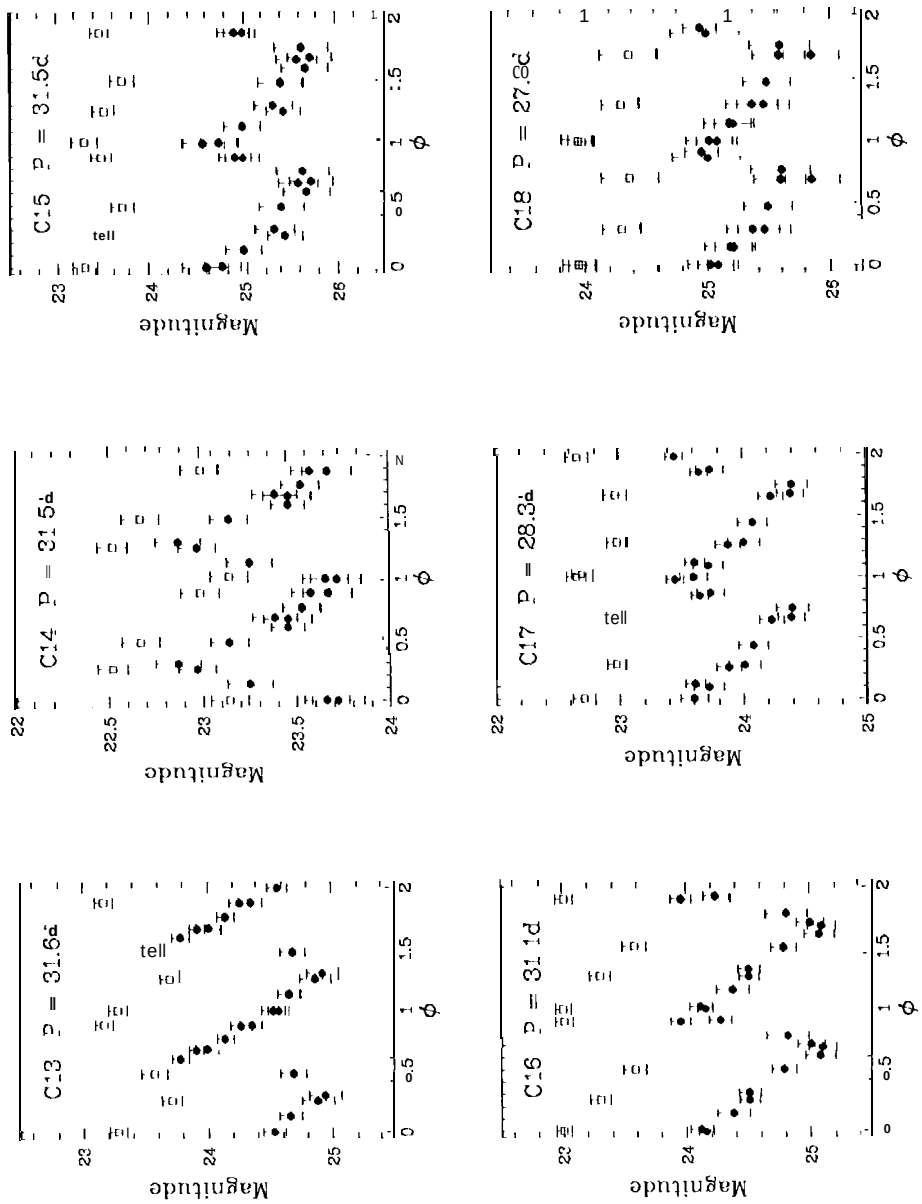

Figure 9c. - Light curves for Cepheids C13 - C18. Filled and open symbols indicate V- and I-band photometry, respectively.

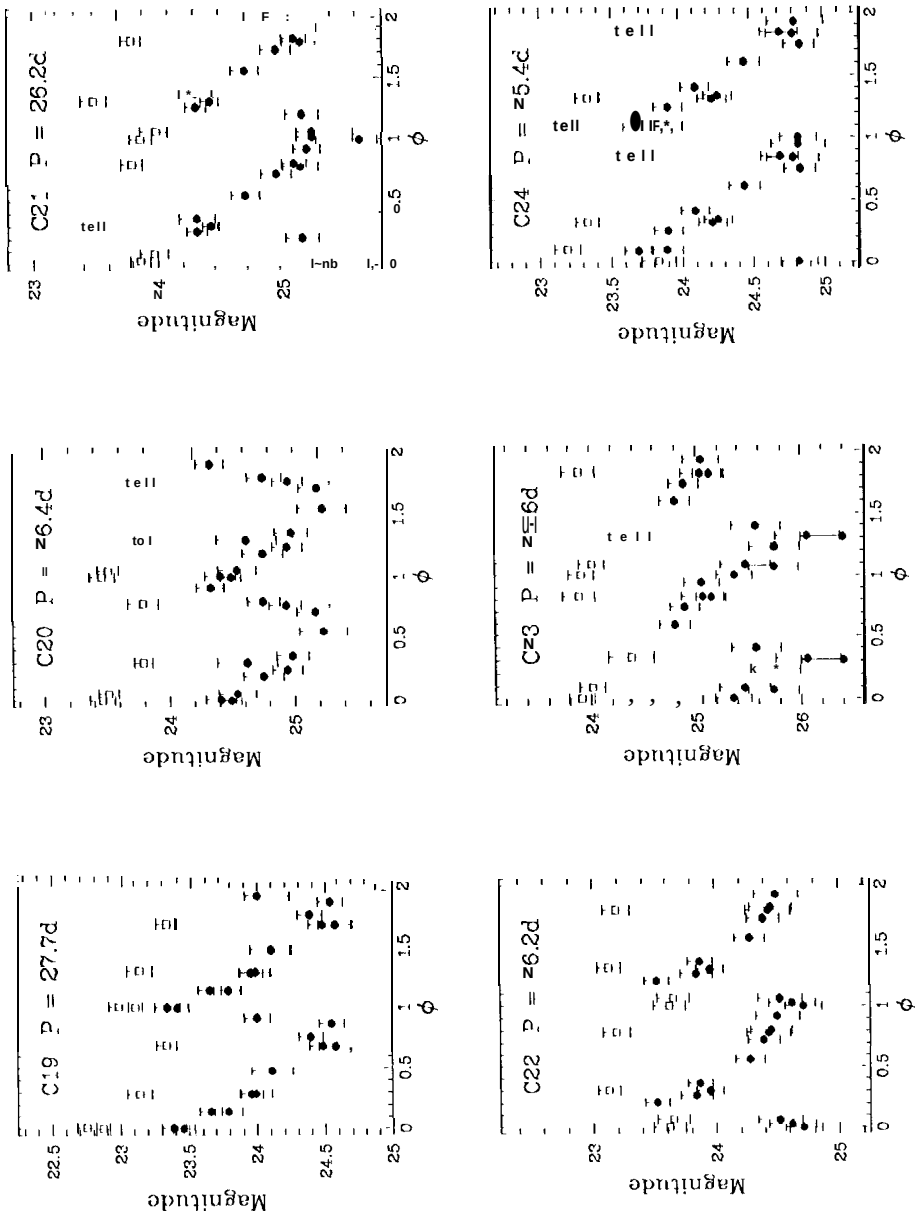

Figure 9(1.- Light curves for Cepheids C19 - C24. Filled and open symbols indicate V- and I-band photometry, respectively.

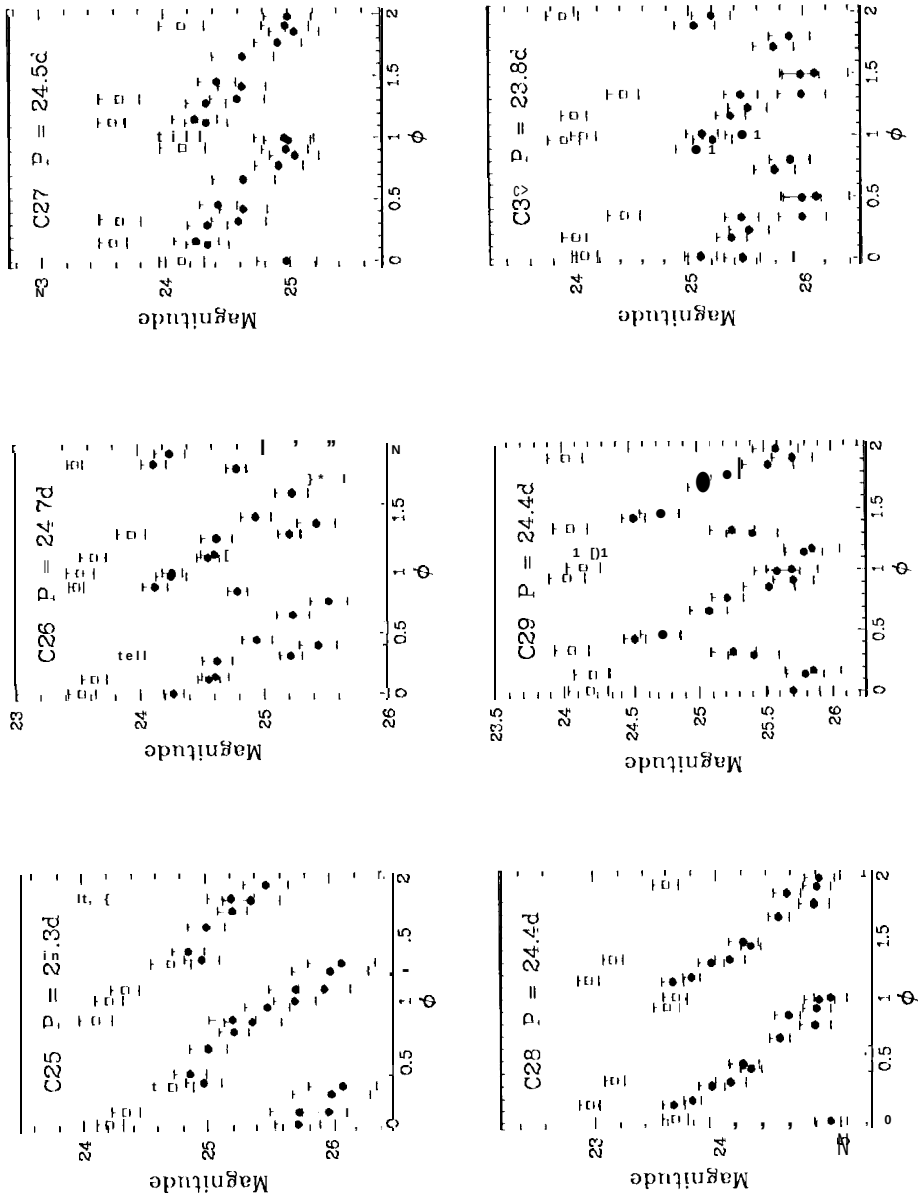

Figure 9c.- Light curves for Cepheids C25 - C30. Filled and open symbols indicate V- and I-band photometry, respectively.

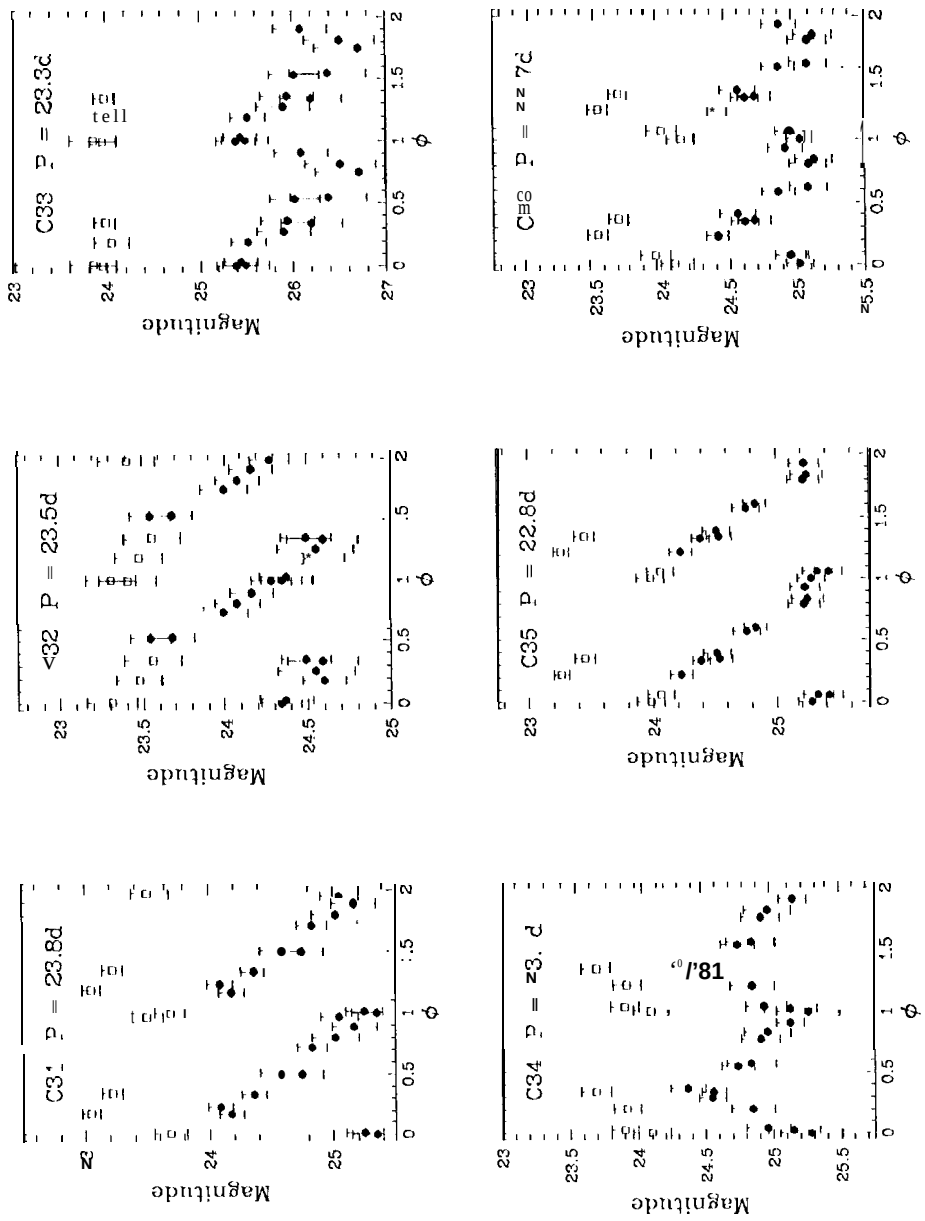

Figure 9f.- Light curves for Cepheids C31 - C36. Filled and open symbols indicate V- and I-band photometry, respectively.

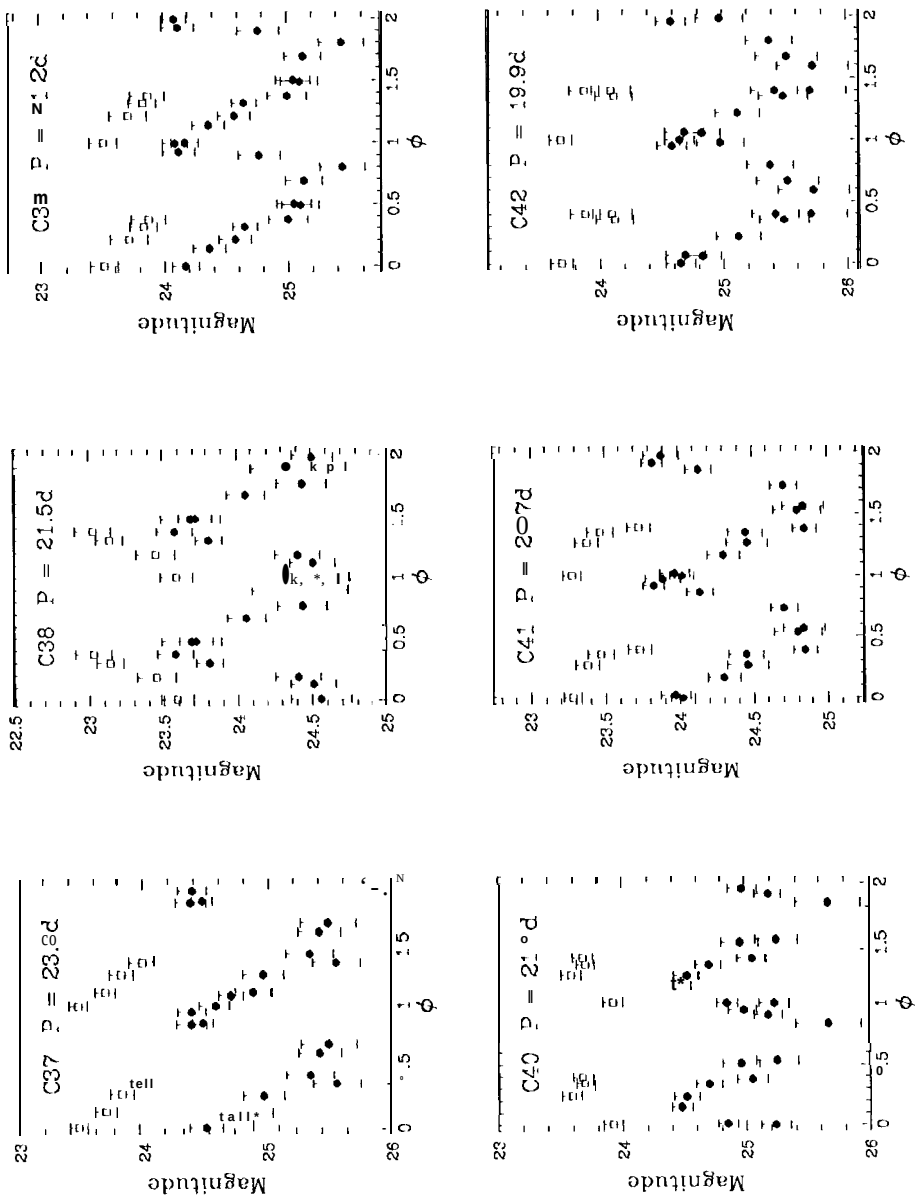

Figure 9g.- Light curves for Cepheids C37 - C42. Filled and open symbols indicate V- and I-band photometry, respectively.

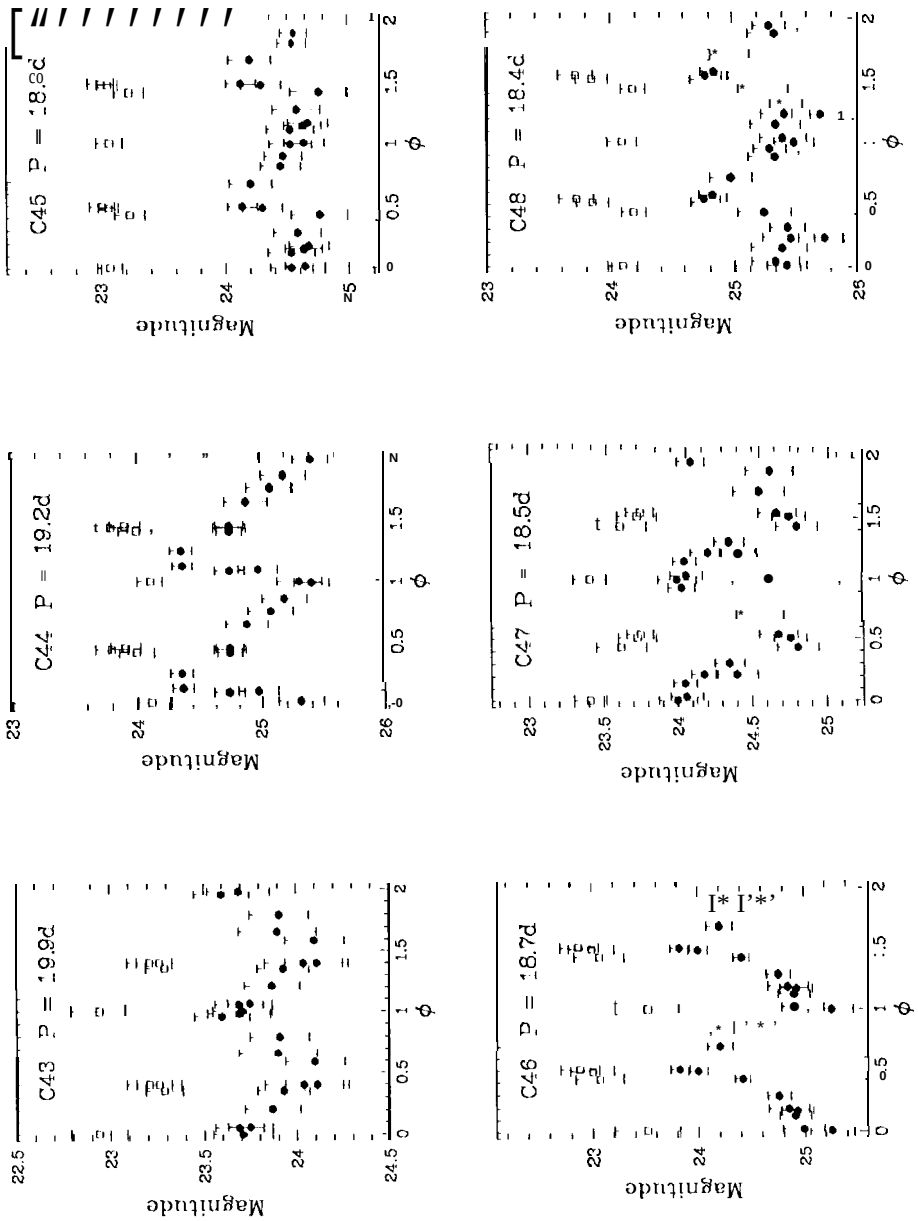

Figure 9h.- Light curves for Cepheids C43 - C48. Filled and open symbols indicate V- and I-band photometry, respectively.

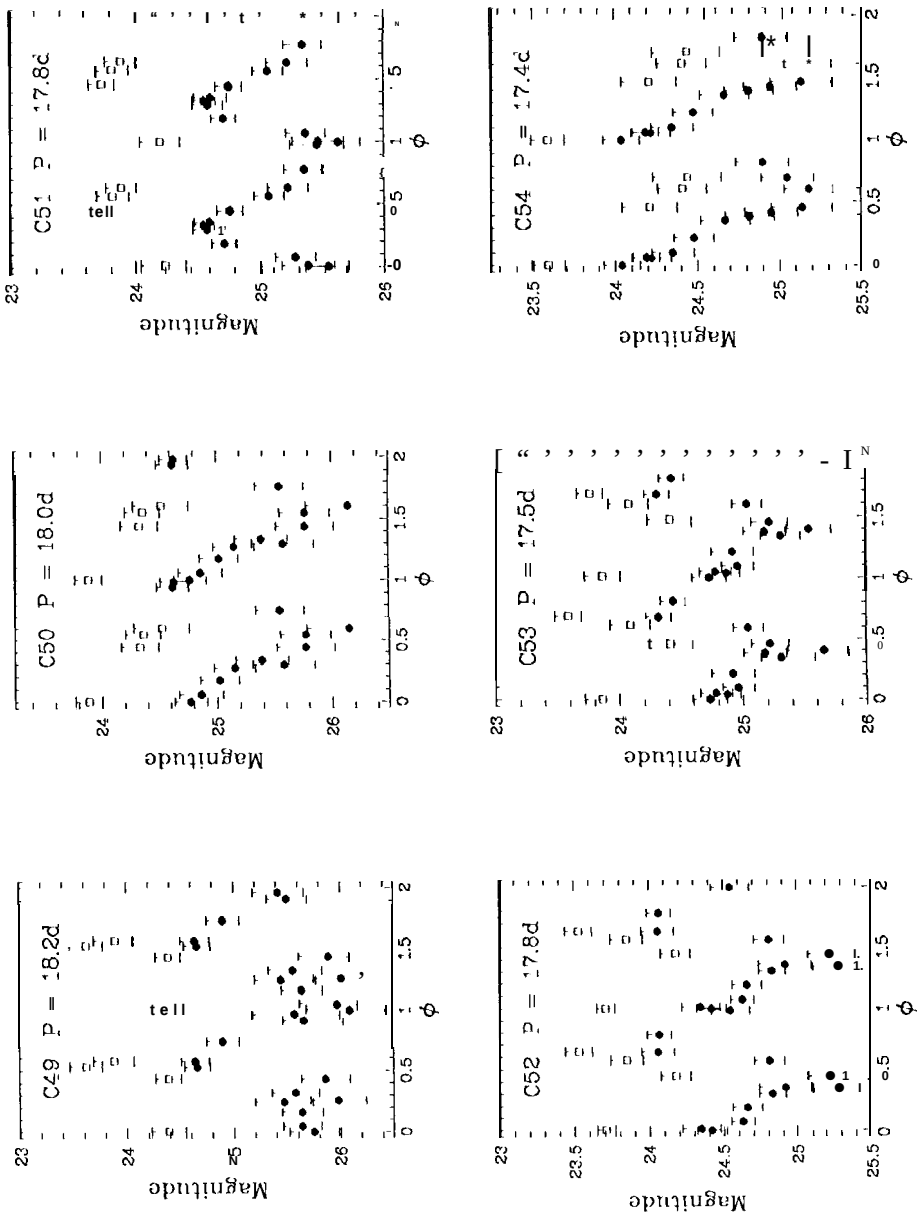

Figure 9i.- Light curves for Cepheids C49 - C56. Filled and open symbols indicate V- and I-band photometry, respectively.

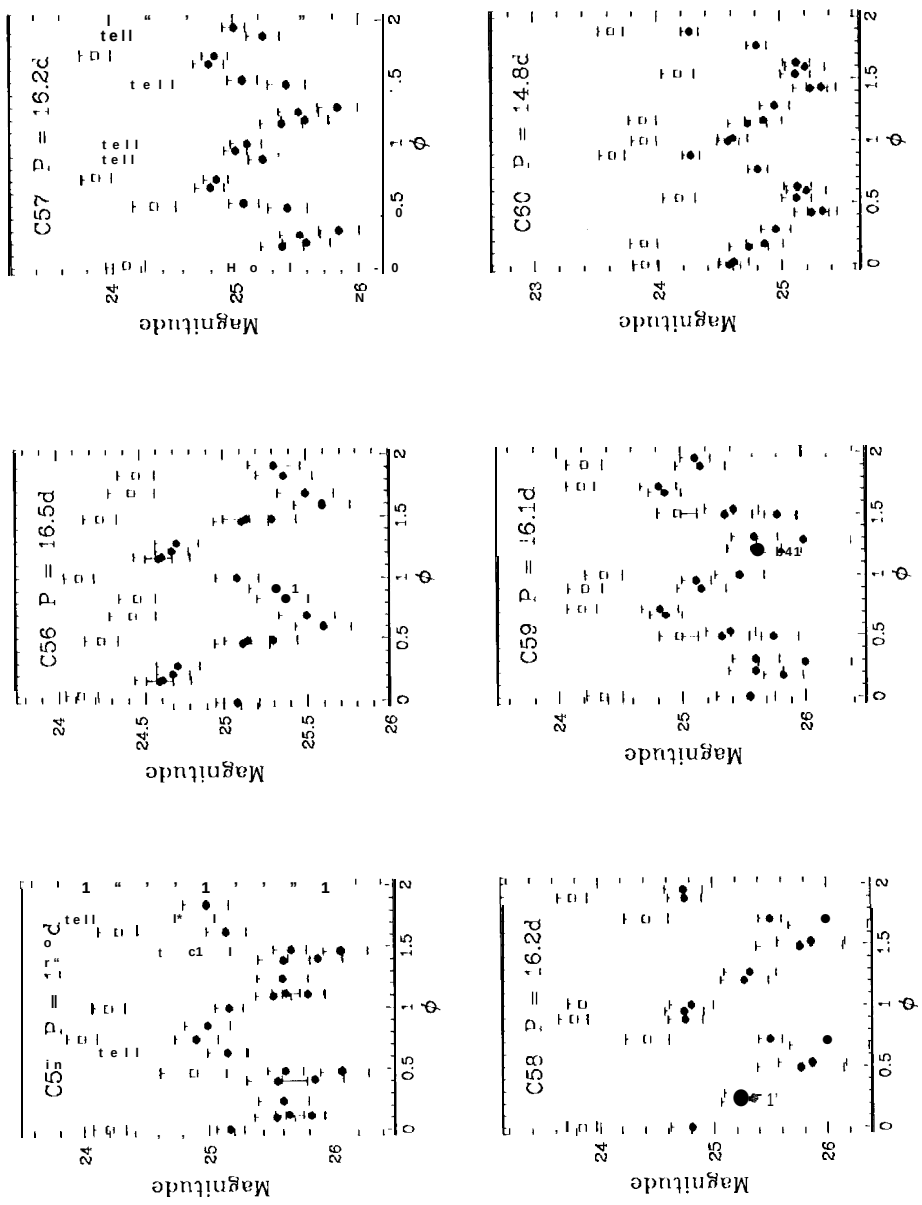

Figure 9j.- Light curves for Cepheids C57 - C60. Filled and open symbols indicate V- and I-band photometry, respectively.

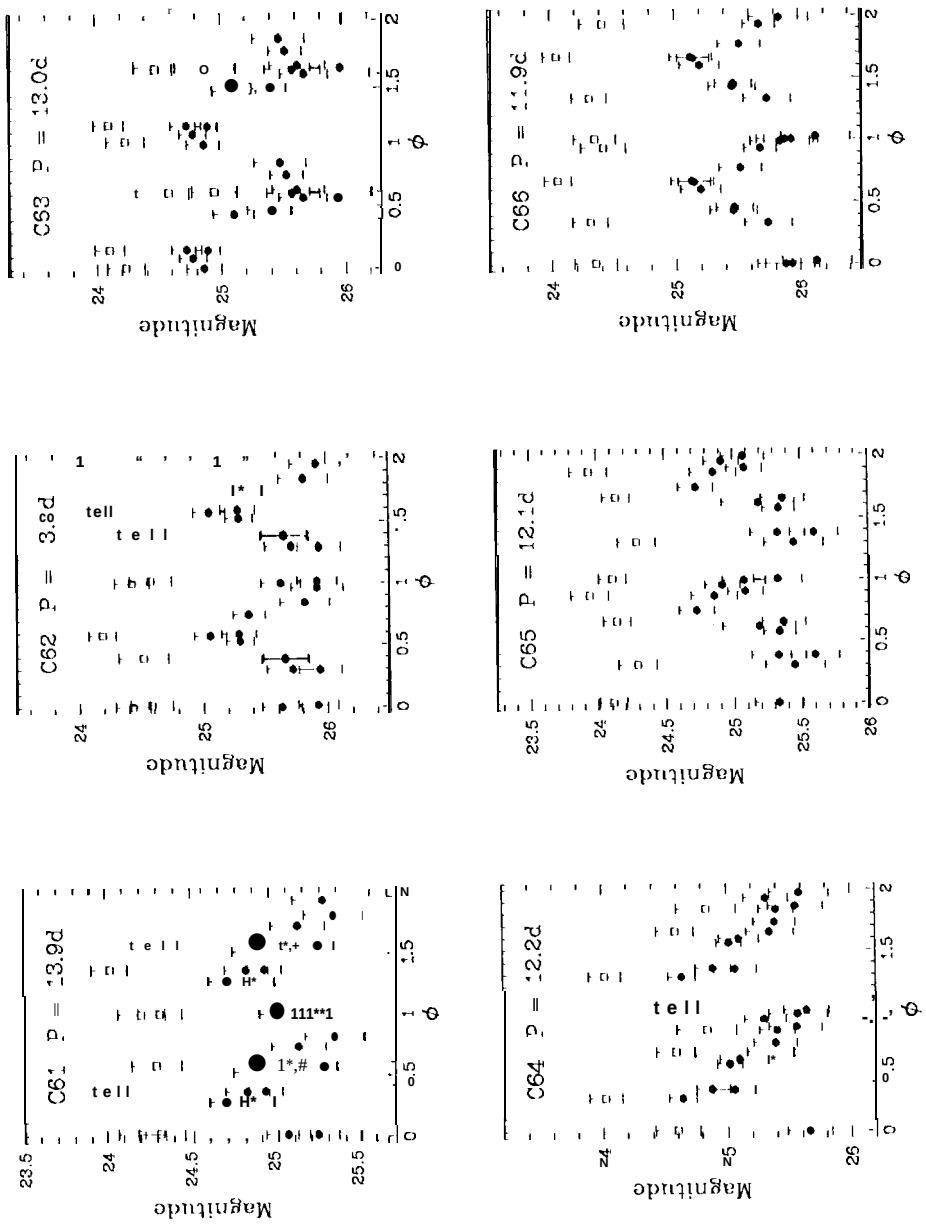

Figure 9k.- Light curves for Cepheids C61 - C66. Filled and open symbols indicate V- and I-band photometry, respectively.

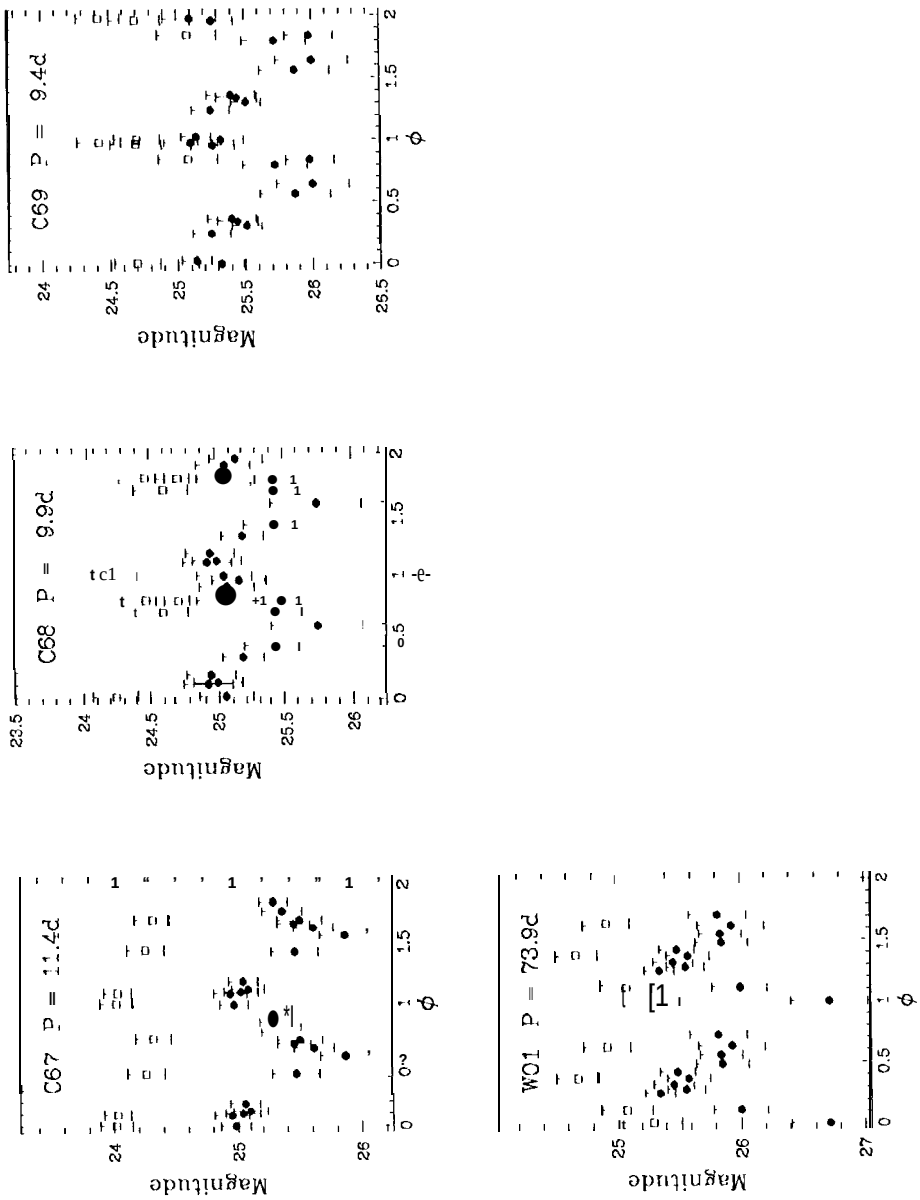

Figure 9l.- Light curves for Cepheids C67 - C69 and W01. Filled and open symbols indicate V- and I-band photometry, respectively.

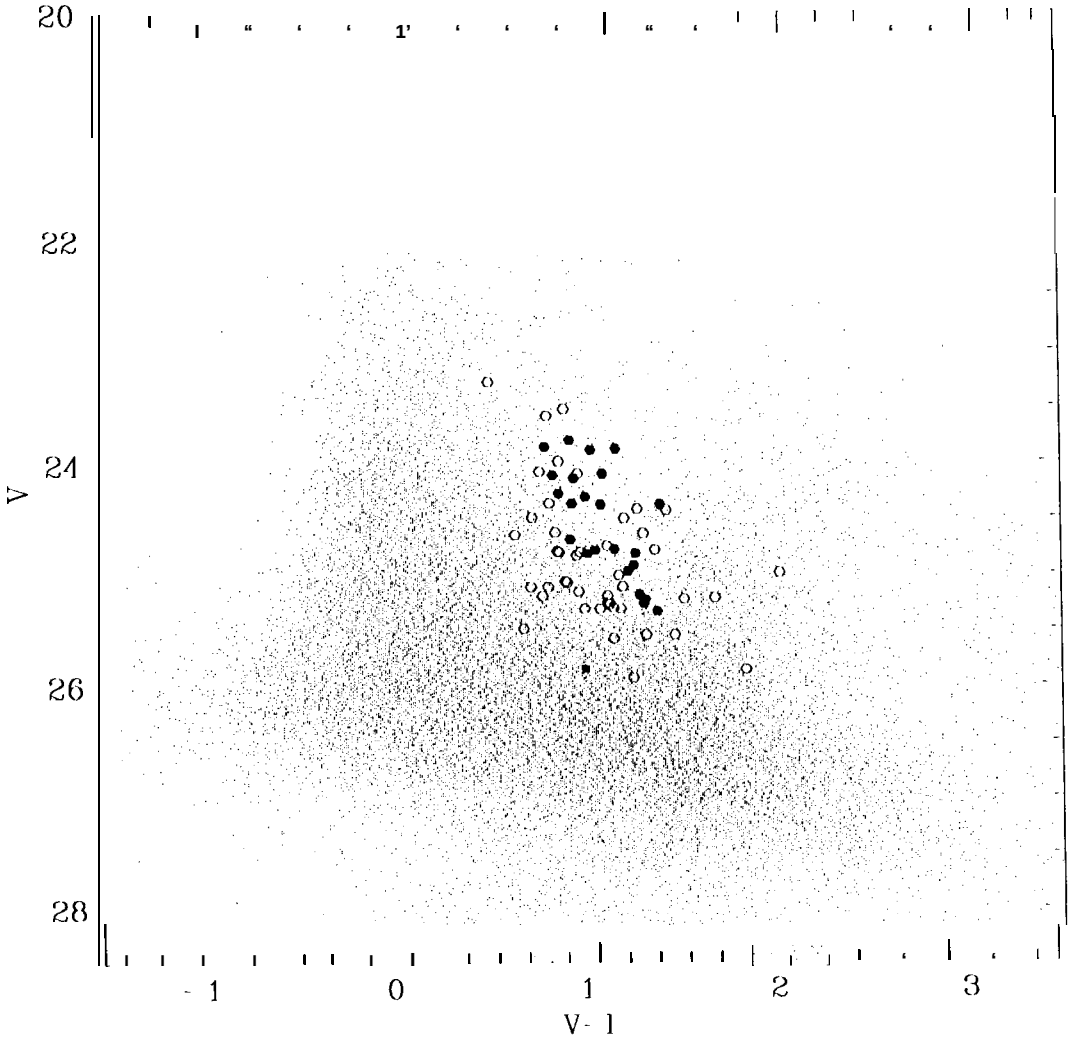

Figure 10.- Color-magnitude diagram of stars in NGC 3621. Cepheids which were used to construct the period-luminosity relations are plotted as filled circles, while the other ones are plotted as open circles. The Population II Cepheid is plotted as a filled square.

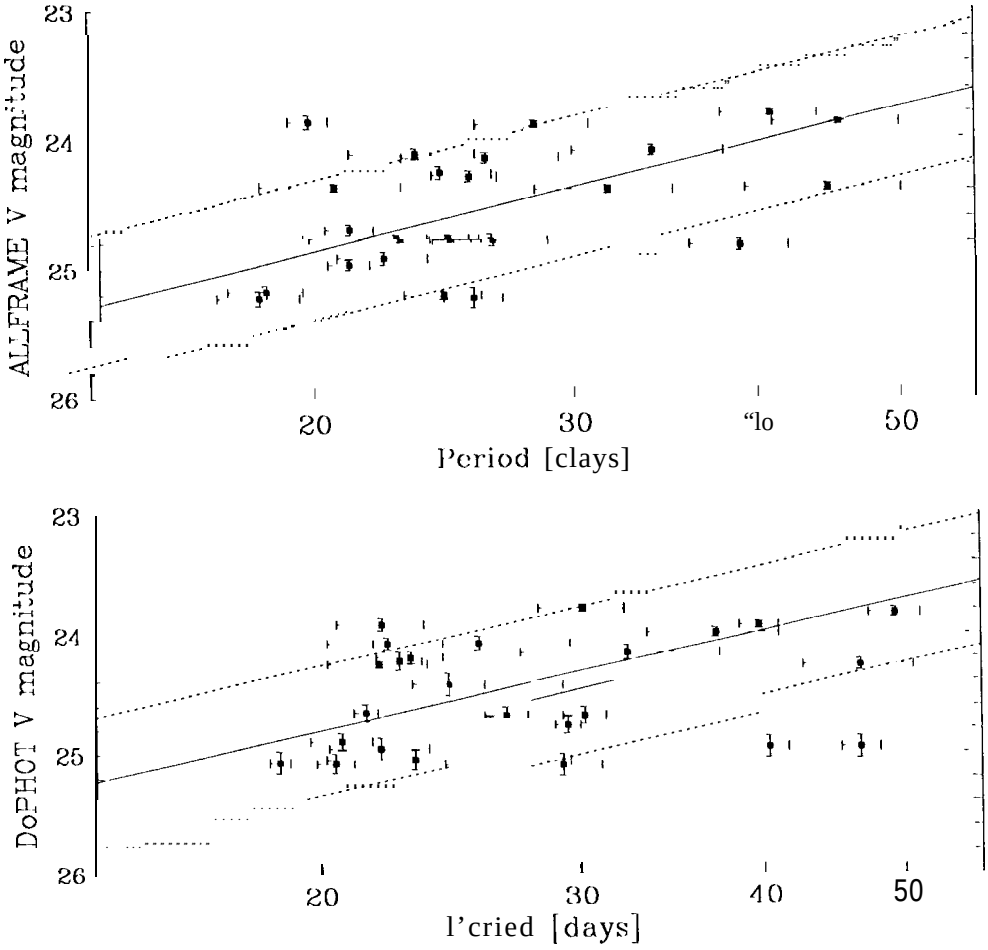

Figure 11.- The V-band period-luminosity relations of high-quality Cepheids (see Table 2) obtained with ALLFRAME (top) and DoPHOT (bottom) photometry. Phase weighted magnitudes are used. The solid lines are the best fits and the dotted lines correspond to the rms dispersion of the LMC period-luminosity relation of Madore & Freedman (1991). The distance moduli obtained from the lines of best fit are 29.85 ± 0.19 and 29.80 ± 0.19, respectively.

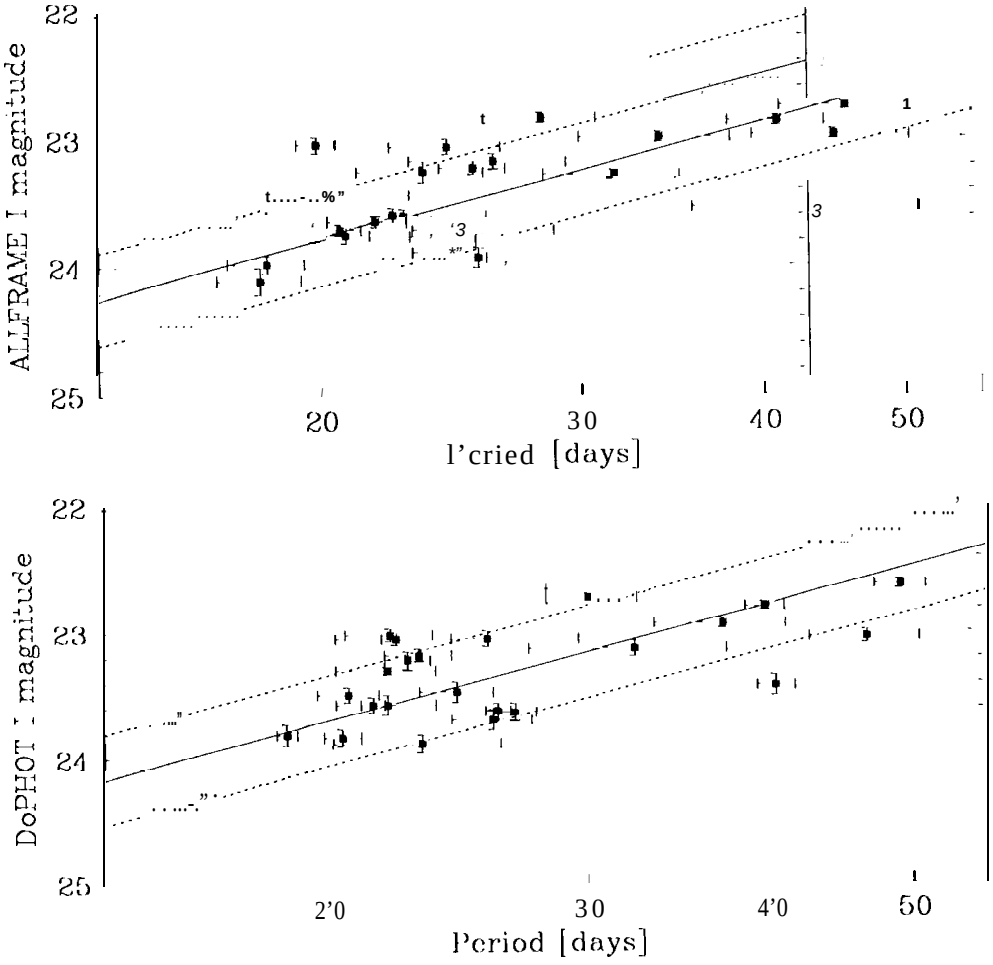

Figure 12.- The I-band period-luminosity relation of high-quality Cepheids (see Table 2) obtained with ALLFRAME (top) and DoPHOT (bottom) photometry. Phase weighted magnitudes are used. The solid lines are the best fits and the dotted lines correspond to the rms dispersion of the LMC period-luminosity relation of Madore & Freedman (1991). The distance moduli obtained from the lines of best fit are 29.58 ± 0.17 and 29.49 ± 0.18, respectively.

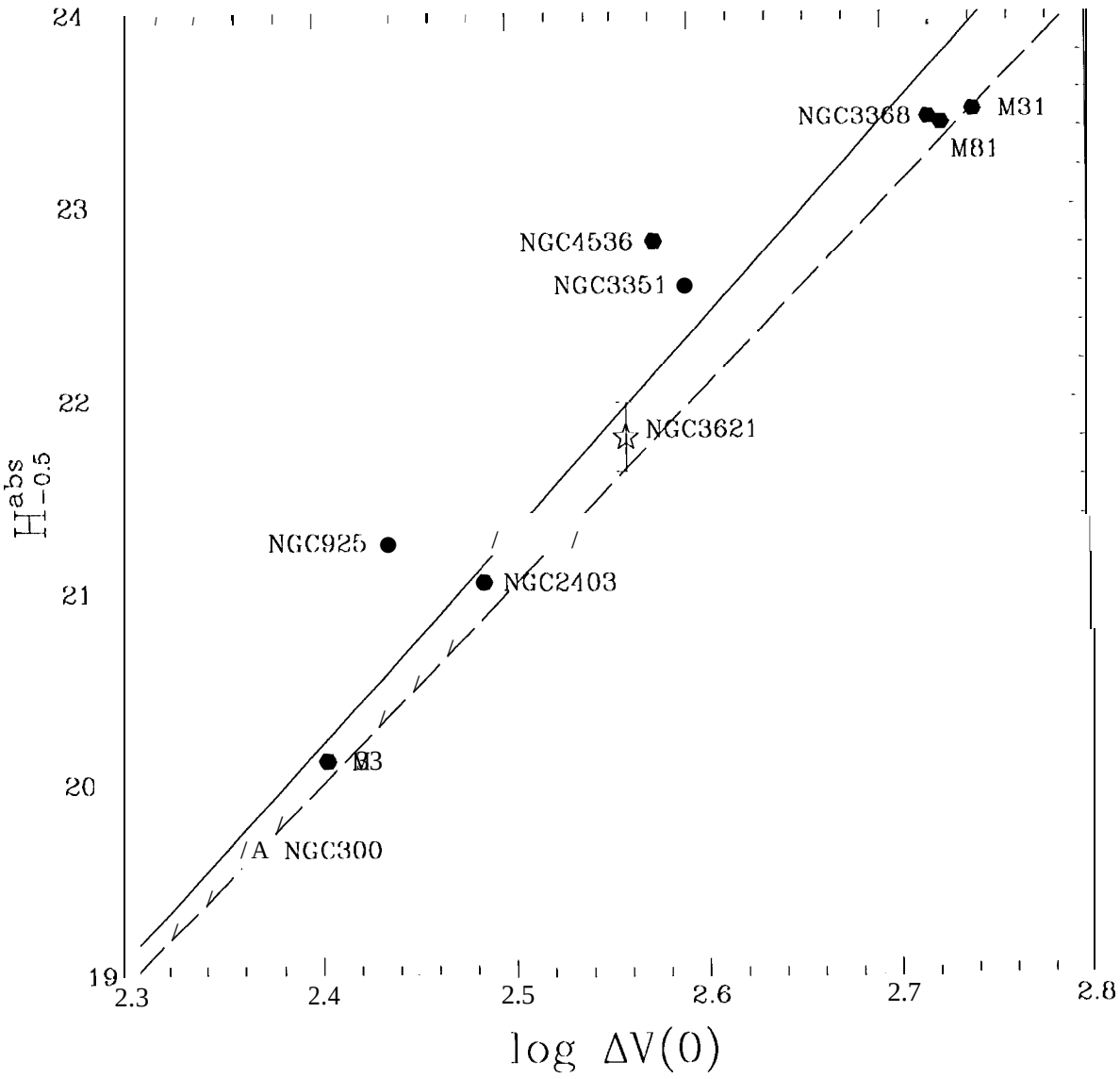

Figure 13.- Calibrators of the Infrared Tully-Fisher Relation (see Table 4). The solid line is given by Equation (9) in §6; the dashed line is the calibration by Freedman (1990).

Table Captions

Table 1: Log of HST WFPC2 observations of NGC 3621. All observations comprise two cosmic-ray split pairs except for the epoch 011 January 4th. The Julian Date quoted is that of the start of the first exposure.

Table 2: The variables found in NGC 3621. The columns provide the following information: (1) the identification, (2) the chip, (3) the period, (4) and (5) the right ascension and declination in (J2000.0), (6) and (7) the phase-averaged ALLFRAME V- and I-band magnitudes, and (8) the description of each of the Cepheids using the key given in the notes to the Table.

Table 3: The different contributions to the error budget of the distance modulus of NGC 3621.

Appendix Table Captions

Table A1: - The gain ratios and 0.5-arcsecond V- and I-band ALLFRAME aperture corrections for each of the four WFPC2 chips.

Table A2: - The zero point calibration adopted for ALLFRAME. m_{F555W} and m_{F814W} are defined to be the ALLFRAME raw magnitudes in the $F555W$ and $F814W$ filters, respectively, for a star in an image with exposure time t.

Tables A3-A6: - Secondary standard photometry for Chips 1-4

Table A7: - V-band ALLFRAME data for each of the Cepheids over the twelve epochs.

Table A8: - I-band ALLFRAME data for each of the Cepheids over the four epochs.

TABLE 1

LOG OF OBSERVATIONS

Obs. Date	MJD	Exp. Time (s)	Filter
27/12/94	49713.857	900 + 900	*F555W*
27/12/94	49713.915	900 + 900	*F814W*
04/01/95	49721.770	900	*F555W*
04/01/95	49721.830	900 + 900	*F814W*
04/01/95	49721.897	900 + 900	*F439W*
15/01/95	49732.891	900 + 900	*F555W*
17/01/95	49734.969	900 + 900	*F555W*
20/01/95	49737.{)18	900 + 900	*F555W*
2?4/01/95	49741,670	900-1 900	*F555W*
24/01/95	49741.734	900 + 900	*F814W*
24/01/95	49741.801	900 + 900	*F439W*
28/01/95	49745.493	900 + 900 + 180	*F555W*
28/01/95	49745.559	180	*F814W*
01/02?/95	4974{).579	800 + 800	*F555W*
06/02/95	49754.739	800 + 800	*F555W*
12/02/95	49760.641	800 + 800	*F555W*
12/02/95	49760.700	900 + 900	*F814W*
18/02/95	49766.877	800-1 800	*F555W*
?5/02/95	4(1773.176	900 + 900	*F555W*

NOTE.- The following reference files were used in the calibration of these exposures. File names follow the conventions adopted by the Space Telescope Science Institute. The file was used for all filters unless indicated otherwise. MASKFILE = e2112084u.r0h; ATODFILE = dbu1405iu.r1h; BIASFILE = e6l10347u.r2h (27/12/94 - 20/1/95) and f1j1615tu.r2h (24/1/95 - 25/02/95); DARKFILE = ebh1547qu.r3h (27/12/95), f151225pu.3h (04/01/95 - 17/01/95), f1i1004iu.r3h (20/01/95), f1k1459hu.r3h (24/01/95- 01/02/95), f220923mu.r3h (06/02/95- 12/02/95), and f2h11352u.r3h (18/02/95 - 25/02/95); FLATFILE = e380935cu.r4h (F555W), e380934lu.r4h (F439W) and e391434fu.r4h (F814W); SHADFILE = e371355eu. r5h (shutter A), e371355iu.r5h (shutter B), depending on the shutter used at the start of the exposure; GRAPHTAB = e8210190m.tmg; COMPTAB = eai1341pm.tmc

TABLE 2

CEPHEID CANDIDATES

ID	Chip	Period (days)	R.A. (J2000.0)	Dec.	V	1	Comments
C01	WF2	60.00	11:18:21.6	- 32:50:19.2	23.52	22.61	ABFd
C02	WF4	45.50	11:18:14.0	- 32:50:58.8	23.88	22.75	ABFf *
C03	PC1	44.65	11:18:16.6	- 32:50:09.3	24.38	22.97	ABCds *
C04	WF3	40.90	11:18:22.4	- 32:51:05.8	23.81	22.86	ABd *
C05	WF2	40.70	11:18:19.5	- 32:49:51.2	24.78	23.40	ABffs
C06	WF4	39.00	11:18:16.3	- 32:50:47.7	24.82	23.53	DdEf *
C07	WF3	38.35	11:18:22.5	32:50 :49.4	23.57	22.76	ABFs
C08	PC1	37,70	11:18:18.3	- 32:50:24.5	24.96	22.{)5	ABC
C09	WF2	34.50	11:18.19.7	- 32:50:02.4	24.09	23.11	aBFs
C10	PC1	34.00	11:18:16.8	32:50 :31.4	24.09	22.99	ABC *
C11	WF4	32.70	11:18:16.0	32:50:50.5	25.94	24.66	ABffs
C12	PC1	32.00	11:18:18.8	32:50 :16.5	25.23	23.74	ABFI
C13	PC1	31.65	11:18:17.1	- 32:50:12.7	24.39	23.28	ABdF *
C14	WF2	31.55	11:18:21.4	- 32:49:32.7	23.28	22.76	ABFFs
C15	WF2	31.45	11:18:20.5	- 32:50:07.1	25.20	23.52	ABdF
C16	PC1	31.15	11:18:18.2	32:50:36.0	24.50	23.28	ABf
C17	PC1	28.35	11:18:19.0	- 32:50:36.3	23.89	22.84	ABf *
C18	WF2	27.75	11:18:19.8	-32:50:20.8"	25.30	24.11	DEsd
C19	WF4	27.70	11:18:16.1	- 32:51:34.8	23.99	22.91	BDF
C20	WF2	26.40	11:18:22.3	- 32:50:30.9	24.78	23.71	AdEF *
C21	PC1	26.25	11:18:18.3	- 32:50:40.2	24.81	23.64	ABdF
C22	WF2	26.20	11:18:20.1	- 32:49:55.0	24.14	23.18	ABF *
C23	WF2	25.60	11:18:19.6	- 32:49:38.8	25.23	23.89	DBds *
C24	WF3	25.40	11:18:23.5	- 32:51:44.2	24.28	23.23	ABCd *
C25	WF2	25.30	11:18:24.4	- 32:49:53.9	25.30	24.14	ABff
C26	WF3	24.70	11:18:19.0	32:51:38.0	24.77	23.76	ABF *
C27	WF4	24.50	11:18:17.3	- 32:50:43.5	24.60	23.55	DEF
C28	WF4	24.40	1:18:17.3	- 32:51:12.8	24,26	23.07	ABFdd *
C29	PC1	24.40	1:18:18.2	- 32:50:39.9	25.21	23.89	ABCd *
C30	WF4	23.80	1:18:15.5	- 32:51:44.8	25.54	24.14	BDF
C31	WF2	23.75	1:18:21.3	32:49 :53.9	24.63	23.31	ABFF
C32	WF2	23.45	1:18:19.4	- 32:50:35.2	24,11	23.26	ABff *
C33	WF2	23.30	1:18:20.3	32:49:40 ()	25.96	24.07	ABffs
C34	WF4	23.10	11:18:16.1	32:51 :26.2	24.80	23.80	DEF
C35	PC1	22.75	11:18:18.3	- 32:50:26.0	24.77	23.60	ABC *
C36	WF4	22.65	11:18:14.7	- 32:51:03.8	24.79	23.74	AEF
C37	WF2	22.15	11:18:21.4	- 32:50:18.3	24.92	23.65	ABdf *
C38	WF2	21.45	11:18:19.7	32:50 :10.8	24.08	23,30	ABffd
C39	WF2	21.'20	11:18:20.0	- 32:50:16.1	24.70	23.75	BDF *

TABLE 2- *Continued*

ID	Chip	P'cried (clays)	R.A. (J2000.0)	D Cc.	*V*	*I*	Comments
C40	WF3	20.95	11:18:18.7	- 32:51:25.2	24.97	23.71	ABdFs *
C41	WF4	20.70	11:18:14.5	32:51 :10.7	24,37	23.44	ABF *
C42	WF2	19.90	11:18:21.6	32:49:46.7	25.16	23.87	ABFds
C43	WF2	19.90	11:18:20.6	- 32:50:01.2	23.86	23.05	BfDF *
C44	WF3	19.20	11:18:18.9	- 32:51:08.3	24.78	23.89	DBFd
C45	WF2	18.80	11:18:20.0	32:49 :48.5	24.43	23.04	DBFs
C46	WF3	8.70	1:18:23.7	32:50 :52.7	24.42	23.13	ABF
C47	WF4	8.45	1:18:18.0	- 32:50:51.0	24.37	23.54	DEF
C48	WF4	8.40	1:18:18.1	- 32:51:11.5	25.18	23.98	AdEF *
C49	WF2	8.20	1:18:19.8	- 32:50:15.6	25.23	24.11	BDs *
C50	WF2	8.00	1:18:20.3	- 32:50:15.4	25.22	24.09	aDffs
C51	PC1	7.80	1:18:17.6	- 32:50:14.3	25.01	23.82	ABsC
C52	WF3	17,75	11:18:23.6	- 32:51:47.3	24.49	23.75	ABC
C53	WF4	17.45	11:18:16.3	- 32:51:26,4	24.79	24.03	BDFF
C54	WF2	17.35	11:18:20.7	- 32:49:59,7	24.63	23.98	ABFd
C55	WF4	17.05	11:18:16.6	- 32:51:00,9	25.28	24.35	DEF
C56	WF2	16.50	11:18:23.2	- 32:50:34.7	25.06	24.14	ABCd
C57	PC1	6.25	1:18:18.2	32:50 :12.5	25.17	24.18	DEFds
C58	WF2	6.20	1:18:19.5	- 32:49:56.6	25.24	24.12	BDds
C59	WF2	6.15	1:18:20.2	- 32:50:10.9	25.30	24.43	aBFs
C60	PC1	4.75	1:18:16.1	- 32:50:20.2	24.81	23.63	ABff
C61	WF4	3.90	1:18:18.2	- 32:51:05.7	25,04	24.14	aBF
C62	PC1	3,80	1:18:18.0	- 32:50:35.5	25.61	24.44	DdEff
C63	WF3	13.00	11:18:20.5	32:51:43.2	25.12	24,29	DBfd
C64	WF2	12.20	11:18:19.3	32:50:42.8	25.11	24,38	DB
C65	WF4	12.10	11:18:17.2	32:51 :09.6	25.19	24.06	DBCF
C66	PC1	11.90	11:18:18.4	32:50:37.5	25.57	24.23	DEFd
C67	PC1	11.45	11:18:17.4	32:50:32.6	25.28	24.15	DBCd
C68	WF2	9.95	11:18:19.5	32:50;29.3	25.21	24.41	aBFsd
C69	WF3	9,40	11:18:21.3	32:51:46.7	25.49	24.78	DBFd
W01	WF1	73.9	11:18:17.4	32:50:29.3	25.85	24.86	aBCd

NOTE. The key to the code used to describe each Cepheid is: (A) well-defined lightcurve, (a) less well-defined lightcurve, (B) *V*-band peak-to-peak lightcurve amplitude of 0,75 mag or greater, (C) isolated star, (1)) poorly sampled lightcurve, (E) low-amplitude lightcurve, (F) crowded field, (FF) very crowded field, (1) bad image defect, (d) affected by cosmic rays, (f) confusion in the wings, (fF) bad confusion in the wings, (i) minor image defect, (s) large sky gradient. (*) indicates that the Cepheid was incorporated into the final sample.

TABLE 3

ERROR BUDGET

Source of uncertainty	Value (mag)	Value (mag)
I-band P-L relation scatter	0.05	
V-band P-L relation scatter	0.08	
$E(V-I)$	0.05	
Unreddened P-L relation		0.07
Photometry errors	0.09	
Distance modulus		0.11
LMC distance modulus	0.10	
Metallicity effect	0.10	
Total error budget		0.18

NOTE - The uncertainties in the I-band P-L relation and the reddening value, $E(V-I)$, are added in quadrature to obtain the uncertainty of the unreddened P-L relation. This is in turn combined with the maximum possible error due to the photometric algorithms to arrive at the uncertainty in the absolute distance modulus relative to the LMC. The uncertainty in the LMC distance modulus and the effects of different metallicities of the LMC and NGC 3621 ([O/H] = -3.60 and -3.05, respectively) are added to arrive at the final uncertainty in the distance modulus.

TABLE 4

H-BAND TULLY-FISHER RELATION DATA

Galaxy Name	$\Delta V(0)$ kill/s	$H^{abs}_{-0.5}$ mag	References
M31	552	-23.49	F90
M33	253	-20.12	F90
M81	531	-23.42	F94a
NGC 300	235	-19.66	F90
NGC 925	273	-21.26	FT81; S96; W84
NGC 2403	306	-91.05	F90
NGC 3351	390	-22.60	A77; SSD87; G96
NGC 3368	523	-23.45	A77; T95
NGC 3621	366	-21.80	FT81
NGC 4536	376	-22.81	A80; S96

NOTE.- A77: Aaronson (1977); A80: Aaronson et al. (1980); F90: Freedman (1990); F94a: Freedman et al. (1994a); FT81: Fisher & Tully (1981); G96: Graham et al. (1996); S96: Saha et al. (1996); SSD87: Staveley-Smith & Davies (1987); T95: Tanvir et al. (1995); W84: Wevers (1984)

TABLE A1

GAIN RATIOS AND ALLFRAME APERTURE CORRECTIONS FOR WFPC2

Chip	Gain Ratio	Aperture Correction F555W	1"s14 W
PC1	1.987	0.067	-0.077
WF2	2.003	0.014	+0.026
WF3	2.006	0.007	+0.032
WF4	1.955	-0.011	+0.010

TABLE 2

CALIBRATION RELATIONS FOR ALLFRAME PHOTOMETRY

Chip	Transformation Equations for ALLFRAME
PC1	$F555W = m_{F555W} + 2.5 \log_{10} t - 1.036$
	$F814W = m_{F814W} + 2.5 \log_{10} t - 1.940$
WF2	$F555W = m_{F555W} + 2.5 \log_{10} t - 0.971$
	$F814W = m_{F814W} + 2.5 \log_{10} t - 1.796$
WF3	$F555W = m_{F555W} + 2.5 \log_{10} t - 0.956$
	$F814W = m_{F814W} + 2.5 \log_{10} t - 1.809$
WF4	$F555W = m_{F555W} + 2.5 \log_{10} t - 0.984$
	$F814W = m_{F814W} + 2.5 \log_{10} t - 1.860$
All	$V = F555W - 0.045 (V-I) + 0.027 (V-I)^2$
	$I = F814W - 0.067 (V-I) + 0.025 (V-I)^2$

TABLE A3

SECONDARY PHOTOMETRY STARS FOR CHIP

R.A. (J2000.0)	Dec.	V	*I*
11:18:16.0	-32:50:28.3	23.31	23.17
11:18:16.0	-32:50:31.5	23.88	23.93
11:18:16.1	-32:50:26.7	23.33	23.23
11:18:16.1	-32:50:26.7	23.85	21.60
11:18:16.1	-32:50:27.2	23.53	23.29
11:18:16.1	-32:50:30.6	23.64	23.52
11:18:16.2	-32:50:07.2	23.48	22.34
11:18:16.2	-32:50:16.4	23.91	23.29
11:18:16.2	-32:50:16.8	23.67	23.32
11:18:16.2	-32:50:22.4	23.79	23.32
11:18:16.2	-32:50:30.7	22.93	22.45
11:18:16.2	-32:50:31.4	23.89	23.70
11:18:16.3	-32:50:10.9	23.69	22.54
11:18:16.3	-32:50:22.8	23.28	23.18
11:18:16.3	-32:50:29.4	23.14	22.83
11:18:16.3	-32:50:37.0	23.85	22.82
11:18:16.4	-32:50:30.1	23.34	23.05
11:18:16.5	-32:50:24.8	23.91	23.46
11:18:16.5	-32:50:36.8	23.73	23.22
11:18:16.6	-32:50:13.6	21.29	20.59
11:18:16.7	-32:50:11.3	23.92	23.15
11:18:16.7	-32:50:28.8	22.80	22.03
11:18:16.7	-32:50:30.3	23.61	23.02
11:18:16.8	-32:50:09.7	23.54	23.02
11:18:16.8	-32:50:36.5	23.08	22.92

TABLE A3- *Continued*

R.A. (J2000.0)	Dec.	V	*I*
11:18:16.9	- 32:50:23.7	23.65	23.74
11:18:16.9	- 32:50:38.6	23.38	23.21
11:18:17.0	- 32:50:10.9	22.06	21.59
11:18:17.0	- 32:50:36.7	23.67	23.50
11:18:17.0	- 32:50:37.1	23.78	23.78
11:18:17.0	- 32:50:39.5	23.41	22.57
11:18:17.0	- 32:50:39.5	23.92	23.73
11:18:17.1	- 32:50:14.9	23.61	23.21
11:18:17.1	- 32:50:36.7	24.01	23.15
11:18:17.2	- 32:50:39.1	23.07	22.68
11:18:17.3	- 32:50:10.2	23.36	22.98
11:18:17.3	- 32:50:36.0	23.18	21.63
11:18:17.3	- 32:50:37.5	23.81	23.58
11:18:17.3	- 32:50:37.7	23.93	23.87
11:18:17.4	- 32:50:19.8	23.89	23.71
11:18:17.5	- 32:50:18.4	21.62	20.97
11:18:17.7	- 32:50:35.7	22.80	21.99
11:18:17.8	- 32:50:26.4	23.85	22.53
11:18:18.0	- 32:50:09.9	23.83	23.69
11:18:18.1	- 32:50:25.0	23.68	22.78
11:18:18.3	- 32:50:09.7	23.28	23.44
11:18:18.3	- 32:50:34.8	23.77	23.33
11:18:18.4	- 32:50:10.7	23.57	23.26
11:18:18.7	- 32:50:15.5	23.97	23.52
11:18:18.7	- 32:50:17.3	22.18	21.98
11:18:18.8	- 32:50:10.9	23.02	22.70

TABLE A4

SECONDARY PHOTOMETRY STARS FOR CHIP 2

R.A. (J2000.0)	Dec.	V	I
11:18:19.2	32:49:58.6	21.85	21.32
11:18:19.5	32:50:07.7	22.61	21.53
11:18:19.5	-32:50:09.3	21.90	21.01
11:18:19.5	-32:50:16.0	21.86	20.97
11:18:19.6	-32:50:09.5	22.28	21.82
11:18:19.8	32:50:03.8	22.24	20.91
11:18:19.8	-32:50:32.1	22.32	22.02
11:18:20.1	-32:50:35.8	21.78	21.46
11:18:20.2	-32:49:43.3	22.47	22.07
11:18:20.2	32:50:11.8	22.47	22.38
11:18:20.8	-32:49:58.8	22.26	21.95
11:18:20.9	-32:50:13.6	22.58	22.19
11:18:20.9	-32:54:38.2	21.70	21.06
11:18:21.1	32:50:25.5	22.54	22.64
11:18:21.2	-32:49:41.6	22.25	22.07
11:18:21.2	-32:50:16.8	22.58	22.31
11:18:21.3	-32:49:50.2	22.58	22.54
11:18:21.3	32:50:25.1	21.97	20.77
11:18:21.4	-32:49:53.6	21.73	21.12
11:18:21.4	-32:50:22.1	22.00	21.26
11:18:21.6	-32:49:33.4	21.88	21.72
11:18:21.9	32:49:33.1	22.46	22.65
11:18:22.2	-32:49:52.6	22.61	22.38
11:18:22.2	-32:49:54.4	22.04	21.32
11:18:22.2	-32:49:56.0	21.77	21.03

TABLE A4. *Continued*

R.A. (J2000.0)	Dec.	V	I
11:18:22.3	-32:49:43.4	21.49	20.96
11:18:22.5	-32:49:56.0	21.89	20.77
11:18:22.8	-32:49:44.3	21.88	21.68
11:18:22.8	-32:49:58.7	22.51	22.34
11:18:22.9	-32:49:48.8	21.36	20.75
11:18:22.9	-32:49:58.7	22.26	21.96
11:18:23.0	-32:49:54.1	22.58	22.83
11:18:23.2	-32:50:03.4	22.54	22.09
11:18:23.3	-32:49:36.6	22.10	21.23
11:18:23.3	-32:49:41.8	21.98	21.67
11:18:23.5	-32:50:03.0	21.63	21.50
11:18:23.5	-32:50:05.0	22.10	21.96
11:18:23.7	-32:49:45.1	22.39	21.54
11:18:23.7	-32:50:04.3	21.16	20.83
11:18:23.8	-32:49:45.0	22.28	21.66
11:18:23.8	-32:50:04.3	22.61	22.87
11:18:23.9	-32:49:48.8	22.35	22.23
11:18:24.1	-32:50:09.1	21.48	20.72
11:18:24.3	-32:49:59.5	21.66	21.43
11:18:24.5	-32:49:50.4	22.55	22.60
11:18:24.5	-32:49:50.4	22.61	22.76
11:18:24.5	-32:50:03.9	22.19	21.14
11:18:24.7	-32:49:53.4	22.42	22.43
11:18:24.7	-32:49:57.5	21.92	21.51
11:18:24.8	-32:49:53.0	22.08	21.85
11:18:25.0	-32:50:09.4	22.56	20.68

TABLE A5

SECONDARY PHOTOMETRY STARS FOR CHIP 3

R.A. (J2000.0)	I) Cc.	V	1
11:18:20.0	- 32:51:46,4	20.07	18.36
11:18:18.9	- 32:50:49.4	20.72	20.02
11:18:19.5	- 32:51:28.0	21.18	19.96
11:18:22.2	32:51 :32.2	21,40	20.08
11:18:23.9	- 32:50:52.2	21.50	20.54
11:18:22.2	- 32:51:29.4	21.51	21.36
11: 8:23.2	- 32:51:03.5	21.77	21.59
11: 8:22.7	- 32:51:31.5	21.79	21.43
11: 8:23.9	32: 50;59.0	21.90	21.74
11: 8:24.0	32:51 :18.4	22.05	21,90
11: 8:21.0	- 32:51:22.4	22.14	21.85
11: 8:23.7	- 32:51:00.4	22.16	22.19
11: 8:20.9	- 32:51:14.4	22.21	21.04
11:18:18.2	- 32:51:50.2	22.29	21.96
11:18:22.3	- 32:51:03.0	22.40	22.34
11:18:20.6	- 32:51:24.3	22.46	22.38
11:18:22.4	- 32:51:02.3	22.56	22.63
11:18:21.1	- 32:51:15.6	22.59	22.21
11:18:21.9	- 32:51:34.1	22.59	20.27
11:18:22.1	- 32:51:41.6	22.60	20.43
11:18:24.2	- 32:51:47.0	22.03	22.68
11:18:21.9	- 32:50:50.0	22.64	22.75
11:18:21.0	- 32:51:16.6	22.68	21.71
11:18:22.5	- 32:50:58.3	22.70	22.79
11:18:21.1	- 32:51:33.1	22.72	22.48

TABLE A5 *Continued*

R.A (J2000.0)	Dec.	V	I
11:18:22.6	32:51:01.6	22.74	21.90
11:18:19.8	32:51:31.4	22.77	22.32
11:18:22.2	32:51:13.7	22.81	21.96
11:18:22.0	32:51:35.1	22.82	23.12
11:18:18.9	32:51:31.3	22.84	22.51
11:18:22.1	-32:50:51.1	22.85	22.85
11:18:18.9	-32:51:18.0	22.86	22.31
11:18:21.1	-32:51:18.3	22.87	22.83
11:18:18.2	-32:51:47.0	22.88	22.62
11:18:20.8	-32:51:36.9	22.91	22.33
11:18:19.3	-32:51:23.8	22.92	21.45
11:18:22.1	32:51:16.1	22.97	22.94
11:18:23.2	-32:51:56.7	22.97	20.92
11:18:19.1	-32:50:47.2	22.98	22.61
11:18:21.5	-32:51:23.8	23.02	22.74
11:18:20.4	32:51:04.6	23.03	22.26
11:18:20.8	-32:51:31.9	23.04	21.94
11:18:21.5	-32:51:38.7	23.07	21.00
11:18:22.3	-32:51:10.1	23.11	22.97
11:18:20.8	32:51:19.2	23.13	22.62
11:18:19.2	-32:51:42.3	23.15	22.95
11:18:22.6	-32:50:56.9	23.16	23.03
11:18:18.8	-32:51:17.5	23.17	20.70
11:18:19.2	-32:51:49.4	23.17	22.69
11:18:19.5	-32:51:46.2	23.18	21.32
11:18:20.9	-32:51:42.5	23.19	22.75

TABLE A6

SECONDARY STANDARD PHOTOMETRY FOR CHIP 4

R.A. (J2000.0)	I) Cc.	V	1
11:18:12.7	-32:50 :43.2	23.39	22.36
11:18:12.8	- 32:51:17.1	23.40	21.36
11:18:13.0	- 32:51:03.3	23.35	23.33
11:18:13.1	- 32:50:57.0	23.35	21.48
11:18:13.1	- 32:51:16.3	23.()()	20.05
11:18:13.4	- 32:50:58.6	22.79	22.58
11:18:13.6	- 32:51:32.5	23.32	22.92
11:18:14.1	32: 51:13.4	23.45	23.12
11:18:14.2	- 32:50:53.3	23.02	22.57
11:18:14.2	- 32:51:14.8	23.33	21.31
11:18:14.6	- 32:51:03.8	23.52	22.34
11:18:14.6	- 32:51:35.7	23.45	23.05
11:18:14.8	- 32:51:21,9	23.28	22.10
11:18:15.1	- 32:51:33.8	23.51	22.81
11:18:15.3	32:51 :50.4	'23.10	22.29
11:18:15.4	- 32:51:05.5	22.77	22.14
11:18:15.5	- 32:51:04.7	**22.70**	22.16
11:18:15.5	- 32:51:37.2	23.09	22.83
11:18:15.5	- 32:51:45.9	23.52	22.84
11:18:15.6	32:50 :50.1	21.88	20.81
11:18:15.6	- 32:51:30.6	23.45	23.60
11:18:15.8	- 32:51:02.1	23.59	23.38
11:18:15.8	- 32:51:06.3	22.67	22.27
11:18:15.9	- 32:51:33.5	23.20	23.12
11:18:15.9	32:51 :35.8	23.52	23,22

TABLE A6 *Continued*

R.A. (J2000.0)	Dec.	V	
11:18:15.9	-32:51:48.1	22.80	22.23
11:18:16.1	-32:50:43.4	23.50	23.21
11:18:16.1	-32:51:30.2	23.55	23.27
11:18:16.1	-32:51:36.2	23.36	22.98
11:18:16.2	-32:50:44.8	23.43	22.87
11:18:16.2	-32:51:26.0	22.76	22.05
11:18:16.3	-32:51:43.0	22.69	22.55
11:18:16.4	-32:50:46.1	23.03	22.38
11:18:16.4	-32:51:21.0	23.34	23.02
11:18:16.5	-32:51:12.9	23.16	22.75
11:18:16.5	-32:51:26.6	23.39	23.24
11:18:16.6	-32:50:56.0	23.54	23.30
11:18:16.6	-32:51:46.2	23.28	21.42
11:18:16.9	-32:50:52.1	23.49	23.44
11:18:17.0	-32:51:39.8	23.64	21.00
11:18:17.1	-32:50:53.0	23.62	23.19
11:18:17.1	-32:51:29.7	23.52	21.59
11:18:17.2	-32:51:17.4	23.50	22.08
11:18:17.3	-32:51:18.8	23.37	21.53
11:18:17.5	-32:51:31.2	22.97	22.56
11:18:17.7	-32:50:44.0	23.43	23.56
11:18:17.7	-32:51:03.0	22.87	22.69
11:18:17.9	-32:50:45.5	22.47	21.91
11:18:18.0	-32:51:18.1	23.09	22.90
11:18:18.2	-32:50:58.0	23.10	20.98
11:18:18.4	-32:51:04.1	22.89	22.19

TABLE A7

V-BAND ALLFRAME PHOTOMETRY - FIRST SIX EPOCHS

ID	2449713.857	2.449721.770	2449732.891	2449734.969	2449737.918	2449741.670
C1	...	23.67 ± 0.14	23.873 0.16	23.78 ± 0.21	23.603 0,13	23.26 ± 0,11
C2	23.66 ± 0.07	23.97:1 0.08	24.123 0.08	24,15:1 0.08	24.224 0,10	24.233 0.11
C3	24.42 ± 0.09	24.65 ± 0.12	24.783 0.09	24.543 0.08	24.13 ± 0.10	23.97 ± ().07
C4	24.313 0.10	24.39 ± 0.10	23.54 ± 0.05	23.493 0.07	23.71 ± 0.07	23.764 0.07
C5	25.47 ± 0.24	25.563 0.20	24.354 0.14	24.443 0.12	24.53 ± 0.13	24.823 0.14
C6	25.364 ().13	24,734 0.08	24.63 ± 0.13	24,504 0.11	24.743 0.10	24.894 0.13
C7	23.57,1 0.11	23.964 0.11	24.144 0.14	23.544 0.28	23.19 ± 0.12	23.28 ± 0.11
C8	24.814 0.12	24.44 ± 0.23	24.67 ± 0.14	24.843 0.09	24.87 ± 0.11	24.953 0.09
C9	23.844 0.21	24.20 ± 0.23	24.53 ± 0.23	24.41 ± ().34	24.41 ± 0.26	23.934 0.22
C10	23,643 0.08	24.08 ± 0.08	24.503 0,27	24.523 0.09	24.543 0.11	24.674 0.09
C11	26.02 ± 0.22	25.92 ± 0.22	25.56 ± 0.19	25.603 (),14	25.853 0.18	25.764 0.15
C12	24.924 0.22	25.163 0.33	25.763 0.31	25,504 0,24	25.424 0.23	24.754 0.15
C13	24.53,1 0.09	24.88 ± 0.13	23.79 ± ().07	23.923 ().()6	24.15 ± 0.07	24.35:1 0.09
C14	23.72 ± 0.14	22.973 0.10	23.464 0.09	23.464 0.13	23.533 0.10	23.584 0.10
C15	24.57,1 0.23	25.434 0.18	25.66 ± 0.25	25,573 0,21	25.625 0.28	24.98:1 0.18
C16	24.16 ± 0.06	24.51 ± 0.08	25.08 ± 0,12	25.10 ± 0.11	24.824 0.17	23.964 0.08
C17	23.604 0,11	24.01 ± 0.13	24.394 ().11	24.40 ± 0.13	23.653 0.07	23.453 0.07
C18	25.084 0.16	25.464 0,21	25.594 0.21	25.604 0.24	25.004 0.28	25.024 0.18
C19	23.463 0.08	23.963 0.08	24.584 ().12	24,403 0.09	24.555 0.09	23.393 0.09
C20	24.49 ± 0.08	24.62 ± 0.24	25.15 ± 0.15	24.754 0.12	24.333 (),11	24.54 ± (),15
C21	25.40 ± ().14	24.424 0.07	24.95 ± ().12	25.093 0.10	25.19 ± 0.10	25.23 ± 0.12
C22	24.71 ± 0.15	23.953 0.11	24.39 ± ().13	24.454 0.17	24.503 0.18	24.52 ± 0.18
C23	25.36:1 0.17	26.40 ± 0.40	24.89:1 0,14	25,14 ± 0.14	25.053 0.17	25.473 0.24
C24	24.82 ± 0.13	24.21 ± 0.09	24.833 0.11	24.78,1 0.18	24.824 0.19	23,894 0.11
C25	25.71 ± 0,17	26.09 ± 0.27	25.223 ().12	25.37 ± 0.23	25.493 0.18	25.953 0.21
C26	24.27 ± 0.08	25.224 0.09	25.534 0.15	24,804 0.08	24.264 0.12	24.564 0.09
C27	24.97 ± 0.24	24.593 ().22	24.92 ± 0.19	25,05:1 0.20	25.004 0.19	24.34:1 0.17
C28	24.924 0.13	24.10 ± ().12	24,79,1 0.12	24.573 0.11	24.83 ± 0.12	23.643 0.09
C29	25.703 0.19	25.264 ().17	25.22 ± 0.12	25.533 0.19	25.593 ().17	25.793 0.14
C30	25.474 0.16	25.984 0.21	25.884 0.18	25.054 0.18	25.11 ± 0,14	25.364 0.13
C31	25.353 0.20	.	25.02 ± 0.19	25,173 0.18	25.254 0.15	24.18 ± 0.09
C32	24.34 i 0.12	24.59 ± 0.21	24.08 ± 0,13	24.16 ± 0.13	24.37 ± 0.16	24.60 ± 0,13
C33	25.393 0.22	26.205 0.33	26.51 ± 0.38	26,09,1 0.29	25.443 0.18	25.524 0.19
C34	25.28 ± 0,'23	24.56 ± 0.09	24.963 0.17	25.15 ± 0,10	24.963 0.16	24.85 ± 0.16
C35	25.284 0.11	24,54 ± 0.10	25.25 ± 0.13	25.23:1 0.12	25.33 ± 0.12	24.234 0.09

TABLE A7- *Continued*

ID	2449713.857	2449721.770	2449732.891	2449734 .{169	2449737.918	2449741.670
C36	25.023 0.10	24.683 0.12	25.123 ().14	24.91 ± ().13	24.953 0.11	24.41 ±0.08
C37	24,584 0.13	25.563 0.19	24.483 0.08	24.39 ± 0.11	24.71 ±0.10	24.97 ±0.16
C38	24.563 0.20	23.583 0.12	24.33 ± ().23	24.51± 0.14	24.51 ±0.15	23.81± 0.09
C39	24.17 ± 0.11	25.004 0.16	24.773 0.17	24.094 0.10	24.36 ± 0.13	24.654 0.10
C40	25.24 ± 0.12	25.05± 0.12	25.19 ± 0.11	24.854 0.08	24.484 0.08	24.70 ± 0.10
C41	24,023 0.08	24.854 0.08	23.834 ().07	23.974 0.10	24.303 0.11	24.45:1 0.12
C42	24.653 0.12	25.71 ±0.29	24.59 ± 0.12	24,693 0.16	25.123 0.18	25.42 ±0.19
C43	23.71 ± 0.16	24.04:1 0.21	23.60,1 0.15	23.75,1 0.12	23.873 0.16	24.11 ± ().17
C44	25.31± 0.18	24.753 0.10	25,41 ± (),14	24.98 ± 0.16	24.36 ±0.09	24.754 0.11
C45	24.53 ± 0,17	24.764 0.'22	24.644 0.16	24.53 ± 0.19	24.58 ± 0.19	24.303 (),16
C46	25.263 0.21	24.42,1 0.07	24.993 0.20	24.91± 0.15	24.76 ± 0.11	24.()() ±0.09
C47	24.00± 0.13	24.81:1 0.14	24.06 ± 0.11	24.054 0.08	24.353 0.10	24.763 0.11
C48	25.494 0.16	25.243 0.21	25.404 0.19	25.344 0.20	25.434 0.14	24.7$4 0.13
C49	25.754 0.23	25.864 ().23	25.644 0.18	25.64 ± 0.19	25.584 0.22	24.66 ± 0.12
C50	24.77 ± 0.14	25.77 ± 0.25	24.863 0.19	25.023 ().17	25.393 ().23	25.774.0.22
C51	25.634 0.18	24.75 ± 0.10	25.374 0.16	24,71 ± 0.10	24.60 ± 0.13	25.073 0.12
C52	24,423 0.10	25,223 0.14	24.633 0.08	24.66 ± 0.10	24.92 ± 0.18	24.81± 0.10
C53	24.734 0.14	25.22 ±0.15	24.96± (), 13	24.92± 0.17	25.18 ± 0.17	25.043 0.12
C54	24.044 0.11	25.144 0.19	24.353 ().13	24.48 ± 0,12	24.82 ± 0.15	25.18 ± 0.15
C55	25.173 0.11	26.084 0.22	25.57 ± 0.11	25.60± 0.20	25,834 ().26	25.154 0.16
C56	25.08 ± 0.13	25.304 0.14	'24.61 ± ().08	24.723 ().13	25.11± 0.17	25.503 0.17
C57	25.10± 0.13		25.384 0.17	25.833 0.16	25.42 ± 0.15	24.85 ± 0.14
C58	24.81± ().19	...	...		25.77:1 ().38	25.51 ± 0.23
C59	25.474 0.20	25.744 0.20	25.824 ().16	25.604 0.19	25.324 0.32	24.823 0.15
C60	24,574-0.09	25.123 0.12	24.953 0.12	25.33 ±0.12	25.13 ± 0.11	24.274 0.07
C61	25.243 0.12	25.273 0.13	24.964 0.10	24.94 ± 0.17	25.16 ± 0.16	25.063 0.13
C62	25.63 ±0.16	25.063 0.13	25.663 0.19	25.30 ± 0.11	25.37± 0.13	25.92 ± 0.16
C63	24.863 0.14	25.973 ().24	25.383 0.19	25,633 ().22	25.483 0.21	24.894 0.10
C64	25.664 0.18	25.35 ±0.19	25,02,1 0,10	25.39± ().17	25.59 ± 0.24	24.643 0.11
C65	25.334 0.18	25.373 0.16	25.343 0.12	24.73 ± ().13	25,084 0.16	25,453 0.22
C66	25.884 0.23	25.13 ± 0.17	25.20 ±0.16	25.523 0.17	26.134 0.28	25.744 0.19
C67	24.984 0.12	25.51 ± 0.18	25.46 ± 0.13	25,303 ().11	25,04 ±0.14	25.473 0.19
C68	25.05 ± 0.20	25.46 ± 0.19	25.07 ± 0.20	25.004 0.18	25.425 ().22	25.12 ± ().15
C69	25.323 0.17	25.98 ± 0.18	25.14 ± 0.11	25.25 ± 0.14	25.87 ± ().26	25.264 ().16
W01	26,724 0.31	26.00,4 0.22	25.35 ± 0.12	25.563 0.15	25.46 ±0.16	25.583 0,17

TABLE A7

V-BAND ALLFRAME PHOTOMETRY - LAST SIX EPOCHS

ID	2449745.493	2449749.579	2449754.739	2449760.641	2449766.877	2449773.176
C1	23.24±0.09	23,324 0.08	23.45 ± 0.08	23,483 0.10	23.603 0.09	...
C2	24.144 0.11	23.654 0.09	23,393 0.08	23.034 0.07	23.99 ± 0.06	24.21 ± 0.08
C3	23.94±0.06	24.203 0.09	24.373 0.08	24.58±0.10	24.834 0.10	24.853 0.09
C4	23.745 0,10	23.86 ± 0.09	24.15 ± 0.09	24.153 0.08	23.68±0.07	23,594 0.07
C5	24.80±0.19	25.074 0.19	25.51±0.31	25.55±0.26	24.243 0.12	24.46 ± 0.12
C6	25.024 0.13	25.19 ±0.13	25,384 0.17	24.80 ± 0.13	24.454 0.10	24,834 0.11
C7	23.304 0.16	23.433 0.16	23.623 0.18	23.864 0.17	24.063 0.19	23.55±0.12
C8	24.93 ± 0.14	25.144 0.12	25.203 0.16	25.33 ±0.15	25.28,1 0.24	24.71 ± 0.08
C9	23.79 ± 0.21	23.87±0.23	24.244 0.19	24.244 0.24	24.41 ± 0.26	23.94 ±0.19
C10	23.67±0.06	23.64±0.09	23.91±0.09	24,223 0.09	24.4{) ±0.09	24.583 0.09
C11	26.074 0.23	26.043 0.19	26.23±0.32	26.493 0.30	25.583 0.19	25.834 0.20
C12	24.823 0.15	25.043 0.18	25.304 0.15	25.724 0.23	25.81±0.20	24.92 ± 0.25
C13	24.57±0.08	24.663 0.09	24.944 0.13	24.69±0.10	24.01 ± 0.10	24.'273 0.08
C14	23.664 0.12	23.254 0.12	22.87 ± 0.12	23.14 ±0.10	23.393 0.12	23.674 0,13
C15	24.74±0.19	24.983 0.19	25.32 ± 0.21	25.39±0,24	25.71±0.23	24,903 0.17
C16	24.124 0.09	24.384 0.13	24.51 ± 0.09	24.793 0.10	25.01 ±0.11	24,284 0.09
C17	23.61±0.08	23.88±0.10	24.08 ± 0.12	24.233 0.10	23.743 0.11	23.723 0.12
C18	25.184 0.20	25.373 0.21	25.494 0.19	25.854 0.22	24.95 ± 0.13	25.21 ± 0.15
C19	23.663 0.08	23.9(I ±0.12	24.11 ± 0.15	24.493 0.10	24.013 0.09	23.79±0.10
C20	24.753 0.16	24.98 ± 0.13	25,233 0.19	24.923 0.12	24.41 ± 0.12	24.94 ± 0.12
C21	25.15 ± 0.13	24.31 ±0.14	24.70 ± 0.11	25.14:1 0.14	25.233 0.12	24.31 ± 0.08
C22	23.52±0.10	23.873 0.10	24.28 ± 0.12	24.435 0.18	24.623 0.19	23.84 ± 0.13
C23	25.75±0.24	25.574 0.23	24.80 ± 0.14	25.06±0.20	25.74±0.24	26.06±0.31
C24	23.90,1 0.10	24.09 ± 0.10	24.44 ± 0.11	24.693 0.13	23.693 0.10	24.253 0.10
C25	26.00±0.31	24.86±0.13	25.01 ± 0.15	25.21 ±0.19	25.723 0.22	24.974 0.14
C26	24.63 ± 0.12	24.953 0.12	25.244 0.13	24.13 ± 0.10	24.61±0.11	25,44 ± 0.15
C27	24.343 0.16	24.433 0.15	24.64 ± 0.25	24.98 ±0.19	24.25,1 0.18	24.634 0.19
C28	23.954 0.10	24.21 ± 0.12	24.50 ± 0.08	24.81 ± 0.11	23.794 0.07	24.274 0.08
C29	25.41 ±0.19	24.724 0,15	25.084 0.14	25.71±0.15	25.853 0.21	24.534 0.08
C30	25.454 0.15	26.103 0.30	25.744 0.18	25.204 0.17	25.51 ± 0.17	25.983 0.16
C31	24.364 0.10	24.584 0.17	24.834 0.12	25.054 0.15	24.093-0.10	24,753 0.17
C32	24.49 ± 0.15	23.55 ± 0.12	24,00 ±0.14	24.28±0.1'2	24.553 0.23	23.683 0.13
C33	25.94±0.29	26.02 ± 0.27	26.71 ± 0.47	25.49±0.25	25,904 0.29	26.384 0.41
C34	24.37 ± 0.13	24.743 0.12	24.914 0.14	25.15 ±0.19	24.55 ± 0.10	24.843 0.18
C35	24.524 0.11	24.76 ± 0.11	25.223 0.13	25.423 0.11	24.394 0.07	24.834 0.09

TABLE A7- *Continued*

ID	2449745.493	2449749.579	244() 754.739	2449760.641	2449766.877	2449773.176
C36	24.564 0.13	24.86 ± 0.12	25.084 0.14	24.96 ± 0.12	24.61 ± 0.10	25,084 0.14
C37	25.353 0.19	25.43: 0.17	24.39 ± 0.12	24.89 ± 0.15		25.503 0.22
C38	23,724 ().11	24,064 ().13	24.584 ().17	24.41 ± 0.15	23.69 ± 0.20	24.44 ± 0.17
C39	25.10,1 ().15	25.13,1 ().15	24.124 ().13	24.57 ± 0.13	25.054 0.14	25.44 ± 0.18
C40	24.963 0.15	. .	24.98 ± 0.12	24.523 0.10	25.25 ± 0.17	25.674 0.26
C41	24.80 ± 0.16	24.71 ± 0.09	23.89 ± 0.12	24.463 0,14	24.84 ± 0.14	24.143 0.09
C42	25.733 0.29	25.383 0.19	2.4.833 0.15	25.49 ± 0.20	25.523 0.25	24.984 0.19
C43	24.103 0.16	23.91 ± 0.16	23.69 ± 0.13	23.93 ± 0.14	23.903 0.21	23.693 0.17
C44	24.89: ().17	25.19 ± 0.18	24.37 ± 0.08	24.754 0.13	25.08 ± 0.18	24.754 0.12
C45	24.21 ± 0.17	24.47,4 0.15	24.67 ± 0,16	24.14 ± 0.12	24.45 ± 0.16	24.634 0.15
C46	24.21 ± 0.12	24.63 ± ().12	24.85 ± 0.19	23.833 0.09	24.26 ± 0.15	24.933 0.15
C47	24,564 0.17	24.03 ± 0.09	24.184 0.09	24.68 ± ().13	24.633 0.16	24.403 0.14
C48	24.973 0.17	25.29 ± 0.13	25.41 ± 0.19	24.853 0.11	25.333 0.21	25.682 0.21
C49	24.904 0.15	25.424 0.24	25.47: 0.27	24.64 ± 0.13	25.50 ± 0.19	25.983 0.26
C50	25.553 0.21	24,633 0.12	25.15 ± 0.18	26.15 ± 0.37	24.62 ± 0.14	25.582 0.27
C51	25.353 (),15	25.474 0.'21	24.58 ± 0.12	25.224 ().16	25.463 ().22	24.55 ± 0.09
C52	24.073 0.08	24,353 0.13	24.83,1 0.09	24.063 0.11	24.553 0.13	25.284 0.17
C53	24.434 0.10	24.78 ± 0.13	25.31 ± 0.16	24.31 ± 0.10	24.87 ± 0.11	25.54 ± 0.18
C54	24.903 0.16	24.19 ± 0.08	24.674 0.15	25.05 ± ().16	24.223 0.12	24.953 (),16
C55	24.994 0.18	25.474 0.14	25.544 0.23	24.904 ().17	25.743 0.20	25,603 0.14
C56	25.31 ± 0.16	24.633 ().17	25.143 0,14	25.37 ± 0.17	24.69 ± 0.10	25.60 ± 0.17
C57	25.01 ± 0.09	25.574 0.19	25,074 0.12	25.244 0.13	25.5230.16	24.80 ± 0.12
C58	24.754 0.17	25.28 ± 0.21	25.87:1 0.30	24.763 ().15	25.334 0.23	26.023 0.35
C59	25.124 0.12	25.603 0.22	25.394 0.20	25.16 ± 0,20	26.003 0.38	24.87 ± 0.13
C60	24.733 0.16	25.243 0.14	24.81 ± 0.08	24.86 ± 0.15	25.20 ± 0.16	24.61 ± 0.12
C61	24.744 0.12	25.054 0.08	25.32:1 0.18	24.85 ± 0.13	25.384 0.18	24,903 0.12
C62	25.943 0.17	25.294 ().14	25.92 ± 0.21	25.663 0.18	25.824 0,20	25.72 ± 0.21
C63	25,093 0.15	25,534 0.13	24.724 0.12	25.59 ± 0.22	24.774 0.11	25.684 0.19
C64	25.103 0.16	25.324-0.18	24.892 0.14	25.40:1 0.14	25.073 0.17	25.564 0.22
C65	25.193 0.27	24.92 ± 0.13	25.333 0.20	24.86 ± 0.17	25.60 ± 0.18	25.094 0,13
C66	25.15 ± 0.13	25.93 ± 022	25.463 ().19	25.683 0.13	25.474 0.15	25.844 0.24
C67	25.373 0.16	25.104 0.14	25.874 0.20	24.95 ± 0.14	25.623 0.16	25.064 0.12
C68	24.953 0.18	25.743 0.34	24,933 0.18	25.42 ± 0.25	25.19 ± 0.15	25.163 0.20
C69	25.404 0.18	25,723 0.24	25.44 ± 0.15	25.104 0.20	26.00 ± 0.27	25.51 ± 0.11
W01	25.493 0.14	25.852 0.21	25.84 ± ().17	25.93 ± 0.27	25.824 0.23	

TABLE A8

I-BAND ALLFRAME PHOTOMETRY

ID	2449713.915	2449721.830	2449741.734	2449760.700
C01	22.623 ().09	22.81±0.10	22.52 ±0.08	22.554 0.09
C02	22.57 ±0.06	22.743 0.06	23.004 0.07	22.564 0.06
C03	22.994 0.07	23.184 0.08	22.774 0.05	23.17 ±0,10
C04	23.19±0.07	23.31 ±0.09	22.763 0.06	23.163 0.08
C05	23.854 0.18	23.95±0.17	23.37 ±0.12	23.803 0.19
C06	24.16 ±0.11	23.55 ±0.09	23.47 ±0.07	23.48 ±0.12
C07	22.753 0.09	22.954 0.08	22,63,1 0.06	22.955 0.09
C08	22.953 0.06	22.843 0.07	22.87,1 0.10	23.24,1 0.07
C09	23.073 0.11	23.174 0.18	23.11 ±(),14	23.11 ±0.19
C10	22,813 0.06	22.963 0.07	23.374 0.09	23.024 0.06
C11	24.66±0.13	24.96±0.21	24.68,1 0.17	24.72 ±0.18
C12	23.62 ±0.21	23.90 ±0.22	23,49,1 0.19	23.91±0.12
C13	23.28,1 ().07	23.714 0.08	23.174 0.07	23.573 ().10
C14	23,144 0.10	22.524 0.08	22.99±0.10	22.67±0.10
C15	23.293 0.13	23.503 ().11	23.474 0.10	23.70 ±0.12
C16	23.003 0.06	23.303 0.08	23.013 0.07	23.584 0.09
C17	22.71 ±0.09	22.983 0.08	22.66 ±0.09	22.974.0.09
C18	23,983 0.11	24.303 0.15	23.95 ±0.13	24.373 0.23
C19	22.87 ±0.05	23.14,1 0.09	22.75 ±().07	23.34 ±0.07
C20	23.464 0.10	23.7{) ±0.07	23.51 ±0.08	23,794 0.12
C21	23.864 0.08	2.3.494 0.10	23.973 0.11	23.79 ±0.08
C22	23.623 0.13	23.133 0.09	23.65 ±0.13	23.193 0.11
C23	23.91 ±0.12	24.383 0.21	24.01 ±0.12	23.893.0.15
C24	23.833 0.12	23.334 0.08	23.19,1 ().()9	23.674 0.13
C25	24.21 ±0.11	24.72 ±0.16	24.344 0.11	24.103 ().13
C26	23.533 0.11	23.943 0.11	23.63 ±0.10	23.504 0.06
C27	24.13 ±0.18	23.643 0.17	23.58,1 0.11	24.15 ±0.18
C28	23.664 0.10	23.163 0.08	22.96±0.08	23.59 ±0.10
C29	24.15 ±0.12	24.064 0.12	24.214.0.13	24.033 0.13
C30	24.07 ±0.11	24.423 ().14	23.99,1 0.11	23.903 0.14
C31	23.693 0.13	23.223 0.08	23.053 0.07	23.503 0.13
C32	23.31 ±().15	23.563 0.17	23.483 ().14	23.41 ±0.17
C33	23.95 ±0.14	23.983 0.11	24.05,1 0.18	23.853 0.25
C34	24.10 ±0.14	23.693 0.11	23.92,1 0.10	23.90 ±0.09
C35	23.983 0.11	23.45 ±0.08	23.26 ±0.06	24.06 ±0.11

TABLE A8 Continued

ID	2449713.915	2440721.830	2449741.734	2449760.700
C36	24.13 ± 0.10	23.674 0.07	23,523 0.07	23.993 ().11
C37	23.473 0.07	23.994 ().1()	23.823 0.09	23.69 ± 0.08
C38	23.59: 0.11	23.034 0.12	23.14 ±0.09	23.45 ± 0.13
C39	23.51 ± 0.11	23.6'73 0.14	23.834 0.11	23.713 0.15
C40	23.923 0.08	23.68 ± 0.08	23.704 0.07	23.592 0.08
C41	23.28± 0.06	23.734 0.08	23.47:1 0.09	23.384 0.08
C42	23.693 0.09	24.10 ± 0.16	23.88:1 0.12	24.123 0.15
C43	22.94± 0.15	23.26:1 0.12	23.21 ± ().12	23,294 0.10
C44	24.11± 0,10	24.00,1 0.14	23.91 ± 0.12	23.80 ± 0.13
C45	23.07 ± 0.10	23.234 0.12	23.06:1 0.08	23.01± 0.10
C46	23.523 ().31	23.07± ().23	23.00 ± 0.21	22.883 0.18
C47	23.41± 0.11	23.624 0.17	23.734 ().13	23.753 0.09
C48	24.09 ± 0.12	24.18 ± 0.10	23. 85± 0.13	23.723 0.14
C49	24.394 0.16	24.394 0.12	23.(32 ±0.15	23.884 0.19
C50	23.893 0.12	24.33 ± 0.16	24.36 ±0.15	24,523 0.24
C51	24.20 ± 0.16	23.73 ± 0.10	23.824 0.13	23.894 0.12
C52	23.71± 0.06	24.18 ± 0.10	23.854 0.11	23.533 0.09
C53	23.864 0.14	24.41 ± ().18	24.08 ± 0.16	23.58 ± 0.10
C54	23.593 0.10	24.21± ().17	24.41± 0.15	24.444-0.21
C55	24.204 0.13	24.884 0.27	24.28 ± 0.16	23,984 0.12
C56	24.134.0.09	24,264 0.10	24.45 ± 0.14	24.48 ± 0.11
C57	24.094 0.14	24.354 0.17	23.89± 0.12	24,074 0.12
C58	23.85± 0.12	. . .	24.423 0.19	23.783 0.13
C59	24.374 0.15	24.974 (). 16	24.19 ± ().12	24.22 ± 0.14
C60	23.894 0.10	24.174 0.13	23,633 0.10	23.883 0.11
C61	24.21± 0.14	24.303 0.15	24.323 0.13	24.02 ±0.11
C62	24,433 0.14	24.19 ± 0.11	24.58 ± 0.17	24.523 0.20
C63	24.23 ± 0.15	24.91 ± 0.22	24.10 ± 0.12	24.493 0.18
C64	24.603 0.18	24,504 0.15	24.024 0.13	24.84± 0.24
C65	24.11± 0.10	24,143 0,10	24.29± 0.14	23.94 ± 0.14
C66	24.353 0.17	24.05± 0.11	24.31± 0.14	24.423 0.18
C67	24.024 ().13	24.324 0.14	24.26,1 0.15	24.034-0.11
C68	24.243 0.17	24.76 ± 0.16	24.47 ± 0.19	24.65 ± 0.26
C69	24.703 0.17	25.084 0.22	24.($\{1 ±0.19	24.42:1 0.16
W0]	25.293 0.24	25,083 ().21	24.68 ± 0.17	24,923 0.19